REGULATION OF DYNEIN-DYNACTIN DURING *DROSOPHILA* GAMETOGENESIS

By

Poojitha Sitaram

Dissertation

Submitted to the Faculty of the

Graduate School of Vanderbilt University

in partial fulfillment of the requirements

for the degree of

DOCTOR OF PHILOSOPHY

in

Cell and Developmental Biology

December, 2013

Nashville, Tennessee

Approved by:

Laura A. Lee

David M. Miller III

Katherine L. Friedman

David M. Bader

Matthew J. Tyska

To Amma, Appa and Dudhu

ACKNOWLEDGEMENTS

I have many people to thank for my accomplishments during the course of my graduate career and for getting me where I am today. I would first like to thank my mentor, Dr. Laura Lee, for all of her guidance and support over the last five years. Laurie is an exceptional mentor and scientist and her first priority is always the well-being of her students. Irrespective of the demanding nature of her schedule for any particular day, if I had an urgent need to discuss my project with her, she would always make time to meet with me. Any skill I possess today with regards to organization or scientific writing, I learnt from Laurie. I can honestly say that I'm a better scientist and worker because of her. And finally, I want to thank Laurie for agreeing to let me visit India about once a year, in spite of her constant worry that I'd get married during one of my visits and never come back!

A bonus of being in Laurie's lab is having the additional support and scientific guidance of Dr. Ethan Lee. Since both Lee labs share lab space and have joint lab meetings, Ethan knows nearly as much about my project as Laurie does, and he has always been available to provide a fresh and unbiased perspective to any roadblocks that Laurie and I have faced over the past several years. I also want to thank Dr. Andrea Page-McCaw who has been equally as valuable to me in sharing her knowledge of *Drosophila* and oogenesis as well as in sharing her lab resources the many, many times I went to her for help. I would also like to thank the members of my committee, Drs. David Miller, Kathy Friedman, Matt Tyska, and David Bader for all their guidance and support during my graduate career.

I would not have been half as successful with my research if it hadn't been for some amazing lab mates and colleagues. My most sincere thanks go to Michael Anderson who, in addition to being a wonderful mentor to me over my first few months in lab, also gave me the starting point for my various projects. I'm also grateful to Julie Merkle and Jamie Rickmyre, as well as to the senior graduate students in Ethan's lab for all of their help in making me feel so welcome and for getting me acclimatized to the lab environment.

Three of my fellow IGP classmates, Sarah Hainline, Brian Hang, and Tony Chen, joined Laurie and Ethan's labs at the same time I did, and they made my graduate school experience seem like an epic adventure equal to the likes of Tolkien's The Lord of the Rings. We faced trials and tough times, but we always supported each other knowing that in the end, we would succeed in throwing the One Ring (and Gollum) into Mount Doom. Additional thanks goes to my bench mate, Tony Chen, for occasionally taking my mind off of conventional science (and reality) with long discussions about Game of Thrones, Doctor Who and many such similar topics. I also want to thank Kenyi Saito and Matt Broadus for various scientific and not-so-scientific conversations during lab meetings and birthday parties, as well as those shouted (or e-mailed back and forth) across the lab.

And of course, I would be remiss if I did not mention Jeanne Jodoin (my best friend forever), who in addition to providing various forms of entertainment such as startling me with dry ice bombs and regaling me with daily stories about her dogs, also became somewhat of a scientific partner to me as we helped each other with certain aspects of our experiments. Unfortunately, to this day, she still stubbornly pronounces "ap-parrot-us" as "apa-rat-us". I would also like to thank Heather Wallace for acting as a

sounding board for all my experimental problems, for listening to me talk about all the books I'd been reading, for assisting me in attempting to catalog the various species of frogs in Nashville (we both failed, miserably), and finally, for being my lunch date nearly every day of the week.

I also want to thank all of my friends, those in and outside Nashville. Friday night dinners and weekend movies with Kamya, Bhava, and Saumitra, and frequent conference calls and holiday visits with Pooja, Vidya, Gunjan, Nandita, Santhosh, and Divya, are partly what kept me sane and contented with life these past few years. My gratitude also goes to all of my extended family members residing in the United States - Radhika Atthai and Ravi Uncle, Tilak Mama and Vidya Manni, Vishnu, and Ramya – for not only putting up with my constant visits, but actually encouraging them.

Last but certainly not least, I want to express my undying gratitude to my family. My Thatha, Ammamma, and Paati may not completely understand why I would want to keep on "studying" instead of getting a lucrative job, but they make no secret of how proud they are of me and my accomplishments. My little brother, Sudu, in spite of not knowing how to express his support through words, has shown me in so many other ways just how much he wants me to succeed in my personal and professional life. And finally, to my Amma and Appa, who have been unwavering pillars of support over my entire life, I want to say thank you. Thank you for your strength, your trust, your endless confidence in me, and most importantly, thank you for just being who you have been for all these years. I would not be where I am today without you.

TABLE OF CONTENTS

LIST OF TABLES

LIST OF FIGURES

CHAPTER I

INTRODUCTION TO DYNEIN AND *DROSOPHILA* GAMETOGENESIS

Introduction

Molecular motors travel along cytoskeletal tracts and perform an array of critical functions within cells. The myosin family of motors is responsible for actin-based motility and is best known for its roles in the regulation of muscle contraction, cell shape, and cell motility. Dynein and kinesin, on the other hand, are microtubule motors that transport cargo by traveling along the microtubule cytoskeleton. The majority of kinesin motors are involved in plus-end-directed transport, whereas dynein powers minus-end-directed transport to mediate retrograde movement of its cargoes.

The focus of my research has been to study the regulation of dynein during *Drosophila* spermatogenesis and oogenesis. In this chapter, I will provide an overview of dynein and its accessory factors with an emphasis on the LIS-1 accessory protein. I will further describe the function and regulation of dynein during *Drosophila* spermatogenesis. I will describe our lab's previous work identifying Asunder as a novel regulator of dynein localization during *Drosophila* spermatogenesis. Finally, I will provide an overview of *Drosophila* oogenesis with emphasis on various patterning events that take place during this process. I will then highlight the critical roles played by dynein for proper progression through *Drosophila* oogenesis.

The Dynein Complex

Two classes of dynein exist within cells. Axonemal dynein, which is found within cells containing cilia or flagella, provides the force for the beating of flagella (Gibbons and Rowe, 1965). More than 20 years after the discovery of axonemal dynein in *Tetrahymena*, cytoplasmic dynein was identified in neurons and shown to play a role in powering retrograde transport along microtubules (Paschal and Vallee, 1987). Two cytoplasmic dynein complexes have been identified: Cytoplasmic dynein 1, which is required for organelle transport and various mitotic events, and cytoplasmic dynein 2, which plays a role in intraflagellar transport (Cole, 2003; Vallee et al., 2004). My work is focused on cytoplasmic dynein 1 (hereafter referred to as dynein), which is the most common form of dynein and is present in all cells containing microtubules.

Dynein is a large multimeric complex composed of six different subunits, which are named based on their relative molecular masses. These include the heavy chain containing the motor domain and five smaller subunits that form the base of the complex, including the intermediate chain, light intermediate chain, and three different light chains (Hook and Vallee, 2006; Pfister et al., 2006). Vertebrates have at least two genes encoding each of the subunits, whereas in *Drosophila* most of the subunits are encoded by single genes.

The core of the dynein complex is composed of a dimer of the large ~500-kDa dynein heavy chain (Fig. 1.1). Each heavy chain contains a C-terminal AAA motor domain that is the site for ATP hydrolysis, which powers the movement of dynein on microtubules, as well as an N-terminal stem through which the heavy chain associates

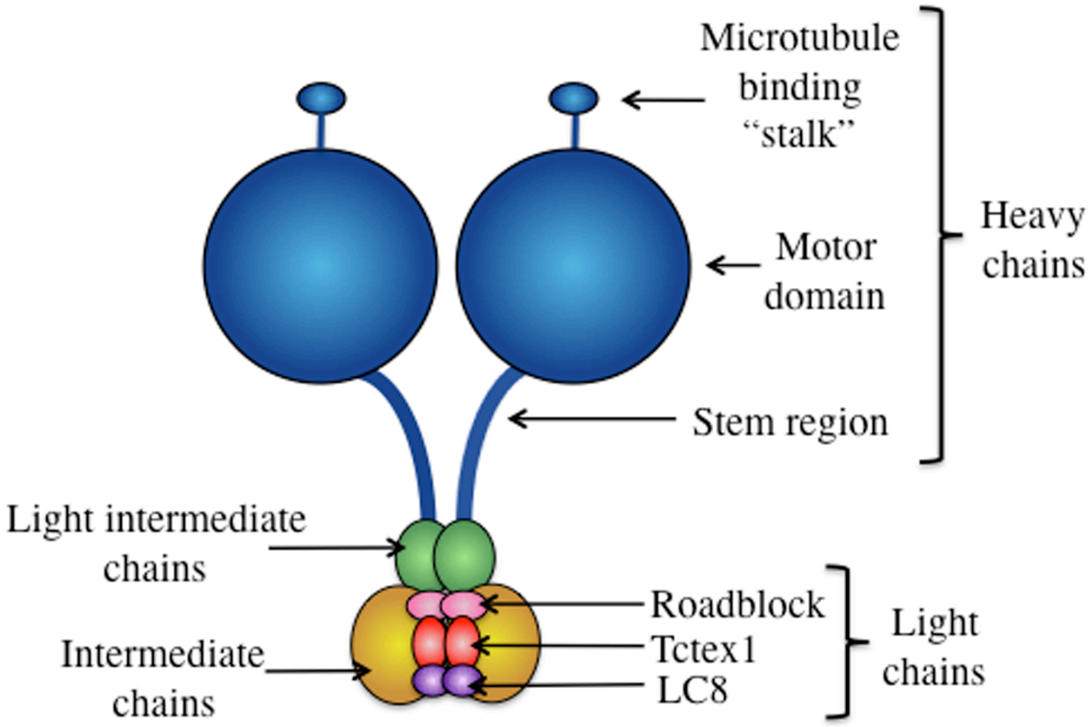

Figure 1.1. The dynein complex. Cartoon depicting the structural model for the association of the cytoplasmic dynein complex subunits. A pair of dynein heavy chains contains the motor domain of the dynein complex. Dynein also associates with microtubules through a microtubule-binding domain in the heavy chain. Associated with the stem region of the heavy chain are dimers of dynein intermediate chains and light intermediate chains. Dimers of three light chain family members associate with the intermediate chain subunits and make up the rest of the dynein complex. Adapted from (Pfister et al., 2006).

with the other subunits of dynein (Vallee and Hook, 2006). The motor domain also contains a 'stalk' region through which dynein associates with microtubules.

A dimer of the ~74-kDa intermediate chain is found associated with the stem of the heavy chains at the base of the dynein complex. The intermediate chain has also been found to directly bind dynein light chains and is predicted to target dynein to its intracellular cargo via its direct association with the p150/Glued subunit of the dynein adaptor protein, dynactin (Karki and Holzbaur, 1995; Ma et al., 1999; Paschal et al., 1992; Pfister et al., 2006; Vaughan and Vallee, 1995). Therefore, intermediate chains appear to serve as a scaffold in the dynein complex.

Also associated with the stem region of the heavy chain is a dimer of the ~50-60-kDa dynein light intermediate chain. In contrast to other subunits, the light intermediate chain is unique to cytoplasmic dyneins, suggesting that its role is specific to intracellular transport (Mische et al., 2008). Additionally, the light intermediate chain has been shown to be required for maintaining the stability of the dynein complex as well as for proper progression through the spindle assembly checkpoint (Mische et al., 2008; Sivaram et al., 2009).

Dimers of three light chain families (Tctex1, Roadblock, and LC8) bind directly to the intermediate chain dimers and have been shown to cooperate in the binding of various intracellular cargoes (Pfister et al., 2006). Different light chain families have been shown to have unique cargo binding properties. Therefore, the specificity of dynein complexes of various subunit compositions for their cargoes appears to depend on the composition of their light chains (Chuang et al., 2001; Tai et al., 2001). Additionally, of

the three light chain families, the Tctex-1 family is the first to be found non-essential in *Drosophila* (Li et al., 2004).

Dynein Function and Regulation

Cytoplasmic dynein is essential for a wide variety of cellular processes. It is required for the transport of diverse cargoes including mRNA, protein, chromosomes, and membrane-bound organelles. Dynein also plays key roles in cell-cycle events, including nucleus-centrosome coupling, nuclear envelope breakdown, spindle assembly/positioning, and chromosome segregation (Gusnowski and Srayko, 2011; Hebbar et al., 2008; Huang et al., 2011; Salina et al., 2002; Splinter et al., 2010; Stuchell-Brereton et al., 2011; Wainman et al., 2009). Additionally, dynein plays a role in developmental processes such as nuclear migration by powering the movement of nuclei along microtubule tracts (Xiang and Fischer, 2004).

Because of the wide range of processes that require its activity, dynein undergoes multiple layers of regulation within the cell. Dynein appears to be primarily regulated by its subunit composition. Different dynein complexes are constructed from a combination of different subunit isoforms, and dynein complexes with different compositions have been shown to mediate distinct functions (Day et al., 2004; Ha et al., 2008; Jin et al., 2007; Jin et al., 2009; Palmer et al., 2009; Sivaram et al., 2009). Dynein performs a variety of functions at different subcellular localizations. Dynein localizes to multiple subcellular sites during the cell cycle, such as the nuclear envelope, centrosomes, kinetochores, spindle microtubules, and the cell cortex (Dujardin and Vallee, 2002; Kiyomitsu and Cheeseman, 2012; Pfarr et al., 1990; Steuer et al., 1990; Tanenbaum et al.,

2010). Additionally, dynein activity within the cell is also regulated by the phosphorylation states of its subunits as well its association with its various accessory factors (Dillman and Pfister, 1994; Gill et al., 1994; Hughes et al., 1995; Salata et al., 2001; Vaughan et al., 2001; Whyte et al., 2008).

Accessory Factors of Dynein

The capacity of dynein to perform its various functions depends on its association with a myriad of accessory factors within the cell. Dynactin is the most well-known and vital accessory factor of dynein. The name "dynactin" or 'dynein activator' was coined based on its *in vitro* capacity to stimulate dynein-mediated vesicle transport, as depletion of dynactin from cells abolishes vesicle transport (Gill et al., 1991; Schroer and Sheetz, 1991). Genetic studies in yeast, filamentous fungi, and *Drosophila* have since demonstrated that dynactin is essential for a majority, if not all, of the *in vivo* functions of dynein (Schroer, 1994; Schroer, 2004). In addition to its roles as a dynein adaptor, dynactin also performs dynein-independent functions within the cell (Blangy et al., 1997; Deacon et al., 2003; Quintyne and Schroer, 2002).

Dynactin is also a large (~1.2 MDa) multi-subunit complex composed of 11 unique subunits, some of which are present in more than one copy, such that each dynactin molecule comprises ~20 individual subunits (Fig. 1.2). The overall structure of dynactin can be divided into two units: the Arp1 rod and the projecting arm. The Arp1 rod is the cargo-binding site of dynactin and is composed of the following proteins: Arp1, Arp11, p62, p25, p27, actin, and capZ α/β (Schroer, 2004). The three remaining dynactin subunits ($p150^{Glued}$, dynamitin, and p24/22) constitute the projecting arm. Dynactin binds

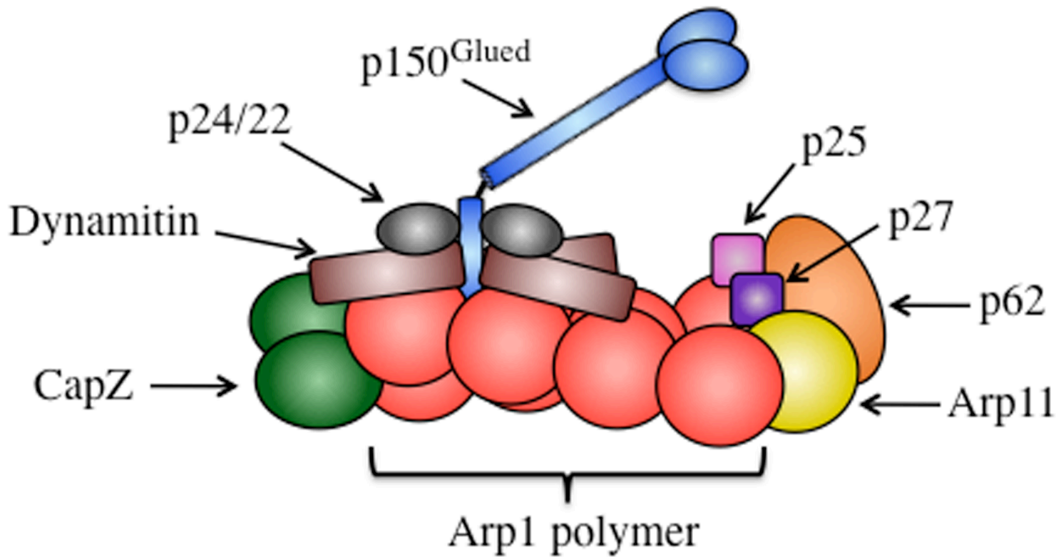

Figure 1.2. The dynactin complex. Cartoon depicting the structural model for the association of the dynactin complex subunits. The current model for the structure of dynactin was generated using information obtained from structural analyses as well as studies of subunit interactions. The cargo-binding domain of dynactin, also known as the Arp1 rod domain, is made up of multiple Arp1 subunits, Arp11, actin, capZ, p62, p27 and p25. The projecting arm is a flexible and extendable structure composed of the remaining three dynactin subunits; p22/24, p50 (also known as dynamitin), and $p150^{Glued}$. Dynactin binds to dynein as well as to microtubules through the subunits of the projecting arm. Adapted from (Schliwa and Woehlke, 2003).

microtubules and dynein through the p150^{Glued} subunit (Karki and Holzbaur, 1995; Vaughan and Vallee, 1995; Vaughan et al., 2002; Waterman-Storer et al., 1995). The individual dynactin subunits are interdependent in that loss or overexpression of any of the subunits can lead to destabilization of the entire complex (Schroer, 2004).

Dynactin, therefore, by virtue of its various subunits, directly interacts with microtubules, dynein intermediate chain, and the subcellular cargoes of dynein. Through these various interactions, dynactin supports the subcellular roles of dynein in two ways: first, by acting as an adaptor protein, mediating the association between dynein and its cargo, and second, by enhancing the processivity of dynein by increasing the time frame during which dynein molecules remain associated with microtubules (Culver-Hanlon et al., 2006; King and Schroer, 2000; Schroer, 2004).

Recent evidence, however, has demonstrated that dynein performs some of its mitotic functions, such as chromosome alignment, spindle pole focusing, and force generation in the spindle, independently of dynactin (Raaijmakers et al., 2013). Dynein acts in concert with its other accessory factors, such as the Lis-1/NudE/NudEL complex, to perform these and other functions. The Lis-1/NudE/NudEL complex regulates dynein force production by acting as a "clutch" to increase attachment of dynein to microtubules and by promoting transport of high molecular weight cargo (Huang et al., 2012; McKenney et al., 2010; Ori-McKenney et al., 2011; Raaijmakers et al., 2013). In fact, dynactin and the Lis-1/NudE/NudEL complex compete to interact with the same site on the dynein intermediate chain, suggesting that different dynein complexes associate with different regulatory elements to perform distinct functions; Lis-1 binds to multiple subunits of dynein and binds to dynactin as well, however, suggesting that certain dynein

complexes can simultaneously associate with both dynactin and Lis-1 (Faulkner et al., 2000; McKenney et al., 2011; Mesngon et al., 2006; Nyarko et al., 2012; Sasaki et al., 2000; Smith et al., 2000). Dynein also interacts with proteins such as ZW10, hSpindly, CENP-F, and BICD2 to promote its targeting to various sites within the cell (Gassmann et al., 2008; Griffis et al., 2007; Raaijmakers et al., 2013; Raaijmakers et al., 2012; Splinter et al., 2010; Starr et al., 1998; Vergnolle and Taylor, 2007; Whyte et al., 2008).

LIS1

Loss or mutation of a single copy of human *Lissencephaly-1* (*LIS1*) causes type I lissencephaly ("smooth brain") associated with the disruption of early migration patterns of neurons (Gambello et al., 2003; Hirotsune et al., 1998; Vallee and Tsai, 2006; Wynshaw-Boris, 2007). Individuals affected with lissencephaly display severe mental retardation, seizures, reduced muscle strength, and typically do not survive past early childhood. As a result of defects in neuronal migration, lissencephaly patients have reduced numbers of cells as well as cellular layers in the cerebral cortex (Reiner and Lombroso, 1998).

Neuronal migration can be divided into two steps. In the first step, the neuron extends leading processes towards specific sites in the nervous system. In the second step, called nucleokinesis, the nucleus and cytoplasmic organelles contained within the cell body travel along microtubule bundles towards the direction of motion (Tsai and Gleeson, 2005). Mouse models have demonstrated that disruption of *Lis1* specifically interrupts the migration of nuclei through the leading processes (Gambello et al., 2003; Hirotsune et al., 1998; Tanaka et al., 2004; Tsai and Gleeson, 2005). Dynein is known to

play a major role in nuclear migration by promoting the interaction of the nucleus with microtubule arrays and microtubule organizing centers (Malone et al., 2003; Tanaka et al., 2004; Tsai and Gleeson, 2005). In fact, a recent study has shown that the apical migration of the nuclei of radial glial progenitor cells of the mouse brain is dependent on the recruitment of dynein to the nuclear envelope (Hu et al., 2013). Disruption of perinuclear dynein was found to cause a mitotic arrest, as these cells undergo mitosis only after the apical migration of the nucleus. These results strongly suggest that lissencephaly arises as a consequence of the disruption of dynein-mediated nuclear migration caused by reduced *Lis1* copy number.

LIS1 appears to be essential for other cellular functions of dynein, as evidenced by the fact that mutations in LIS1 lead to defects in centrosome movements, nuclear envelope breakdown, spindle assembly, and chromosome segregation, all of which are regulated by dynein (Faulkner et al., 2000; Hebbar et al., 2008; Li et al., 2005; Tai et al., 2002). LIS1 and dynein also colocalize at various sites within the cell such as the cell cortex, kinetochores, nuclear envelope, and spindle poles. The localizations of LIS1 and dynein have been shown to be interdependent; this dependence, however, appears to vary with the organism studied as well as the site to which they are localized (Cockell et al., 2004; Coquelle et al., 2002; Lam et al., 2010; Lee et al., 2003; Siller et al., 2005; Zhang et al., 2003).

Similar to the core dynein subunits, LIS1 is dimeric. Each LIS1 polypeptide contains an N-terminal homodimerization domain and a C-terminal β-propeller domain characterized by the presence of several WD-repeat motifs (Tai et al., 2002; Tarricone et al., 2004). LIS1 has been shown to directly bind the dynein heavy and intermediate

chains as well as the dynamitin subunit of dynactin through its WD-repeat region and the binding of LIS1 enhances the motor activity of dynein (Faulkner et al., 2000; Mesngon et al., 2006; Sasaki et al., 2000; Smith et al., 2000). The NudE and NudEL proteins have been shown to further tether LIS1 to dynein in order to facilitate the transport of high-load cargoes such as nuclei and centrosomes, and this function likely explains the observed defects in nuclear and neuronal migration when LIS-1 levels are reduced (McKenney et al., 2010).

Meiosis

Accurate partitioning of cytoplasmic and genetic material is critical for successful cell division. There are two main forms of cell division in eukaryotes. Somatic cells typically undergo a canonical cell cycle with DNA synthesis during "S" phase, a mitotic "M" phase, and intervening gap phases (G1, which precedes S phase, and G2, which precedes M phase). Germ cells, however, undergo a unique form of cell division that involves one round of DNA replication followed by two consecutive rounds of nuclear division to allow the formation of haploid gametes (Miller et al., 2013). Meiosis is critical for sexual reproduction and forms the basis for genetic diversity as it permits the recombination of genomes from two individuals to produce offspring that differ genetically from both parents (Alberts et al., 2007).

The steps in mitotic and both meiotic divisions are similar in nature and are referred to by the same terms (prophase, metaphase, anaphase, telophase, and cytokinesis), although the chromosome alignment and separation in mitosis is more like that in meiosis II (Alberts et al., 2007). The first meiotic division follows interphase

during which DNA replication takes place in the premeiotic S phase. In meiosis I, however, the duplicated homologous chromosomes rather than the sister chromatids are joined together by means of a protein complex called the synaptonemal complex to form a structure called a bivalent. These bivalents undergo recombination and crossing over, where one or more fragments of the maternal chromatid are exchanged for the corresponding paternal chromatid by the production of double-stranded breaks in the DNA. At the end of meiosis I, these homologous chromosomes separate and are then segregated into two daughter cells. After a very brief (and sometimes absent) interphase, these cells progress through meiosis II, which takes place without any additional DNA replication. In meiosis II, similar to mitosis, the sister chromatids align at the metaphase plate, are pulled apart during anaphase II, and are segregated into two daughter cells such that the end products of both meiotic divisions are four haploid cells, each with either a single maternal or paternal copy of each chromosome.

Given the critical role of meiosis in reproduction, mistakes that occur during the meiotic divisions can have serious consequences. Errors of meiosis most commonly occur during the process of chromosome segregation (Alberts et al., 2007). Improper separation or nondisjunction of homologous chromosomes in meiosis I or of sister chromatids in meiosis II result in some haploid daughter cells lacking a certain chromosome while others have more than one copy of the same chromosome. Such defective divisions result in a condition called aneuploidy. Aneuploidy is the leading cause of fetal loss and birth defects (Hassold and Hunt, 2001). A surprisingly high number of human embryos (~20%) are produced with aneuploid gametes, however, only a small percent of these embryos survive (O'Connor, 2008). Aneuploidy involving the

sex chromosomes is generally much better tolerated than aneuploidy of the autosomal chromosomes, which is often associated with mental retardation and other severe defects. The occurrence of nondisjunction of homologous chromosomes during meiosis I in human females further increases with age as a result of the extended meiotic prophase I arrest in older human oocytes (Hassold and Chiu, 1985).

Since the beginning of the 20th century, *Drosophila* gametogenesis has been a very useful model system for studying the process of meiosis. For example, the chromosome theory of heredity was based on the analysis of atypical meiotic segregation in *Drosophila* ovaries (Bridges, 1916). Studies of *Drosophila* gametogenesis have provided key insights into various aspects of meiosis and the functions of a host of genes that are required during meiosis (Anderson, 1925; Boschi et al., 2006; Collins et al., 2012; Herskowitz and Muller, 1954; Kracklauer et al., 2010; Lindsley and Sandler, 1977; Orr-Weaver, 1995; Sitaram et al., 2012; Wainman et al., 2009).

Drosophila Spermatogenesis

Drosophila spermatogenesis is an excellent system for studying the regulation of cell division. The stages of *Drosophila* spermatogenesis are well defined (Fig. 1.3) (Fuller, 1993). The hub cells at the apical tip of the testes are in contact with germline stem cells that are enclosed within a pair of somatic cyst progenitor cells. The germline stem cells divide asymmetrically to produce spermatogonial cells, each of which is enclosed by a pair of cyst cells, which are a product of cyst progenitor cell division. The spermatogonial cells undergo four rounds of synchronous mitotic divisions with incomplete cytokinesis to generate 16 primary spermatocytes. These 16 cells remain

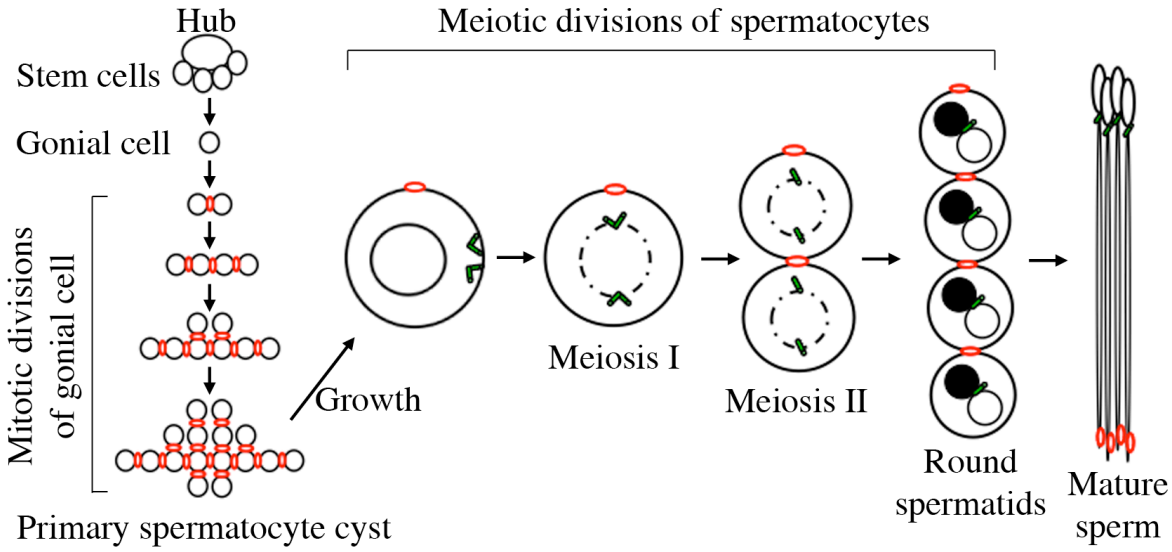

Figure 1.3. *Drosophila* spermatogenesis. Cartoon depicting the various stages of *Drosophila* spermatogenesis. Germline stem cells divide asymmetrically to produce spermatogonial cells that undergo four rounds of mitosis with incomplete cytokinesis to produce 16-cell cysts of primary spermatocytes. Connections formed between cells as a result of incomplete cytokinesis are represented by red circles. Primary spermatocytes undergo an extended period of dramatic growth and gene expression and then divide meiotically to produce four round spermatids. Centrosomes of spermatocytes and basal bodies of spermatids are shown in green. These immature spermatids elongate and differentiate to form mature sperm.

interconnected by cytoplasmic bridges and enclosed within the two cyst cells throughout spermatogenesis.

The 16 cells within a cyst then undergo premeiotic DNA replication followed by a prolonged G2 phase lasting up to 90 hours during which cell volume increases ~25-fold (Fuller, 1993). The primary spermatocytes then undergo meiosis I to yield 32-cell cysts of secondary spermatocytes. After a short-lived interphase II, the secondary spermatocytes undergo meiosis II to generate 64-cell cysts of haploid round spermatids.

Spermatids undergo a complex process of differentiation to develop into mature sperm (Fuller, 1993). In early stages of spermatid differentiation, the mitochondrial mass undergoes a very striking and unique transformation. Two giant mitochondrial aggregates form from the fusion of individual mitochondria within each spermatid, and these two aggregates form multiple layers that interleave with each other and are wrapped to form a densely packed phase-dark sphere called the Nebenkern. In the elongation step that follows, the spermatids undergo dramatic changes in cell shape. Within the growing sperm tail, the spherical mitochondrial derivative unfurls and elongates with the flagellar axoneme that extends from the basal body. At the end of the late stages of spermatid elongation and maturation, individualization takes place along the entire length of the spermatid bundle. During this process, excess cytoplasm is expelled, and the connections between the spermatids within a cyst are lost, thereby leading to the formation of individualized spermatozoa.

Centrioles are generally dispensable for mitosis, but spermatocytes that lack centrioles form highly abnormal meiotic spindles and fail to initiate cytokinesis (Basto et al., 2006; Bettencourt-Dias et al., 2005). Centrioles are also required to form the sperm

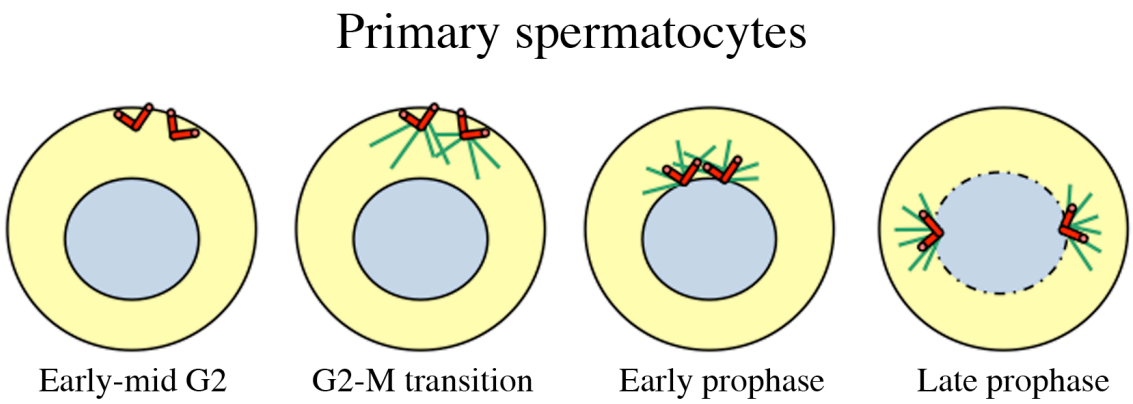

Figure 1.4. Centrosome movements in *Drosophila* primary spermatocytes. Centrosomes (red) associate with the cell cortex in early G2 spermatocytes. At this stage, one of the centrioles organizes a primary cilium of unknown function. The centrosomes nucleate astral microtubules (green) and detach from the cell cortex at the G2-M transition and are found attached to the nucleus (blue) in prophase spermatocytes. They then move along the nuclear envelope and separate to opposite poles by the end of prophase to initiate the formation of the meiotic spindle.

axoneme. In *Drosophila* male meiosis, centrosomes undergo dramatic changes in position similar to centrosome movements observed in the mitotic cell cycle of polarized epithelial cells (Fig. 1.4) (Reinsch and Karsenti, 1994). In primary spermatocytes, centrosomes migrate to the cortex at the end of S phase. By late G2, the centrosomes nucleate astral microtubules, and by early prophase, they dissociate from the cortex and attach to the nuclear surface. As reported for mitosis, this attachment may promote early meiotic events such as microtubule-induced nuclear envelope breakdown and chromosome capture by spindle microtubules (Beaudouin et al., 2002; Salina et al., 2002).

Regulation of Dynein in *Drosophila* Spermatogenesis

Dynein is essential for proper progression through *Drosophila* spermatogenesis (Anderson et al., 2009; Li et al., 2004). Dynein displays a dynamic localization throughout spermatogenesis: it is dispersed uniformly throughout the cytoplasm during early and mid-G2, and it becomes enriched on the nuclear surface by the end of G2. Dynein accumulates at the centrosomes at prophase of meiosis I and II and is enriched at the spindle poles from prometaphase through the completion of telophase. Dynein is additionally observed at the kinetochores during prometaphase. At the end of the meiotic divisions, dynein localizes in the form of a hemispherical cap on the nuclear surface of immature spermatids.

Perinuclear dynein is important for the proper movement of the centrosomes and their attachment to the nuclear membrane (Fuller, 1993; Reinsch and Gonczy, 1998). This anchored pool of dynein appears to promote stable attachment of nuclei and

centrosomes by mediating minus-end directed movement of nuclei along astral microtubules (Reinsch and Gonczy, 1998). Dynein mutation disrupts nucleus-centrosome attachments in *Drosophila* and *C. elegans* embryos (Gonczy et al., 1999; Robinson et al., 1999). The dynein-mediated interaction between the nucleus and centrosomes is important for a variety of biological processes such as nuclear-envelope breakdown, nuclear positioning, and nuclear migration (Beaudouin et al., 2002; Morris, 2000; Reinsch and Gonczy, 1998; Salina et al., 2002).

Our lab has previously identified the *Drosophila* gene *asunder* (*asun*) as a critical regulator of dynein-dynactin localization and nucleus-centrosome coupling during spermatogenesis (Anderson et al., 2009). The attachment between nucleus and centrosomes is lost in the majority of *asun* primary spermatocytes, resulting in a strong prophase arrest. The spermatocytes that escape this arrest exhibit defects in meiotic spindle assembly, chromosome segregation, and cytokinesis. Additionally, a loss of nucleus-basal body coupling was observed in *asun* spermatids.

asun late G2 spermatocytes and spermatids have reduced perinuclear localization of dynein-dynactin, the earliest defect that we have observed in *asun* testes (Anderson et al., 2009). Combined with our understanding of the cellular roles of dynein motors, we hypothesized that all of the subsequent phenotypes observed in *asun* testes are a direct result of the loss of the perinuclear localization of dynein. This hypothesis was further corroborated by the dominant enhancement of the *asun* phenotype by the loss of single gene copies of certain dynein and dynactin subunits (Anderson et al., 2009).

The role of LIS-1 during *Drosophila* spermatogenesis has not been previously characterized. In Chapter II, I will describe my work in determining the role played by

Drosophila LIS-1 in regulating the localization of dynein-dynactin during spermatogenesis by characterizing the spermatogenesis defects associated with a hypomorphic allele of *Lis-1*. I will further describe my proposed model for the regulation of dynein localization and nucleus-centrosome coupling by cooperation between *Lis-1* and *asun* during *Drosophila* spermatogenesis.

Drosophila **Oogenesis**

Drosophila oogenesis is a powerful model system for studying various aspects of cell and developmental biology. A typical ovary is made up of 16-18 independent "egg assembly lines" known as ovarioles (Bastock and St Johnston, 2008; Spradling, 1993). Each ovariole consists of a specialized anterior region, the germarium, and six to seven sequentially more mature egg chambers separated by interfollicular stalk cells (Spradling, 1993). Within the germarium, the germline stem cells undergo asymmetric cell divisions that give rise to cystoblasts (Fig. 1.5). The cystoblasts undergo 4 rounds of mitotic divisions with incomplete cytokinesis to produce 16-cell cysts of germline cells. One germline cell within each cyst is specified to develop into the oocyte while the other 15 germline cells develop into nurse cells. All the cells within a common cyst are interconnected by cytoplasmic bridges called ring canals. Two of the 16 cells within a cyst contain four ring canals; two cells contain three ring canals; four cells contain two ring canals; and the remaining eight cells have only one ring canal. The oocyte invariably develops from one of the two cells with four ring canals (de Cuevas et al., 1997). Individual egg chambers are formed when a cyst of germline cells separates from the

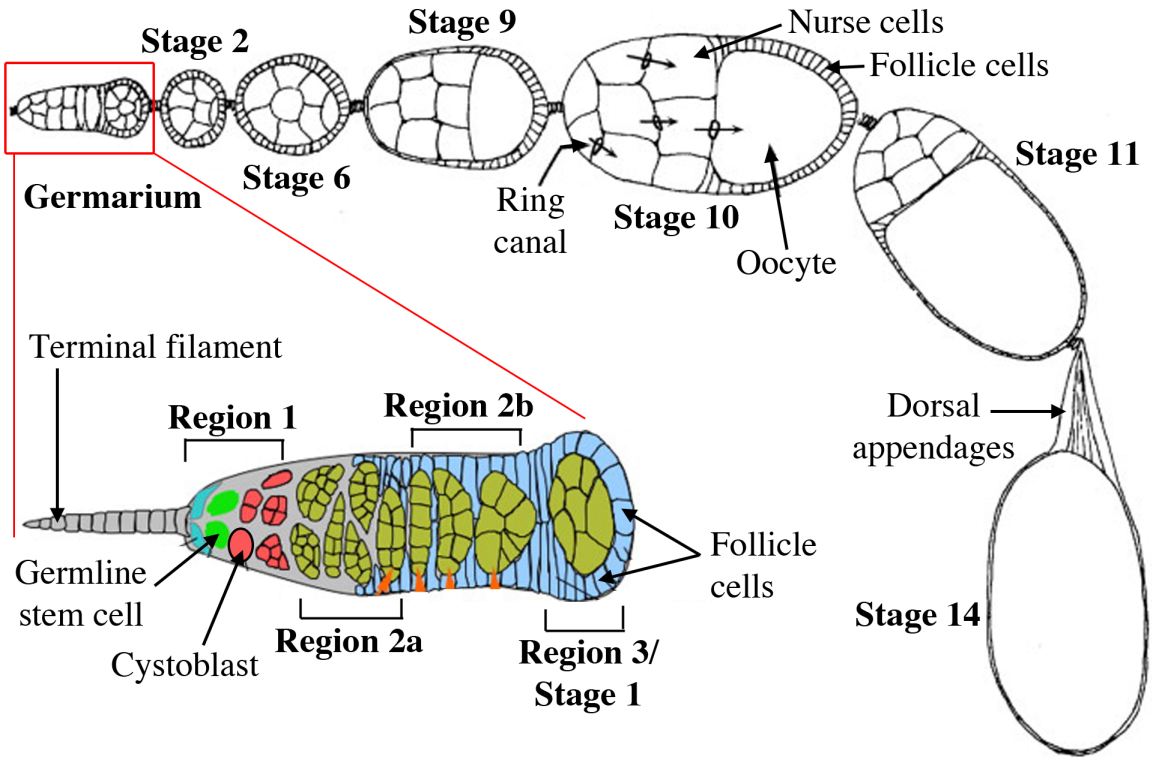

Figure 1.5. *Drosophila* oogenesis. Cartoon depicting the stages of *Drosophila* oogenesis. Within the germarium, germline stem cells (bright green) undergo asymmetric division to produce cystoblasts, which then divide mitotically four times with incomplete cytokinesis to produce 16-cell cysts. One of the 16 cells becomes specified to develop into the oocyte while the others form nurse cells. Each of the 16-cell cysts is enveloped by a single layer of follicle cells and detaches from the germarium to form an egg chamber. The development of the egg chambers into mature eggs is divided into 14 stages based on morphology. Adapted from (Ong and Tan, 2010; Roulier et al., 1998).

germarium, enveloped by a single layer of somatic follicle cells (Spradling, 1993). Wild-type egg chambers are always oriented with the oocyte located at the posterior pole.

The development of the egg chambers into mature eggs has been divided into 14 stages based on egg chamber morphology (Fig. 1.5) (Spradling, 1993). Stage 1 egg chambers are those formed immediately after separation from the germarium. These egg chambers gradually increase in size and undergo a wide variety of morphological changes. The final stage 14 egg chambers represent the mature eggs. By this stage, the oocyte comprises most of the volume of the egg chamber, and the nurse cells have degenerated. The development of a single germline stem cell to form a mature egg is a long process, taking roughly one week (Bastock and St Johnston, 2008).

The mature egg is a highly polarized structure. It is enveloped by the eggshell (or chorion), which is formed by the somatic follicle cells and characterized by several prominent features (Spradling, 1993). In the anterior of the chorion, a cone-shaped structure called the micropyle, which is formed by a group of 40-50 follicle cells, facilitates sperm entry prior to fertilization. Located in the dorsal-anterior region above the micropyle exist a pair of dorsal filaments (or appendages), each formed by a population of 150 follicle cells. The "paddle-shaped" distal region of each dorsal appendage supports gas exchange in eggs deposited under water. Found below the dorsal appendages is a structure known as the operculum, which serves as a larval "exit door" when the larva hatches from the egg.

Patterning Events during *Drosophila* Oogenesis

Determination of eggshell polarity depends on key patterning events that occur throughout *Drosophila* oogenesis (de Cuevas and Spradling, 1998; Lin and Spradling, 1995). The determination of the future oocyte is the earliest event that provides asymmetry to the developing 16-cell cyst. This event is thought to occur by the first mitotic division within the germarium as a result of the asymmetric localization and distribution of a germline-specific membranous organelle called the fusome.

As the descendants of a single germline cell continue to divide mitotically, the fusome grows and branches asymmetrically into each daughter cell. By the time a 16-cell cyst is completed, the oldest cell within the cyst from which the other 15 cells developed retains the largest amount of fusomal material, while younger cells contain proportionately less fusome (de Cuevas and Spradling, 1998). As the future oocyte always contains more fusome material than its 15 sibling cells, it is thought that the distribution of the fusome provides the initial signal for the determination of the oocyte (de Cuevas and Spradling, 1998; Grieder et al., 2000; Lin and Spradling, 1995). In the germarium, the fusome architecture also dictates the organization of the microtubules within the cysts. Nurse cell centrosomes migrate into the future oocyte in a fusome-dependent manner, thereby allowing a microtubule-organizing center (MTOC) to form in the posterior of the oocyte and adding another layer of asymmetry (Bolivar et al., 2001; Lin et al., 1994).

Microtubules originating from the MTOC in the posterior of the oocyte pass through cytoplasmic bridges into adjacent nurse cells and facilitate the transport of

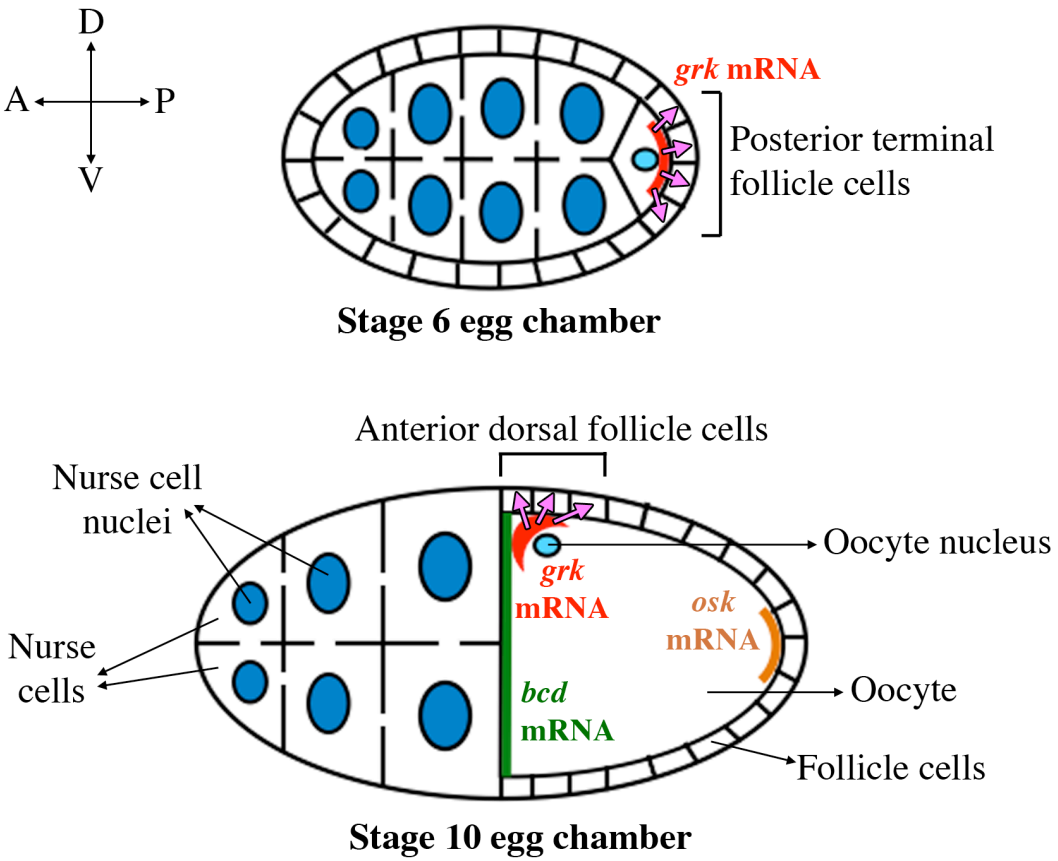

Figure 1.6. Localization of patterning factors during *Drosophila* oogenesis. In early-stage egg chambers, *grk* mRNA (red) and the oocyte nucleus (light blue) are both localized to the posterior of the oocyte. Grk signals to the posterior follicle cells (pink arrows) and initiates a signaling cascade. As a result of this signaling cascade, in late-stage egg chambers, the anterior-posterior axis of the future embryo is established by localization of *osk* mRNA (orange) to the posterior of the oocyte and *bcd* mRNA (green) to the anterior of the oocyte. *grk* mRNA (red) and the oocyte nucleus (light blue) become localized to the anterior-dorsal region of the oocyte where Grk signals to the anterior-dorsal follicle cells (pink arrows) to initiate a signaling cascade to establish the dorsal-ventral axis of the future embryo. Dorsal is to the top; anterior is to the left.

maternal mRNAs and proteins from the nurse cells into the oocyte (Pokrywka and Stephenson, 1991; Theurkauf et al., 1992). The transport of key maternal mRNAs into the oocyte and their asymmetric localization within the oocyte is critical for proper polarization of the embryo (Becalska and Gavis, 2009). In particular, proper localization of *oskar* (*osk*) and *nanos* (*nos*) trancripts (to the posterior pole), *bicoid* (*bcd*) transcripts (to the anterior pole), and *gurken* (*grk*) transcripts (to the posterior initially and later to the anterior-dorsal region of the oocyte) is critical for proper establishment of the embryonic body axes (Fig. 1.6). *grk* mRNA is most critical as it is required in early egg chambers for the initiation of anterior-posterior patterning and in late stage egg chambers for the initiation of dorsal-ventral patterning.

Within the oocyte, in addition to the asymmetric localization of various mRNAs and proteins, the oocyte nucleus also exhibits dynamic localization. In early egg chambers, the oocyte nucleus is observed at the posterior of the oocyte with the MTOC located between the oocyte nucleus and the posterior pole of the oocyte. In stage 7 egg chambers, the posterior follicle cells produce an unknown signal that induces the microtubules nucleated by the MTOC to exert a force on the oocyte nucleus, thereby pushing it to the anterior-dorsal region of the oocyte (Zhao et al., 2012). This asymmetric positioning of the oocyte nucleus breaks the radial symmetry of the oocyte and, in conjunction with the anterior-dorsal localization of the *grk* mRNA, plays an important role in dorsal-ventral axis formation (Gonzalez-Reyes et al., 1995; Roth et al., 1995).

Regulation of Dynein in *Drosophila* Oogenesis

Dynein is essential for proper progression through oogenesis, and its localization is therefore strictly regulated. Similar to spermatogenesis, dynein exhibits dynamic changes in localization during oogenesis, and these changes correspond with specific stages of egg chambers. In the earliest stages of oogenesis, dynein first accumulates within the oocyte in germarium region 2b and remains within the oocyte throughout oogenesis (Li et al., 1994). Dynein begins to accumulate on the surface of the oocyte nucleus in newly formed egg chambers and remains enriched there in early to mid-stage egg chambers. When egg chambers reach stage 9 of oogenesis, the enrichment of dynein on the oocyte nuclear surface is lost, and dynein localizes to the posterior pole of the oocyte. Identical to its role in spermatogenesis, LIS-1 is required for the proper localization of dynein during *Drosophila* oogenesis (Swan et al., 1999).

Dynein is critical for proper patterning at various stages of oogenesis. Within the germarium, dynein has been shown to be required for maintaining the integrity of the fusome, as mutation of the dynein heavy chain results in the formation of a fusome with a highly fragmented architecture (Bolivar et al., 2001). As a consequence of the aberrant fusome formation, dynein mutants also exhibit defects in oocyte determination and centrosome migration (Bolivar et al., 2001; de Cuevas and Spradling, 1998; Lin and Spradling, 1995; McGrail and Hays, 1997; McKearin, 1997; Mische et al., 2008; Swan et al., 1999).

Dynein plays a major role in the transport of various mRNAs from the nurse cells into the oocyte (Becalska and Gavis, 2009; Clark et al., 2007; Mische et al., 2007). Additionally, after the establishment of the microtubule organizing center and formation

of a microtubule network within the oocyte, both families of microtubule motors, dynein and kinesin, are critical for the transport of certain mRNAs by mediating their movement along the microtubules to their specific sites within the oocyte (Becalska and Gavis, 2009; Duncan and Warrior, 2002; Januschke et al., 2002). The localization of the *osk* mRNA to the posterior pole is thought to be primarily dependent on the microtubule plus-end-directed kinesin-1, and the localization of the *bcd* mRNA to the anterior pole is thought to be primarily dynein-dependent (Becalska and Gavis, 2009; Brendza et al., 2000; Cha et al., 2001; Duncan and Warrior, 2002; Januschke et al., 2002; Zimyanin et al., 2008). Localization of *grk* mRNA, which is required for the formation of both major axes, is also dependent on dynein (MacDougall et al., 2003; Rom et al., 2007; Swan et al., 1999). Dynein is also required for maintenance of the anterior-dorsal position of the oocyte nucleus in stage 10 egg chambers (Bolivar et al., 2001; Januschke et al., 2002; Lei and Warrior, 2000; McGrail and Hays, 1997; Schnorrer et al., 2000; Swan et al., 1999; Zhao et al., 2012). It is therefore clear that dynein plays a major role in the transport of molecules and structures to facilitate proper dorsal-ventral axis formation.

As mentioned earlier, *asun* is a critical regulator of dynein during *Drosophila* spermatogenesis (Anderson et al., 2009). ASUN has also been previously identified as an *in vitro* substrate of PNG kinase (Lee et al., 2005). *pan gu* (*png*) encodes a serine/threonine protein kinase expressed exclusively in the female germ line of *Drosophila* and maternally deposited within the egg (Fenger et al., 2000; Lee et al., 2005). *png* was identified to be a critical regulator of the syncytial cell cycles of early embryogenesis in *Drosophila* (Shamanski and Orr-Weaver, 1991). Northern blot analysis of *Drosophila* tissues revealed that *asun* transcripts, while detected in the testes, are

present at much higher levels in ovaries and early embryos, suggesting that *asun* may play roles in oogenesis and/or embryogenesis (Stebbings et al., 1998). We were unable, however, to detect any significant defects in oogenesis or early embryogenesis in females homozygous for the *f02815* allele of *asun*, the allele used in characterizing the male germline defects associated with mutation of *asun* (Anderson et al., 2009). We attributed the lack of defects in $asun^{f02815}$ females to the hypomorphic nature of the *f02815* allele.

In Chapter III, I will describe my work in determining the role played by *Drosophila* ASUN in regulating dynein localization and function during oogenesis by characterizing females homozygous for a null allele of *asun* ($asun^{d93}$), thereby demonstrating that ASUN plays a conserved role in regulating the localization of dynein in *Drosophila* gametogenesis. Additionally, in Chapter IV, I will describe my preliminary results from a dominant enhancement screen to identify potential interactors of *asun*.

CHAPTER II

REGULATION OF DYNEIN LOCALIZATION AND CENTROSOME POSITIONING BY *Lis-1* AND *asunder* DURING *DROSOPHILA* SPERMATOGENESIS

The contents of this chapter have been published (Sitaram et al., 2012)

Introduction

Dynein is a minus-end-directed microtubule motor that exists in two forms. Axonemal dynein promotes microtubule sliding for beating of cilia and flagella. Cytoplasmic dynein moves processively along microtubules and, in addition to organelle positioning and transport, plays key roles in cell cycle events, including nucleus-centrosome coupling, nuclear envelope breakdown, spindle assembly/positioning, and chromosome segregation (Gusnowski and Srayko, 2011; Hebbar et al., 2008; Huang et al., 2011; Salina et al., 2002; Splinter et al., 2010; Stuchell-Brereton et al., 2011; Wainman et al., 2009). Dynein is a large complex composed of four subunit types: heavy (containing motor activity), light, intermediate, and light intermediate chains (Hook and Vallee, 2006; Susalka and Pfister, 2000).

Dynactin and LIS1 are dynein accessory factors (King and Schroer, 2000; Mesngon et al., 2006). LIS1 directly binds several dynein and dynactin subunits through its C-terminal WD-repeat domain, and LIS1 binding enhances dynein motor activity (Faulkner et al., 2000; Mesngon et al., 2006; Sasaki et al., 2000; Smith et al., 2000; Tai et al., 2002). The importance of LIS1 for dynein function is evidenced by the fact that *LIS1*

mutants have defects in many dynein-dependent processes (Faulkner et al., 2000; Hebbar et al., 2008; Li et al., 2005; Tai et al., 2002).

Loss or mutation of one copy of human *LIS1* causes type I lissencephaly ("smooth brain"), a brain malformation disorder associated with neuronal migration defects (Gambello et al., 2003; Hirotsune et al., 1998; Vallee and Tsai, 2006; Wynshaw-Boris, 2007). Neuronal migration requires proper migration and positioning of the nucleus (Malone et al., 2003; Tanaka et al., 2004; Tsai and Gleeson, 2005). Dynein plays a major role in regulating these processes by promoting interaction of the nucleus with microtubules and microtubule organizing centers.

The *Drosophila* homolog of human *Lis1* plays key roles during neurogenesis and oogenesis, presumably via its regulation of dynein. *Drosophila Lis-1* neuroblasts have defects in centrosome migration, bipolar spindle assembly, centrosomal attachment to spindles, and spindle checkpoint function (Siller and Doe, 2008; Siller et al., 2005). In *Drosophila* oocytes, *Lis-1* regulates nuclear migration and positioning (Lei and Warrior, 2000). A detailed characterization of the role of *Lis-1* in *Drosophila* spermatogenesis, however, has not been reported.

Drosophila spermatogenesis is an ideal system for studying cell division. Meiotic spindles of spermatocytes are large and hence convenient for cytological analysis, relaxed checkpoints facilitate the study of cell cycle mutants, and alterations in the highly regular appearance of immature spermatids are diagnostic of meiotic division defects (Cenci et al., 1994; Rebollo and Gonzalez, 2000). The stages of *Drosophila* spermatogenesis are well defined (Fuller, 1993). Germline stem cells give rise to spermatogonia, which undergo four synchronous mitotic divisions with incomplete cytokinesis to generate 16-

cell cysts of primary spermatocytes. After premeiotic S phase, primary spermatocytes enter G2, a prolonged growth period. Meiosis I yields 32-cell cysts of secondary spermatocytes, and meiosis II generates 64-cell cysts of haploid spermatids. Immature, round spermatids differentiate into mature sperm. A unique feature of spermatids in *Drosophila* and other insects involves formation of a multi-layered mitochondrial aggregate, the Nebenkern, which provides energy for beating of the sperm flagella.

We previously identified *asun* as a regulator of dynein-dynactin localization during *Drosophila* spermatogenesis (Anderson et al., 2009). *asun* spermatocytes and spermatids show defects in nucleus-centrosome and nucleus-basal body coupling, respectively. Dynein mutation disrupts nucleus-centrosome attachments in *Drosophila* and *C. elegans* embryos (Gonczy et al., 1999; Robinson et al., 1999). A pool of dynein anchored at the nuclear surface is thought to promote stable interactions between the nucleus and centrosomes by mediating minus-end directed movement of the nucleus along astral microtubules (Reinsch and Gonczy, 1998). We observed reduction of perinuclear dynein in *asun* male germ cells that we hypothesize causes loss of nucleus-centrosome and nucleus-basal body coupling (Anderson et al., 2009).

Drosophila Lis-1 was previously reported to be required for male fertility, although its role in the male germ line has not been further characterized (Lei and Warrior, 2000). In this study, we have analyzed the role of *Lis-1* during *Drosophila* spermatogenesis. We found that *Lis-1* regulates centrosome positioning in spermatocytes and promotes attachments between the nucleus, basal body, and Nebenkern in spermatids. LIS-1 colocalizes with dynein-dynactin at the nuclear surface and spindle poles of male germ cells and is required for recruiting dynein-dynactin to these sites. We

provide evidence to support our model that *Lis-1* and *asun* cooperate to regulate dynein localization and centrosome positioning during *Drosophila* spermatogenesis.

Materials and Methods

Drosophila stocks

y w was used as "wild-type" stock. Transgenic flies expressing β1-tubulin (product of *βTub56D* gene) fused at its C-terminal end to GFP and under control of the *Ubi-p63E* (ubiquitin) gene promoter were a gift from H. Oda and Y. Akiyama-Oda (JT Biohistory Research Hall, Osaka, Japan). Transgenic flies expressing GFP-PACT and DMN-GFP were gifts from J. Raff (University of Oxford, Oxford, UK) and T. Hays (University of Minnesota, Minneapolis, MN), respectively. Transgenic flies expressing GFP-ASUN were previously described (Anderson et al., 2009). *tctex-1*^{e155} was a gift from T. Hays. *piggyBac* insertion lines *asun*^{f02815} and *f01662* were from the Exelixis Collection (Harvard Medical School, Boston, MA). *Lis-1*^{k11702}, *Df(2R)JP5*, *Df(3R)Exel6178*, and *piggyBac* transposase were from Bloomington Stock Center (Indiana University, IN).

Cherry-LIS-1 transgenic fly lines

cDNA encoding *Drosophila* LIS-1 (clone LD11219, *Drosophila* Gene Collection) with an N-terminal Cherry tag was subcloned into vector tv3 (gift from J. Brill, The Hospital for Sick Children, Toronto, Canada) for expression of Cherry-LIS-1 under control of the testes-specific *β2-Tubulin* promoter (Wong et al., 2005). Transgenic lines

were generated by *P*-element-mediated transformation via embryo injection (Rubin and Spradling, 1982).

Generation of a null allele of *asun*

piggyBac insertion lines $asun^{f02815}$ and *f01662* were used to generate a two-gene (*belphegor* (*bor*) and *asun*) deletion line via FLP-mediated recombination of FRT sites in the transposons as previously described (Parks et al., 2004). A 4-kb genomic fragment containing *bor* and flanking regions (Fig. S9) was PCR-amplified from BAC clone BACR05P04 (*Drosophila* Genomics Resource Center, Indiana University, IN) and subcloned into pCaSpeR4. A stop codon was added to 5' *asun* coding region, and a transgenic line was made using this construct. $asun^{d93}$ flies are homozygous for the *bor asun* two-gene deletion and *bor* transgene.

Male fertility assay

Individual males (two days old) were placed in vials with five wild-type females (two days old) and allowed to mate for five days. The mean number of adult progeny eclosed per vial was determined (25 males tested per genotype).

Cytological analysis of live and fixed testes

Live and fixed testes cells were prepared for phase contrast or fluorescent microscopy as described (Anderson et al., 2009). Acetylated tubulin antibodies (6-11B-1, 1:50, Sigma-Aldrich) were also used herein. Wild-type and mutant testes were isolated and prepared for microscopy in parallel and under identical conditions for all

experiments. Our designation of "late G2" and "prophase" primary spermatocytes corresponds to S5/S6 and M1a spermatocytes, respectively, in the staging system of Cenci et al (1994). We used four criteria to score primary spermatocytes as being in prophase: 1) well-separated centrosomes, 2) initiation of chromatin condensation (as evidenced by DAPI staining), 3) the presence of robust arrays of microtubules surrounding centrosomes (visualized by using the beta1-tubulin-GFP transgene), and 4) lack of appreciable nuclear envelope breakdown (as evidenced by clear demarcation between nucleus and cytoplasm when viewing beta1-tubulin-GFP in the cytoplasm) (Fuller, 1993; Rebollo et al., 2004). Confocal images were obtained with a Leica TCS SP5 confocal microscope and Leica Application Suite Advanced Fluorescence (LAS-AF) software using maximum-intensity projections of Z-stacks collected at 0.75 μm/step with a 63X objective.

Immunoblotting

Homogenized testes extracts from newly eclosed flies were analyzed by SDS-PAGE (four testes pairs/lane) and immunoblotting using standard techniques. Primary antibodies were used as follows: dynein heavy chain (P1H4, 1:2000), dynein intermediate chain 1 (74.1, 1:1000, Santa Cruz), Dynamitin (1:250, BD Biosciences or ab56687, 1:1000, Abcam), mCherry (1:500, Clontech), beta-tubulin (E7, 1:1000, Developmental Studies Hybridoma Bank), Cdk1 (PSTAIR, 1:1000, Upstate), and GAPDH (14C10, 1:1000, Cell Signaling). HRP-conjugated secondary antibodies and chemiluminescence were used to detect primary antibodies.

Mammalian cell experiments

HeLa cells were maintained and transfected as described (Anderson et al., 2009). Plasmids for expression of N-terminally tagged versions of *Drosophila* ASUN and/or LIS-1 in cultured human cells were generated by subcloning into pCS2. For colocalization, HeLa cells were transfected with Cherry-LIS-1 and GFP-ASUN constructs using Lipofectamine 2000 (Invitrogen), treated with nocodazole (5 μg/ml) at 24 hr, fixed 5 min at –20˚C with methanol, and mounted in ProLong Gold Antifade Reagent with DAPI (Invitrogen). Images were obtained using an Eclipse 80i microscope (Nikon) with Plano-Apo 100X objective. For coimmunoprecipitation, lysates of transfected HEK293 cells coexpressing HA-ASUN with c-Myc tag or c-Myc-tagged *Drosophila* LIS-1 were made in non-denaturing lysis buffer (50 mM Tris-Cl pH 7.4, 300 mM NaCl, 5 mM EDTA, 1% Triton X-100). Lysates (500 μg) were incubated with anti-c-Myc agarose beads (40 μl; Sigma) for 3 hours with shaking at 4˚C. Beads were washed 3X in lysis buffer and boiled in 6X sample buffer. Samples were analyzed by SDS-PAGE and immunoblotting with c-Myc (9E10, 1:1000) and HA (CAS 12, 1:1000) antibodies.

Results

***Lis-1* is required for spermatogenesis**

To analyze the role of *Lis-1* in *Drosophila* spermatogenesis, we obtained a male-sterile allele, *Lis-1*^{k11702}, with a *P*-element insertion in the 5'-UTR of *Lis-1* (Fig. 2.1A) (Lei and Warrior, 2000). We found that homozygous and hemizygous *Lis-1*^{k11702} males uniformly failed to produce any progeny (Fig. 2.1B). Fertility of *Lis-1*^{k11702} males was

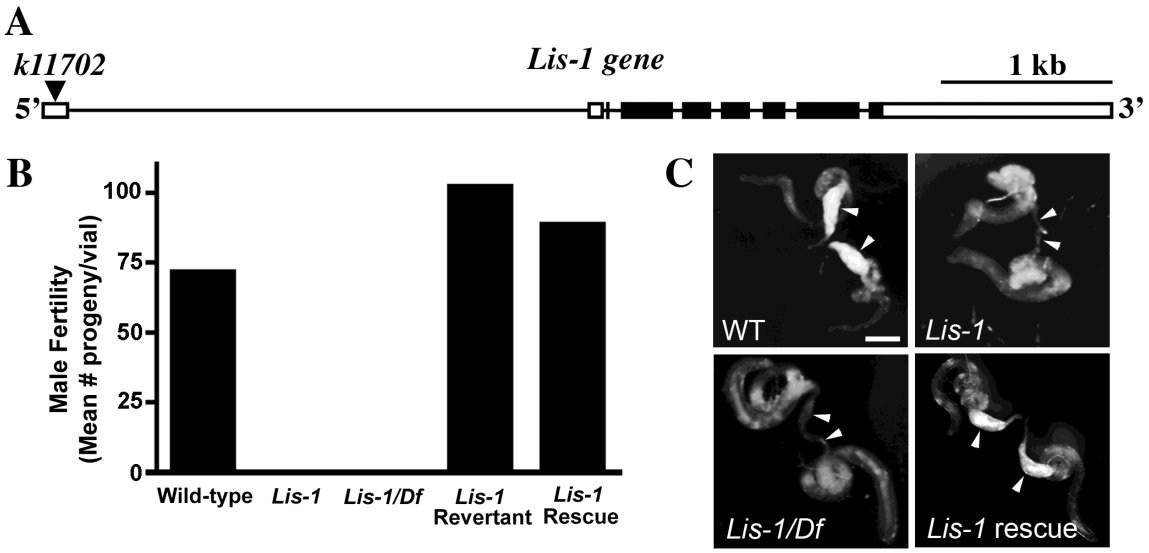

Figure 2.1. *Lis-1*^{k11702} males are sterile. (A) *Lis-1* gene structure. Coding regions and UTRs are represented as filled and unfilled boxes, respectively, introns as thin lines, and transposon *k11702* as a triangle. For simplicity, only one splice variant (transcript RA; www.flybase.org) is shown. (B) Bar graph of male fertility. *Lis-1*^{k11702} male sterility is fully reversed by precise *P*-element excision ("revertant") or by transgenic rescue. (C) Testes and seminal vesicles dissected from males withheld from females for six days. Seminal vesicles of wild-type males are engorged with mature sperm, whereas flaccid seminal vesicles of *Lis-1* males indicate failed spermatogenesis that is reversed by transgenic rescue. Arrowheads, seminal vesicles. Bar, 250 μm. *Df(2R)JP5* ("*Df*") and a transgenic line expressing Cherry-LIS-1 in male germ cells were used in B and C.

fully restored via transgenic expression of Cherry-tagged LIS-1 in male germ cells or by precise *P*-element excision; the former fully rescued all other *Lis-1*^{k11702} phenotypes presented herein (Fig. 2.1B; data not shown). To assess mature sperm production, we examined *Lis-1*^{k11702} seminal vesicles (Fig. 2.1C). Although the size and shape of *Lis-1*^{k11702} testes appeared normal, seminal vesicles were empty, suggesting that *Lis-1*^{k11702} male sterility results from disruption of spermatogenesis.

Lis-1 spermatocytes have abnormal centrosome positioning and meiotic spindle formation

We sought to determine the earliest stage at which spermatogenesis is disrupted in *Lis-1*^{k11702} testes. As in wild-type, we observed 16-cell cysts of primary spermatocytes in *Lis-1*^{k11702} testes (26/26 cysts scored), indicating successful completion of four rounds of spermatogonial divisions. *Lis-1*^{k11702} spermatocytes, however, exhibited profound defects in centrosome positioning and meiotic spindle structure.

During the G2 growth phase of wild-type primary spermatocytes, centrosomes are anchored at the cell cortex; at G2/M, centrosomes migrate back toward the nucleus and begin to separate from each other (Fuller, 1993; Rebollo et al., 2004). Once reattached to the nuclear surface, centrosomes move to opposite poles during prophase. ~90% of *Lis-1*^{k11702} prophase spermatocytes had centrosomes positioned at the cortex rather than the nuclear surface, presumably due to failure to break their cortical associations; wild-type cells rarely (<0.5%) showed this configuration (Figs 2.2A-M, 2.3). Cortical centrosomes of *Lis-1*^{k11702} prophase spermatocytes appeared to separate normally and undergo migration to opposite poles. >10% of *Lis-1*^{k11702} prophase spermatocytes had free

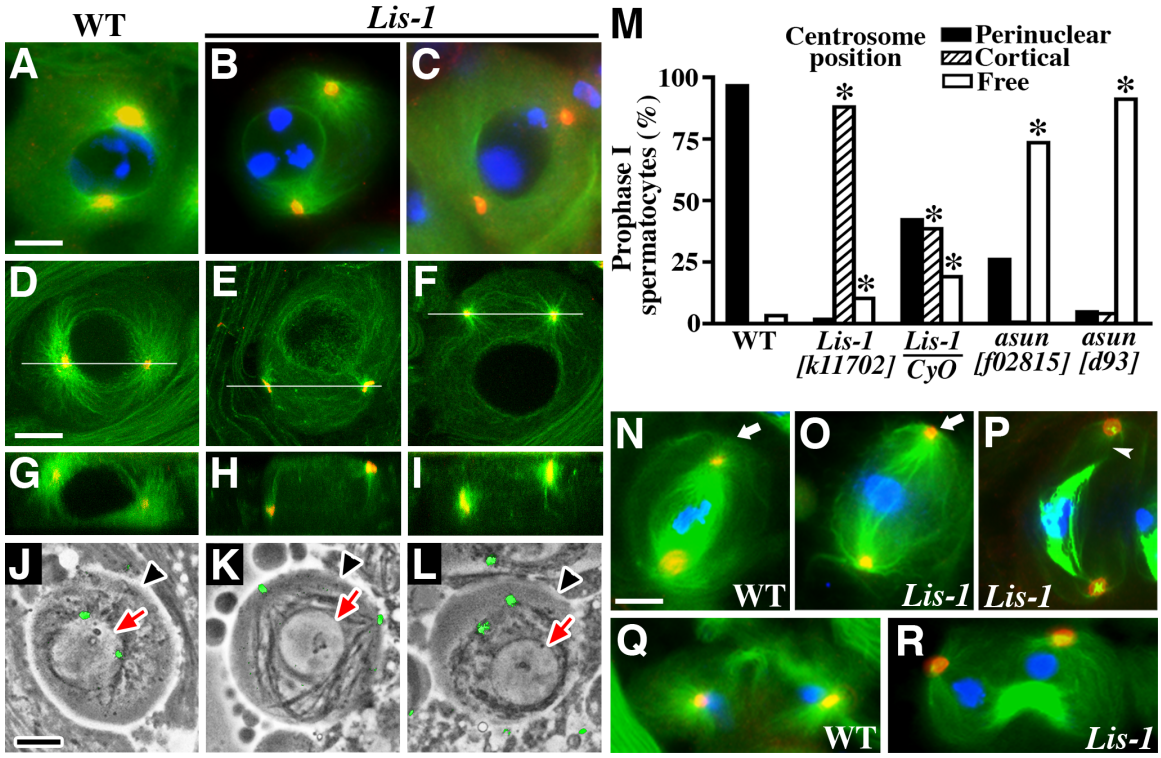

Figure 2.2. Defective centrosome positioning in *Lis-1* spermatocytes. (A-L) Centrosomes normally at the nuclear surface (A,D,G,J) are cortical (B,E,H,K) or free (C,F,I,L) in *Lis-1*^{k11702} prophase I spermatocytes. (A-I) Spermatocytes expressing β-tubulin-GFP (green) stained for γ-tubulin (red; centrosome marker). (A-C) Epifluorescent micrographs. DNA in blue. (D-I) XY projections (D-F) and corresponding XZ optical sections (G-I). White bars mark positions of corresponding XZ optical sections. (J-L) Phase/fluorescence overlay images of spermatocytes expressing GFP-PACT (green; centriole marker). Red arrows and black arrowheads mark the surface of the nucleus (phase-light) and plasma membrane, respectively, of each cell. (M) Quantification of centrosome positioning defects in *Lis-1* and *asun* prophase I spermatocytes expressing β-tubulin-GFP and stained for γ-tubulin (>100 cells scored per genotype). Asterisks, $p<0.0001$ (Fisher's exact test). (N-R) Centrosomes of metaphase (N-P) and telophase (Q,R) spindles are at the cortex (arrows) and often detached (arrowhead) in *Lis-1*^{k11702} but not wild-type spermatocytes. Bars, 10 μm.

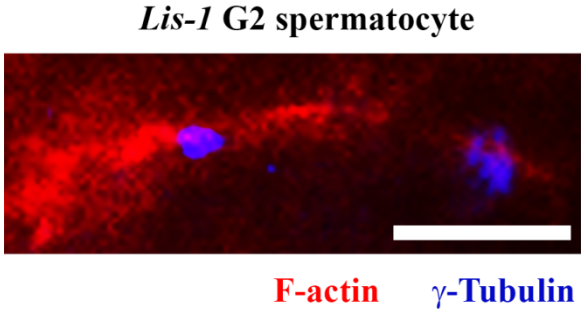

Figure 2.3. Cortical centrosomes in *Lis-1* spermatocytes. *Lis-1*^{k11702} prophase I spermatocyte stained for F-actin to mark the cortex (phalloidin; red) and γ-tubulin (blue) to mark centrosomes. Centrosomes that normally migrate to the nuclear surface at meiotic entry remain close to the cortex in *Lis-1*^{k11702} prophase I spermatocytes. Bars, 10 μm.

centrosomes (unattached to the cortex or nuclear surface) similar to those of *asun* mutants, a phenotype observed in ~3% of wild-type cells (Anderson et al., 2009). ~60% of prophase spermatocytes heterozygous for *Lis-1*^{k11702} had either cortical or free centrosomes.

In dividing *Lis-1*^{k11702} spermatocytes, meiotic spindles were typically associated with cortically positioned centrosomes (~95% vs. <2% for wild-type during metaphase; Fig. 2.2N-R). These observations suggest that cortical centrosomes present in *Lis-1* prophase I spermatocytes assemble meiotic spindles, although we have not excluded the possibility that spindles form normally in the mutants followed by pushing of centrosomes to the cortex during spindle elongation. *Lis-1*^{k11702} spindles were relatively long and wavy with occasional detachment of cortical centrosomes from spindle poles; centrosomal detachment from mitotic spindle poles has similarly been reported for *Lis-1* neuroblasts and early embryos (Robinson et al., 1999; Siller et al., 2005; Wojcik et al., 2001). Despite defects in centrosome positioning and meiotic spindle structure, cytokinesis and chromosome segregation surprisingly did not appear to be grossly affected in *Lis-1*^{k11702} spermatocytes, as most round spermatids contained a single nucleus of uniform size (99%; 612/619 spermatids) (Fuller, 1993).

We previously reported that *asun* is required for centrosome positioning in *Drosophila* spermatocytes (Anderson et al., 2009). Most *asun*^{f02815} spermatocytes arrest in prophase I with free centrosomes. We did not, however, find an increased fraction of *Lis-1*^{k11702} spermatocytes in prophase (Fig. 2.4). Microtubules on the nuclear surface have been implicated in nuclear envelope breakdown at prophase exit (Beaudouin et al., 2002; Salina et al., 2002). We found an accumulation of microtubules (both total and

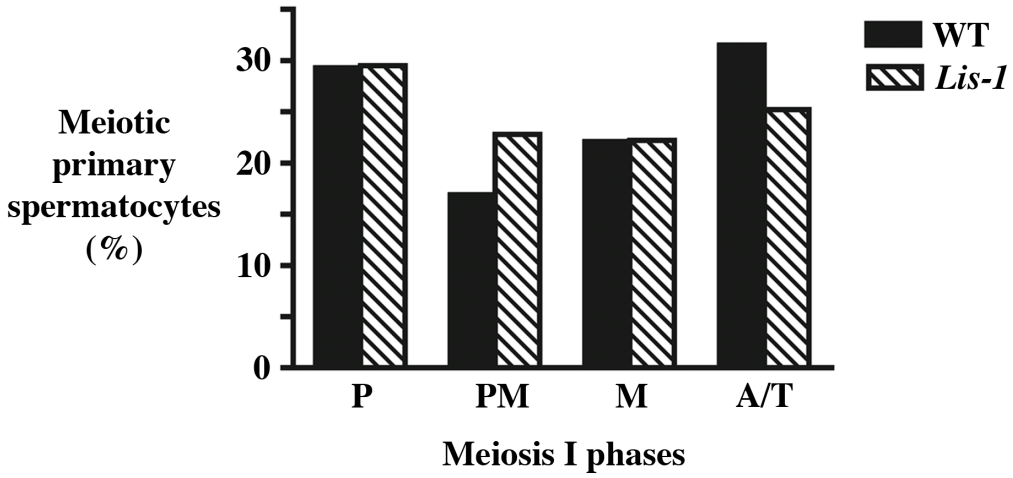

Figure 2.4. Staging of meiotic spermatocytes in *Lis-1* testes. Bar graph shows percentages of primary spermatocytes in prophase (P), prometaphase (PM), metaphase (M), or anaphase/telophase (A/T) from *Lis-1*^{k11702} versus wild-type testes. >350 spermatocytes were scored per genotype.

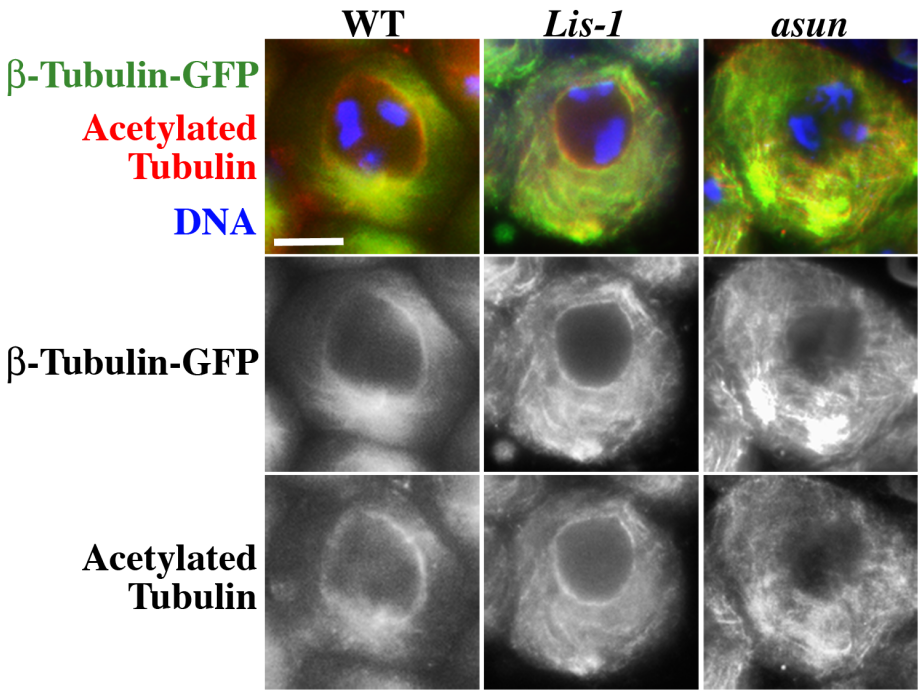

Figure 2.5. Normal pattern of microtubules on the nuclear surface of *Lis-1*, but not *asun*, spermatocytes. Prophase I spermatocytes expressing β-tubulin-GFP (green) stained for DNA (blue) and acetylated tubulin (red). Microtubules (both total and acetylated) observed on the nuclear surface of wild-type and *Lis-1*^{k11702} cells are absent from *asun*^{f02815} cells. Bar, 10 μm.

acetylated) surrounding the nucleus of wild-type and *Lis-1*^{k11702} prophase spermatocytes that was absent in *asun*^{f02815} mutants (Fig. 2.5); this difference may explain the prophase arrest observed in *asun*^{f02815}, but not *Lis-1*^{k11702}, mutants.

Lis-1 spermatids lack nucleus-Nebenkern-basal body attachments and have abnormal Nebenkern morphology

Wild-type round spermatids contain a phase-light nucleus and a phase-dark mitochondrial aggregate (Nebenkern) of roughly equal size; both organelles associate with a centriole-derived basal body at the site of nucleus-Nebenkern linkage (Fig. 2.6A) (Fuller, 1993). Given the lack of nucleus-centrosome attachments in *Lis-1* spermatocytes (Fig. 2.2), we assessed nucleus-basal body attachments in *Lis-1* spermatids using male germline expression of GFP-tagged Pericentrin/AKAP450 centrosomal targeting (PACT) domain to label basal bodies (Martinez-Campos et al., 2004). We observed nucleus-basal body uncoupling in most *Lis-1*^{k11702} hemizygous spermatids (Fig. 2.6B-D). Furthermore, we frequently observed loss of Nebenkern-basal body and nucleus-Nebenkern attachments in *Lis-1*^{k11702} hemizygous spermatids (Fig. 2.6B-D). These results suggest that LIS-1 is required to maintain normal linkages between the nucleus, Nebenkern, and basal body during spermatogenesis. Nebenkerne of wild-type spermatids typically have a round, uniform shape (Fig. 2.6E). In *Lis-1*^{k11702} spermatids, however, we occasionally observed Nebenkerne with abnormal morphology (Fig. 2.6F-H). These findings suggest that LIS-1 plays a role in Nebenkern formation and/or maintenance.

During spermatid elongation, the Nebenkern unfurls and elongates with the growing axoneme (Fuller, 1993). Because the basal body nucleates the axoneme, we

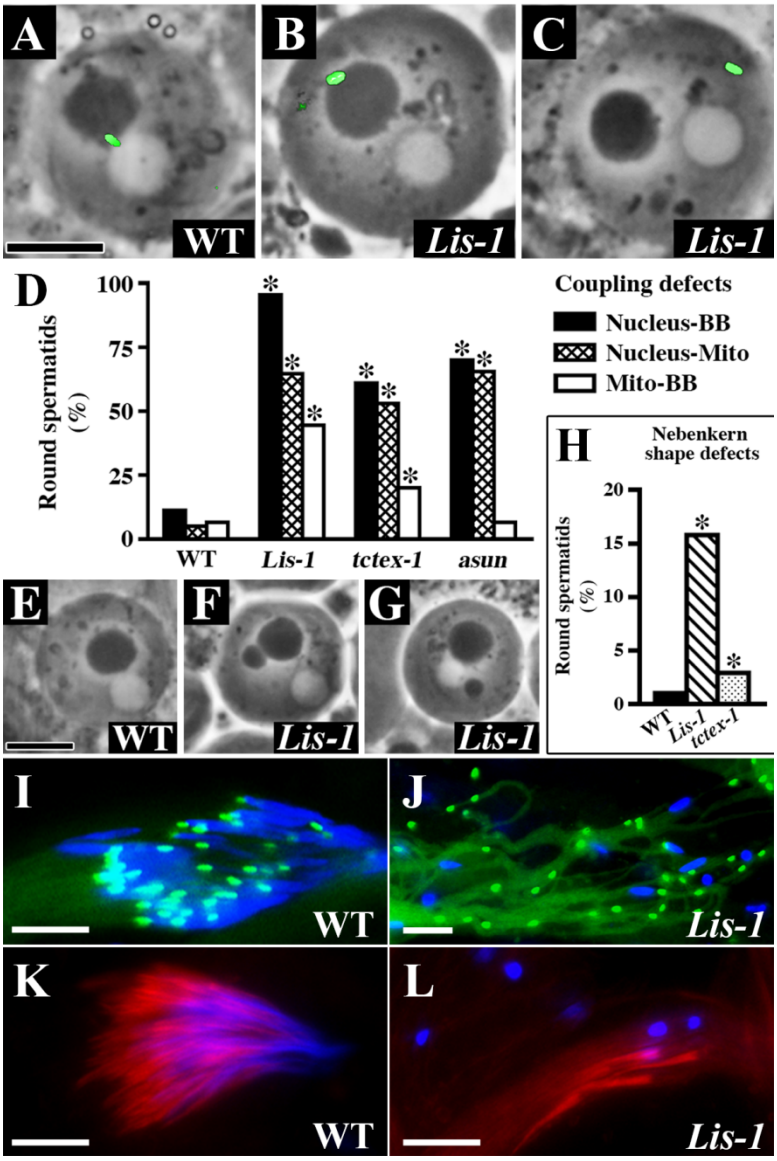

Figure 2.6. *Lis-1* spermatid defects. (A-C) Phase/fluorescence overlay images of round spermatids expressing GFP-PACT (green). Normal associations between the nucleus (phase-light), Nebenkern (phase-dark), and basal body (green) are lost in *Lis-1*^{k11702} spermatids. (D) Quantification of coupling defects in *Lis-1*, *tctex-1*, and *asun* round spermatids observed in phase/fluorescence overlay micrographs. A given spermatid may have been scored as defective in more than one category (loss of nucleus-basal body (BB), nucleus-Nebenkern (Mito), and/or Nebenkern-basal body coupling). (E-G) Phase-contrast images reveal abnormal Nebenkern morphology in *Lis-1*^{k11702} round spermatids. (H) Quantification of Nebenkern morphology defects in *Lis-1* and *tctex-1* spermatids. (I-L) Elongating bundles of spermatids expressing GFP-PACT (green; I,J) or stained with phalloidin (red; marks individualization cones; K,L). DNA in blue. *Lis-1*^{k11702} bundles are disorganized compared to wild-type. Bars, 10 μm. Genotypes used for graphs: *Lis-1*^{k11702}*/Df(2R)JP5*, *tctex-1*^{e155}*/Df(3R)Exel6178*, *asun*^{f02815}*/asun*^{d93} (>500 spermatids scored per genotype). Asterisks, $p<0.0001$ (Fisher's exact test).

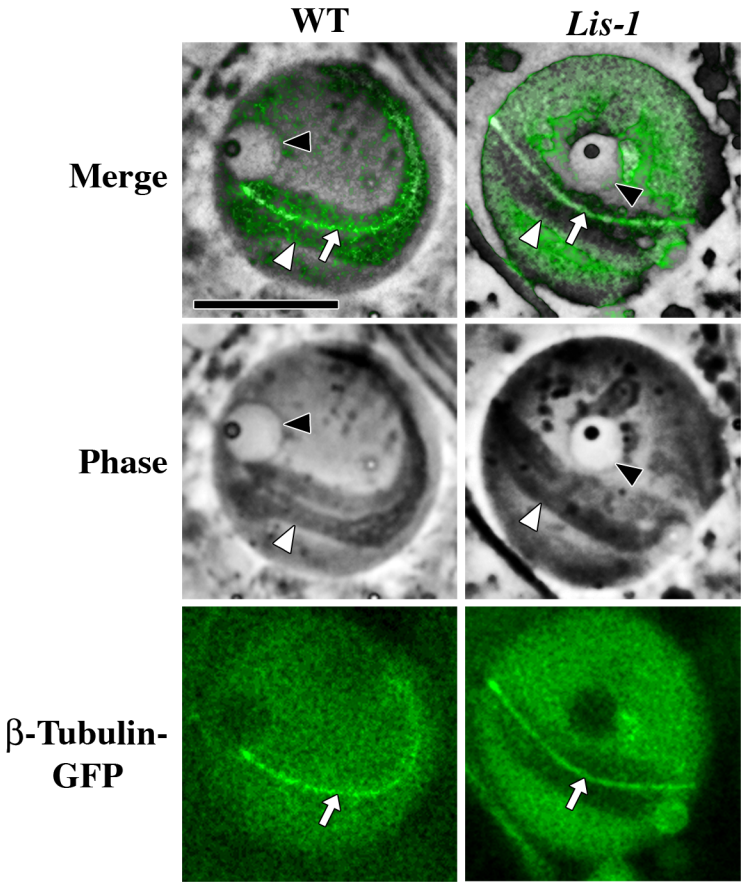

Figure 2.7. Mitochondria associate normally with sperm tails in elongating spermatids of *Lis-1* testes. Overlaid images (fluorescence on phase-contrast) of elongating spermatids expressing β-tubulin-GFP (green). In wild-type spermatids, mitochondria (white arrowhead) unravel and elongate alongside the axoneme (arrow), which is nucleated by the basal body. *Lis-1*^{k11702} spermatids show normal association between mitochondria and the axoneme despite uncoupling of the basal body and nucleus (black arrowhead). Bar, 10 μm.

asked if Nebenkern-basal body uncoupling in *Lis-1*^{k11702} spermatids would affect this process. We found that the Nebenkern properly associated with the axoneme in early elongating *Lis-1*^{k11702} spermatids, suggesting that Nebenkern-basal body coupling is not essential for this process (Fig. 2.7) (Anderson et al., 2009; Inoue et al., 2004).

Defects in late spermatogenesis in *Lis-1* testes

Spermatids must undergo elongation and individualization to form functional sperm (Fuller, 1993). During elongation, nuclei and associated basal bodies are positioned at the proximal tips of growing spermatid bundles, and round nuclei acquire a needle-like shape (Fig. 2.6I). During individualization, actin investment cones move in unison along the axoneme length, resolving cytoplasmic bridges between spermatids formed in a common cyst (Fig. 2.6K). In *Lis-1*^{k11702} testes, however, we observed unattached round nuclei and basal bodies dispersed throughout the length of elongating spermatid bundles as well as sparse, disorganized investment cones (Fig. 2.6J,L). These results suggest that LIS-1 is required for positioning of spermatid nuclei within growing bundles. The random distribution of investment cones within elongating *Lis-1*^{k11702} spermatid bundles may reflect loss of nuclear positioning, as investment cones are thought to originate at the nuclear surface (Texada et al., 2008).

LIS-1 localization during spermatogenesis mirrors dynein-dynactin

Our results suggested roles for *Lis-1* in the regulation of centrosome positioning, meiotic spindle assembly, nucleus-Nebenkern-basal body associations, Nebenkern

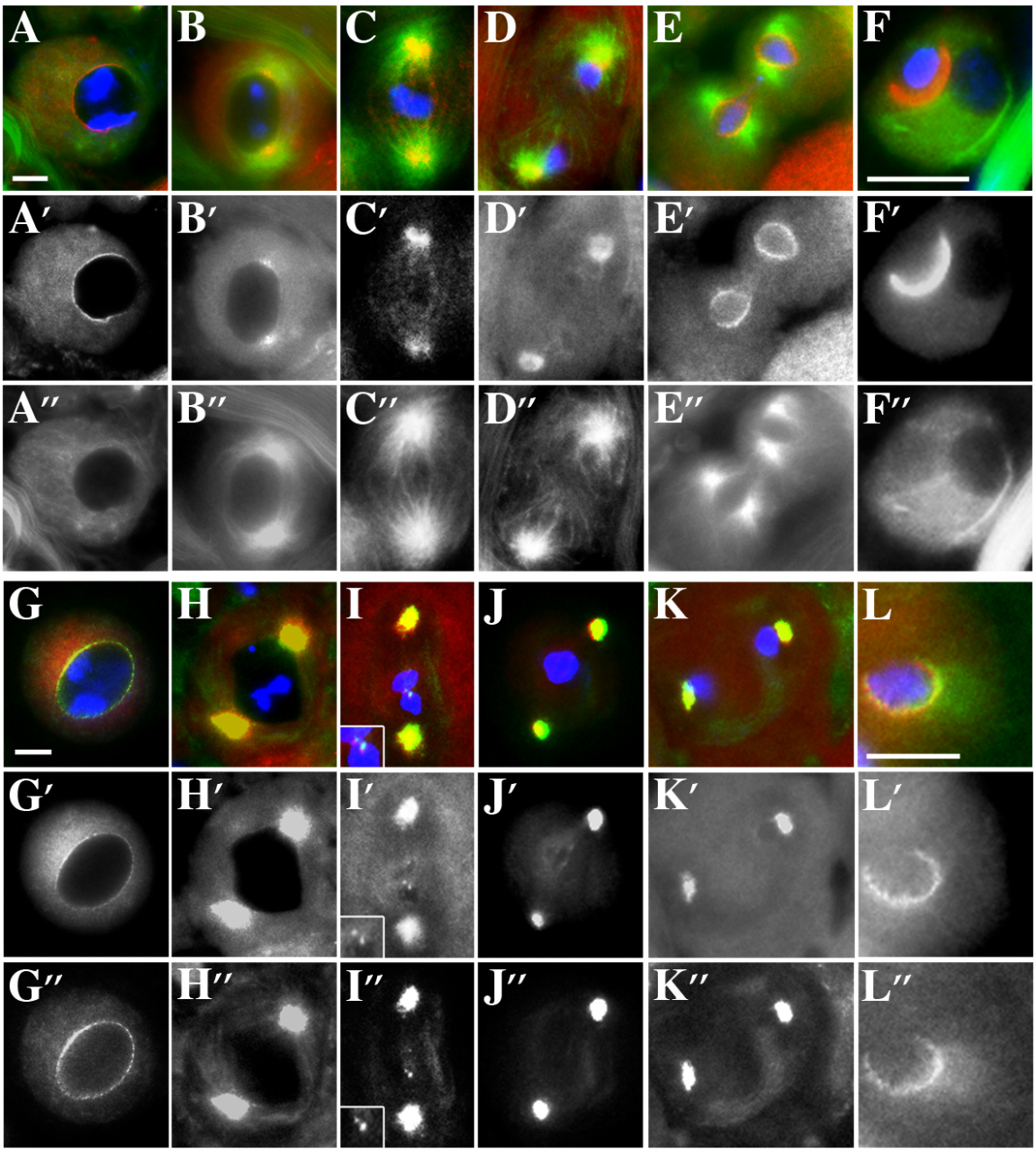

Figure 2.8. Colocalization of LIS-1 and dynactin during male meiosis. (A-F) Wild-type male germline cells coexpressing Cherry-LIS-1 (red, A1-F1; grayscale, A2-F2) and β-tubulin-GFP (green, A1-F1; grayscale, A3-F3). (A) Late G2 spermatocyte. (B) Late prophase I. (C) Metaphase I. (D) Telophase I. (E) Early prophase II. (F) Round spermatid. (G-L) Wild-type male germline cells show colocalization of Cherry-LIS-1 (red, G1-L1; grayscale, G2-L2) and DMN-GFP (green, G1-L1; grayscale, G3-L3). (G) Late G2 spermatocyte. (H) Prophase I. (I) Prometaphase I. Inset shows colocalization of Cherry-LIS-1 and DMN-GFP at kinetochores (J) Metaphase I. (K) Telophase I. (L) Round spermatid. DNA in blue. Bars, 10 μm.

morphogenesis, and nuclear positioning during *Drosophila* spermatogenesis. To gain insight into how *Lis-1* affects these processes, we examined the subcellular localization of LIS-1 during spermatogenesis using transgenic flies coexpressing Cherry-LIS-1 and β-tubulin-GFP. LIS-1 is dispersed in the cytoplasm during early G2 with enrichment around the nucleus by late G2 (Fig. 2.8A; data not shown). Perinuclear LIS-1 becomes focused at centrosomes during prophase I and II (Fig. 2.8B,E). Throughout both meiotic divisions, LIS-1 concentrates at spindle poles (Fig. 2.8C,D; data not shown). In early spermatids, LIS-1 forms a hemispherical cap on the nuclear surface (Fig. 2.8F). Similar localizations have been reported for LIS-1 during mitosis; in contrast to these studies, however, we did not detect LIS-1 at the cortex during *Drosophila* male meiosis (Cockell et al., 2004; Coquelle et al., 2002; Faulkner et al., 2000; Li et al., 2005; Tai et al., 2002).

Cherry-LIS-1 localization during *Drosophila* spermatogenesis is strikingly similar to that of dynein-dynactin, suggesting that LIS-1 and dynein-dynactin may colocalize at these sites (Anderson et al., 2009). We examined male germ cells coexpressing Cherry-LIS-1 and GFP-tagged Dynamitin (DMN), the p50 subunit of dynactin, which colocalizes with dynein throughout spermatogenesis (McGrail and Hays, 1997; Wojcik et al., 2001). We found that LIS-1 colocalized with dynactin at the nuclear surface of G2 spermatocytes and spermatids (Fig. 2.8G-L). In prometaphase spermatocytes, LIS-1 colocalized with dynactin at kinetochores (Fig. 2.8I). These results are consistent with tight association between LIS-1 and dynein-dynactin complexes during *Drosophila* spermatogenesis, as has been reported in other systems (Faulkner et al., 2000; Mesngon et al., 2006; Sasaki et al., 2000; Smith et al., 2000; Tai et al., 2002).

Lis-1 male germ cells show loss of dynein-dynactin localization

Although *Lis-1* is an established regulator of dynein-dynactin, its mechanism of action is unclear. Localizations of LIS-1 and dynein-dynactin within cells have been shown in several cases to be dependent on each other, although their interdependency varies with the model system and subcellular sites (Cockell et al., 2004; Coquelle et al., 2002; Lam et al., 2010; Lee et al., 2003). We examined localization of dynein-dynactin complexes in *Lis-1*^{k11702} male germ cells using antibodies against dynein heavy chain and transgenic expression of DMN-GFP (McGrail and Hays, 1997). Dynein-dynactin is normally enriched at the nuclear surface of G2 spermatocytes and round spermatids and at spindle poles of meiotic spermatocytes (Anderson et al., 2009; Li et al., 2004). We found a significant reduction in dynein-dynactin localization to these sites in *Lis-1*^{k11702} testes (>95% of G2 spermatocytes and >80% of spermatids, >200 cells scored each; Figs 2.9, 2.10). Immunoblotting revealed normal levels of core dynein-dynactin proteins in *Lis-1*^{k11702} testes, suggesting that decreased enrichment at these sites was not due to decreased stability of complex components (Fig. 2.11).

tctex-1 male germ cells have *Lis-1*-like phenotypes

We hypothesized that the defects we observed in *Lis-1*^{k11702} male germ cells are a consequence of decreased dynein function. To test this hypothesis, we sought to assess spermatogenesis in dynein-dynactin mutants. Most null mutations in *Drosophila* dynein-dynactin subunits are lethal, however, thus complicating an analysis of their roles during spermatogenesis. We used flies null for the *Drosophila* ortholog of Tctex-1, the 14-kDa dynein light chain, because they are viable but male sterile (Li et al., 2004).

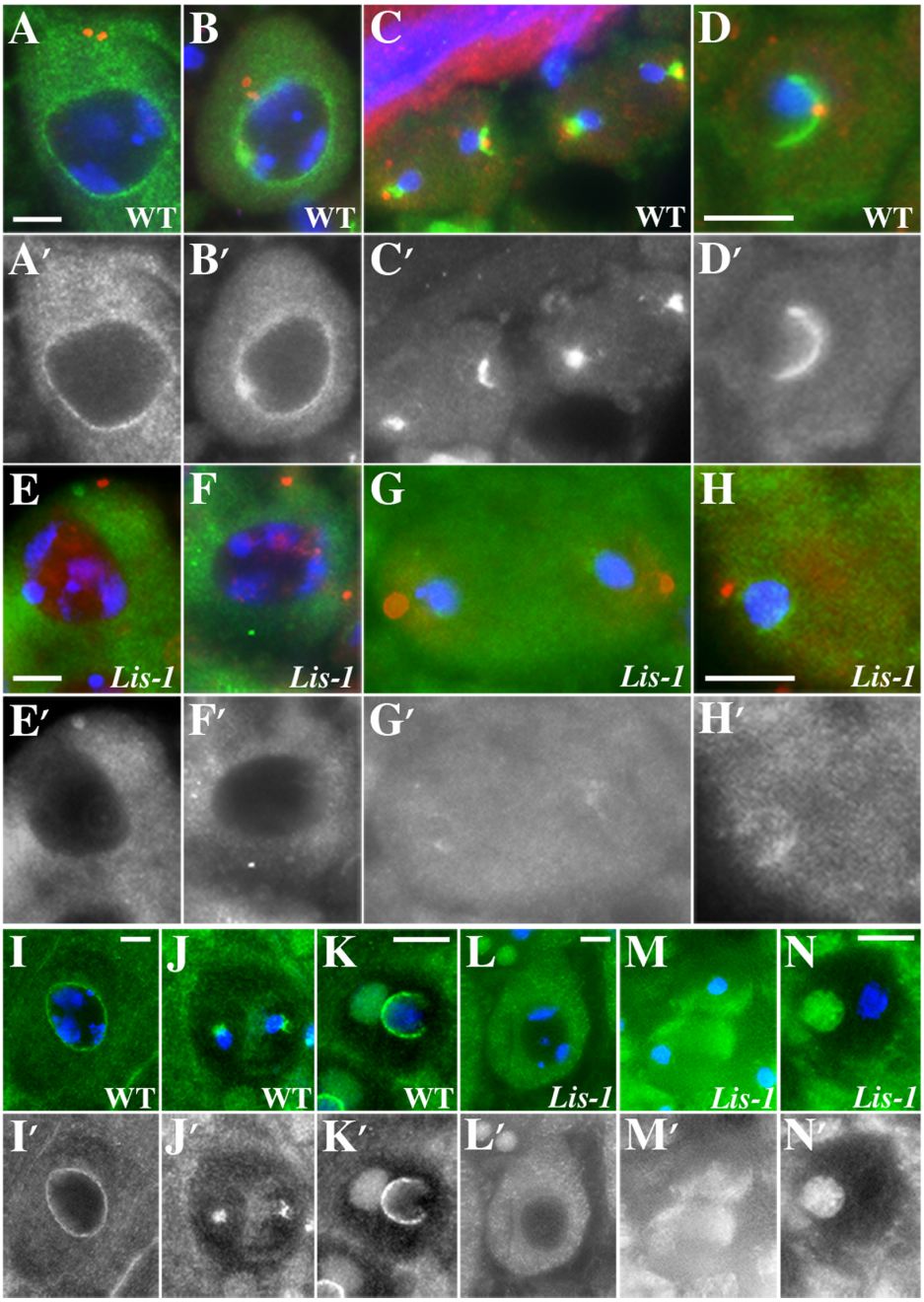

Figure 2.9. Loss of dynein-dynactin localization in *Lis-1* male germline cells. (A-H) Male germline cells stained for dynein heavy chain (green, A1-H1; grayscale, A2-H2) and PLP (red; centriole marker). (I-N) Male germline cells expressing DMN-GFP (green, I1-N1; grayscale, I2-N2). *Lis-1*^{k11702} cells have reduced dynein-dynactin localization relative to wild-type. Late G2 (A,E,I,L), prophase I (B,F), and telophase (C,G,J,M) spermatocytes and round spermatids (D,H,K,N) shown. DNA in blue. Bars, 10 μm.

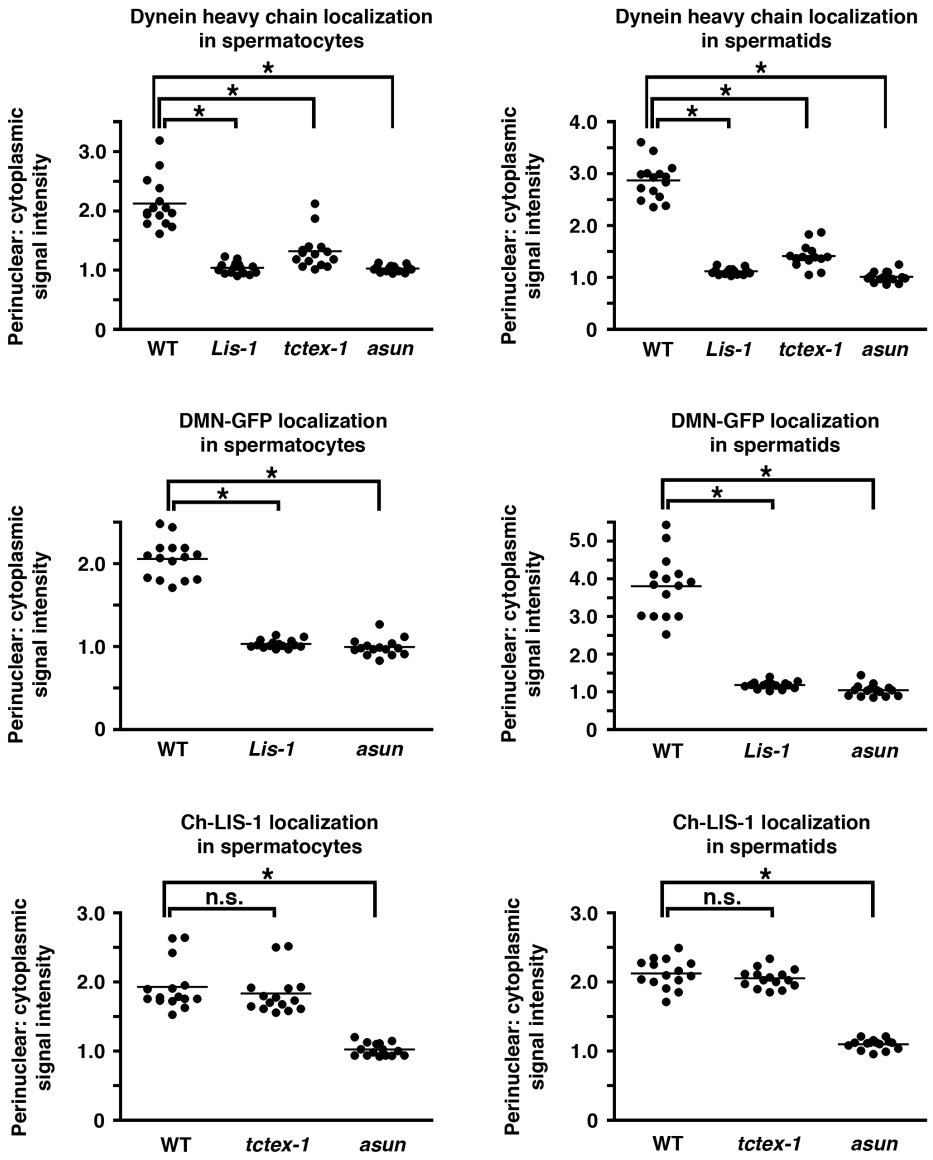

Figure 2.10. Quantification of perinuclear dynein, dynactin, and LIS-1. Late G2 spermatocytes or round spermatids in wild-type or mutant testes stained for dynein heavy chain or with transgenic expression of DMN-GFP or Cherry-LIS-1 were identified by fluorescence microscopy. The alleles used were *Lis-1*^{k11702}, *tctex-1*^{e155}*/Df(3R)Exel6178*, and *asun*^{f02815}. Following image acquisition, the average intensity of the signal (dynein heavy chain, DMN-GFP, or Cherry-LIS-1) within a small rectangular region was sampled near the nuclear surface and in the surrounding cytoplasm using Adobe Photoshop, and the ratio of the intensities (perinuclear: cytoplasmic) was determined. Data are shown as scatter plots in which each dot represents the ratio obtained for one cell and horizontal lines represent mean ratios; for each plot, at least 15 cells from at least three testes pairs were scored per genotype. Statistical analysis was performed using an unpaired Student's *t*-test. Asterisks mark mutants with significantly lower mean ratios compared to wild-type cells ($p<0.0001$). n.s. indicates that mean ratios were not significantly different from that of wild-type cells.

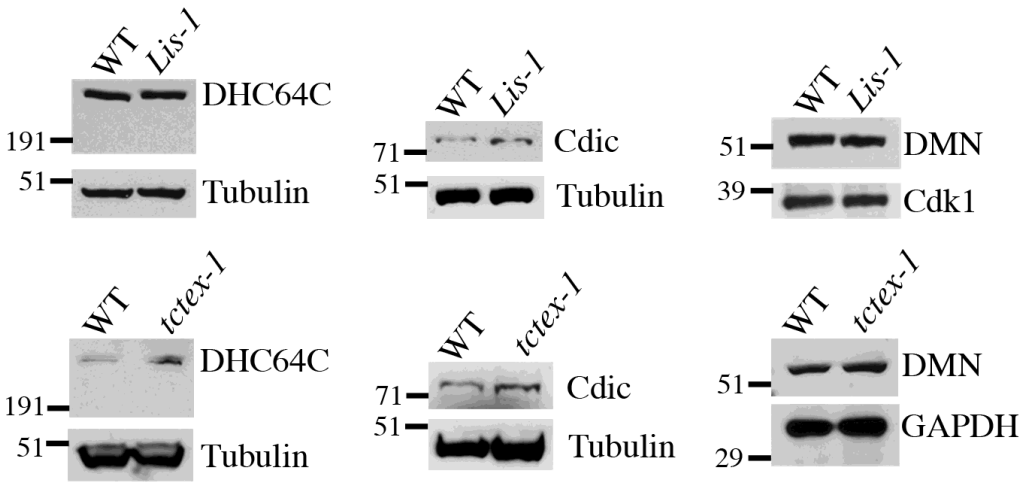

Figure 2.11. Normal levels of dynein-dynactin components in *Lis-1* and *tctex-1* testes. Immunoblots show wild-type levels of dynein heavy chain (DHC64C), dynein intermediate chain (DIC), and DMN (dynactin subunit) in extracts of *Lis-1*^{k11702} and *tctex-1* testes. Loading controls: α-tubulin, Cdk1, or GAPDH.

In *tctex-1* male germ cells (*tctex-1*^{e155}*/Df(3R)Exel6178* used in this study), we identified all *Lis-1*^{k11702} phenotypes described above, albeit to a lesser degree. Both cortical and free centrosomes were observed at higher rates in *tctex-1* prophase spermatocytes (~14% and ~17%, respectively) compared to wild-type cells (<0.5% and ~3%, respectively; $p<0.001$) (Fig. 2.12A-I). *tctex-1* spermatids exhibited loss of wild-type nucleus-basal body, nucleus-Nebenkern, and Nebenkern-basal body attachments and occasionally had Nebenkern shape defects (Figs 2.6D,H, 2.12J-L). We observed significant loss of dynein localization to the nuclear surface of *tctex-1* G2 spermatocytes and spermatids (87% and 64% of cells, respectively; >200 cells scored each) and spindle poles during meiotic divisions (Figs 2.12M-R, 2.10). Another group previously reported nucleus-basal body coupling defects and reduced perinuclear dynein in *tctex-1* spermatids (Li et al., 2004). We observed a less severe degree of reduction of perinuclear dynein in *tctex-1* male germ cells compared to *Lis-1*^{k11702}; this difference might explain the lower percentage of spermatocytes with centrosome positioning defects in *tctex-1* vs *Lis-1*^{k11702} testes (Fig. 2.10). Wild-type levels of core dynein-dynactin subunits were detected in *tctex-1* testes by immunoblotting, suggesting that loss of dynein localization is not secondary to decreased levels of complex components (Fig. 2.11).

Our phenotypic characterization of *Lis-1*^{k11702} male germ cells suggested that LIS-1 is required for proper subcellular localization of dynein. To test for a reciprocal requirement, we assessed Cherry-LIS-1 localization in *tctex-1* male germ cells. We found that *tctex-1* spermatocytes and spermatids had wild-type levels of Cherry-LIS-1 on the nuclear surface (>200 of each cell type scored), suggesting that LIS-1 can be recruited to this site independent of dynein complexes (Figs 2.10, 2.13).

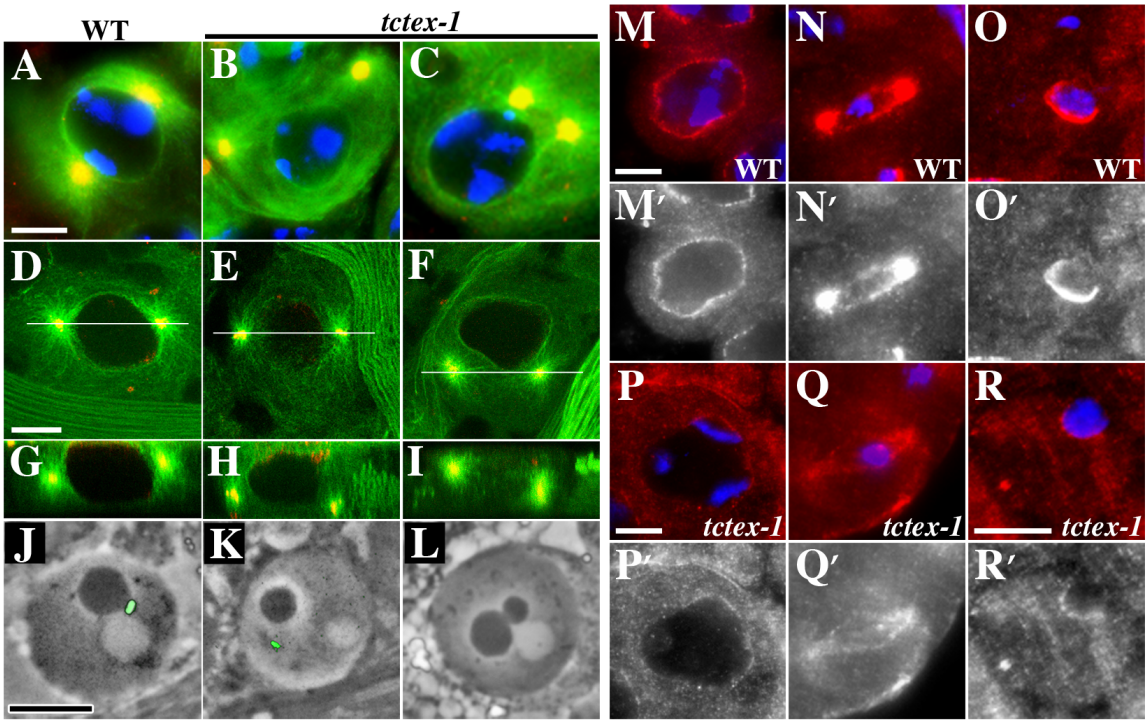

Figure 2.12. Dynein light chain mutant male germline cells exhibit *Lis-1* phenotypes. (A-I) Prophase I spermatocytes expressing β-tubulin-GFP (green) stained for γ-tubulin (red). Roughly one-third of *tctex-1* spermatocytes have cortical (B,E,H) or free (C,F,I) centrosomes (normally at nuclear surface; A,D,G). (A-C) Epifluorescent micrographs. DNA in blue. (D-I) XY projections (D-F) and corresponding XZ optical sections (G-I). White bars mark positions of corresponding XZ optical sections. (J,K) Phase/fluorescence overlay images of round spermatids expressing GFP-PACT (green) show wild-type nucleus-Nebenkern-basal body interactions that are lost in *tctex-1* mutants. (L) Phase-contrast image of *tctex-1* spermatid with defective Nebenkern morphology. (M-R) Male germline cells stained for dynein heavy chain (red, MI-R1; grayscale, M2-R2) and DNA (blue). *tctex-1* cells have reduced dynein localization relative to wild-type. Late G2 (M,P) and metaphase II (N,Q) spermatocytes and round spermatids (O,R) shown. Bars, 10 μm.

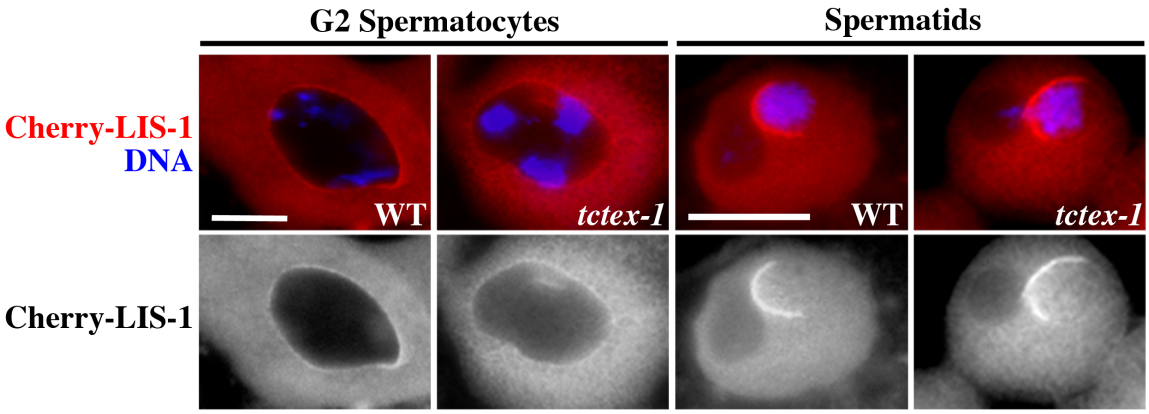

Figure 2.13. Normal LIS-1 localization in *tctex-1* male germline cells. Male germline cells expressing Cherry-LIS-1 and DNA-stained. Cherry-LIS-1 localizes to the nuclear surface in late G2 spermatocytes and round spermatids from both wild-type and *tctex-1* testes. Bar, 10 μm.

Lis-1 dominantly enhances *asun*

We previously identified *asun* as a regulator of dynein during *Drosophila* spermatogenesis (Anderson et al., 2009). Both $asun^{f02815}$ (hypomorphic allele) and $Lis\text{-}1^{k11702}$ male germ cells both show loss of nucleus-centrosome and nucleus-basal body attachments, likely due to reduction of perinuclear dynein. Given these shared phenotypes, we questioned whether ASUN and LIS-1 might cooperate in regulating spermatogenesis. We tested for genetic interactions between *asun* and *Lis-1* and found that the phenotype of $asun^{f02815}$ males carrying a single copy of $Lis\text{-}1^{k11702}$ was strongly enhanced; similar results were obtained using a deficiency that uncovers *Lis-1* (Fig. 2.14; data not shown). The testes of these $Lis\text{-}1^{k11702}$/+; $asun^{f02815}$ males were small compared to $Lis\text{-}1^{k11702}$/+ or $asun^{f02815}$ males (Fig. 2.14A-C). The reduction in size ranged from mild to severe; an example of the latter is shown in Fig. 2.14C. Conversely, we did not detect dominant enhancement of *Lis-1* by *asun* (data not shown).

We found an extreme paucity of sperm bundles in $Lis\text{-}1^{k11702}$/+; $asun^{f02815}$ testes compared to $asun^{f02815}$ testes, suggesting a block in spermatogenesis that would account for the reduced size of $Lis\text{-}1^{k11702}$/+; $asun^{f02815}$ testes (Fig. 2.14D,E). Although $asun^{f02815}$ testes contain an increased fraction of prophase I spermatocytes, cells at all stages of spermatogenesis can be readily identified (Anderson et al., 2009) (Fig. 2.14F). We observed a preponderance of late G2 primary spermatocytes in $Lis\text{-}1^{k11702}$/+; $asun^{f02815}$ testes with very few cells beyond this stage of spermatogenesis, indicative of a severe G2 block (Fig. 2.14G). This phenotype was more severe than meiotic phenotypes observed in male flies homozygous for $Lis\text{-}1^{k11702}$ (no block), $asun^{f02815}$ (prophase block), or a null allele of asun (prophase block, described below); thus, it does not appear to represent

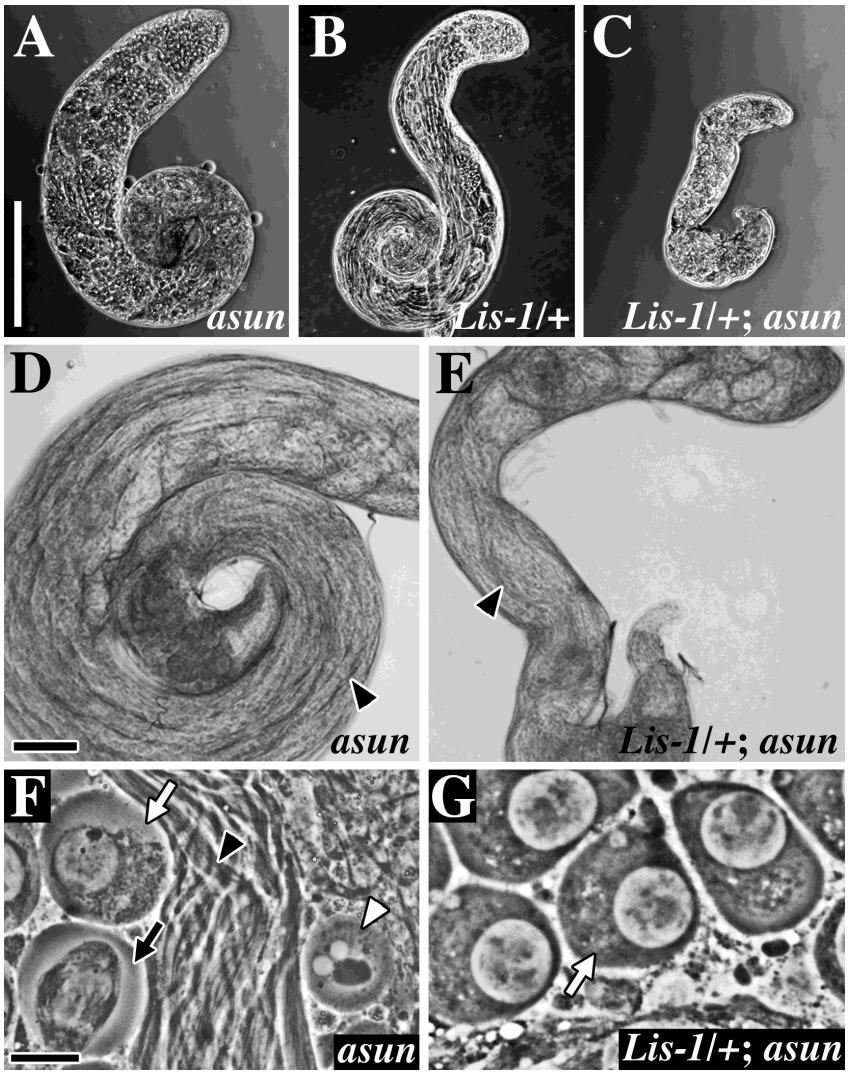

Figure 2.14. *Lis-1* dominantly enhances *asun*. (A-C) Phase-contrast images of whole testes show reduced size of *Lis-1*^{k11702}/+;*asun*^{f02815} compared to *asun*^{f02815} and *Lis-1*^{k11702}/+. Bar, 250 μm. (D,E) Higher magnification images show paucity of sperm bundles (arrowheads) in *Lis-1*^{k11702}/+;*asun*^{f02815} testes compared to *asun*^{f02815}. Bar, 50 μm. (F,G) Phase-contrast image shows *asun*^{f02815} male germ cells at various stages of spermatogenesis: G2 spermatocytes (white arrow), dividing spermatocytes (black arrow), round spermatids (white arrowhead), and sperm bundles (black arrowhead); most cells from *Lis-1*^{k11702}/+;*asun*^{f02815} testes are G2 spermatocytes (white arrow). Bar, 10 μm.

merely an additive effect of the two alleles. These findings suggest that *Lis-1* and *asun* cooperate in the regulation of *Drosophila* spermatogenesis.

asun null phenotype

In contrast to *Lis-1*^{k11702}, we rarely observed cortical centrosomes in *asun*^{f02815} prophase spermatocytes (Fig. 2.2M). Our previous studies suggested that *asun*^{f02815} is a hypomorphic allele (Anderson et al., 2009). We questioned whether lack of the cortical centrosome phenotype in *asun*^{f02815} spermatocytes might be due to low allele strength. To obtain a null allele of *asun*, we generated a two-gene deletion that removed most of the *asun* coding region and its entire neighboring gene, *belphegor* (*bor*) (Fig. 2.15A). *bor* is predicted to encode an ATPase of unknown function. Homozygous lethality of this deletion was rescued by a *bor* transgene, thus demonstrating that *bor*, but not *asun*, is essential for viability. Males homozygous for the two-gene deletion and carrying the *bor* transgene (referred to hereafter as *asun*^{d93}) were completely sterile. All *asun*^{d93} phenotypes reported herein were fully rescued via male germline-specific expression of GFP-ASUN, confirming that they were due to loss of *asun* (data not shown).

Nucleus-centrosome uncoupling was more severe in *asun*^{d93} than *asun*^{f02815} prophase spermatocytes (Figs 2.2M, 2.15B-D). As for *asun*^{f02815}, cortical centrosomes were rare in *asun*^{d93} prophase spermatocytes, suggesting that centrosome detachment from the cortex during late G2 requires LIS-1 but not ASUN (Fig. 2.2M). As expected based on our study of *asun*^{f02815}, perinuclear dynein-dynactin enrichment was greatly diminished in *asun*^{d93} spermatocytes and spermatids (Figs 2.10, 2.15E,F; data not shown) (Anderson et al., 2009). *asun*^{d93} round spermatids, which were scarce due to strong

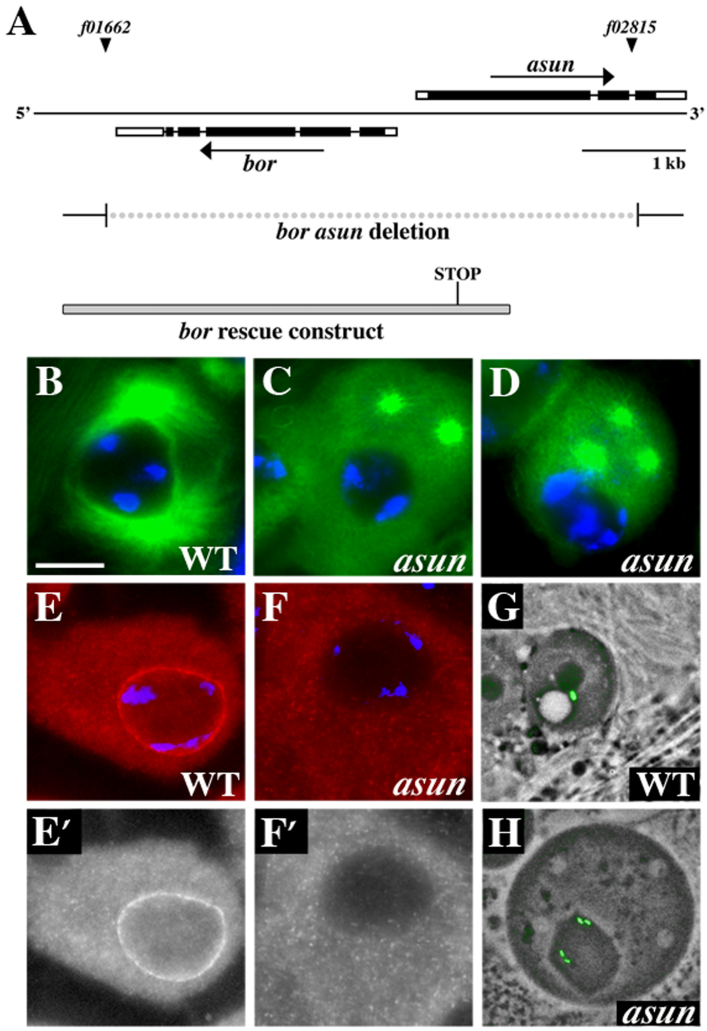

Figure 2.15. The *asun* null phenotype. (A) Schematic diagram of the *asun* gene region. Coding regions and UTRs are represented as filled and unfilled boxes, respectively; introns as thin lines; and *piggyBac* transposons *f01662* and *f02815* as triangles. The breakpoints of a *bor asun* two-gene deletion (generated through FLP-mediated recombination of FRT sites within the transposons) and the design of the *bor* transgene used for rescue are shown. $asun^{d93}$ flies are homozygous for the *bor asun* two-gene deletion and the *bor* transgene. (B-D) Prophase I spermatocytes expressing β-tubulin-GFP (green) and stained for DNA (blue). In wild-type spermatocytes (B), two centrosomes are attached to the nuclear surface. $asun^{d93}$ spermatocytes have two to four free centrosomes (C,D). (E,F) Late G2 spermatocytes stained for dynein heavy chain (red, E1,F1; grayscale, E2,F2) and DNA (blue). $asun^{d93}$ cells (F) have loss of perinuclear dynein relative to wild-type (E). (G,H) Phase/fluorescence overlay images of round spermatids expressing GFP-PACT (green; basal body marker). Each wild-type spermatid (G) has one Nebenkern (phase-dark) comparable in size to the nucleus (phase-light); the nucleus, Nebenkern, and basal body are all tightly associated. Each $asun^{d93}$ spermatid (H) has one large Nebenkern attached to several basal bodies and unattached, small nuclei. Bar, 10 μm.

prophase I arrest, contained multiple nuclei and four basal bodies, indicative of severe cytokinesis defects (99%; 99/100 cells) (Fig. 2.15G,H). *asun*^{d93} spermatids exhibited nucleus-basal body and nucleus-Nebenkern coupling defects; in contrast to *Lis-1*^{k11702} spermatids, however, Nebenkern-basal body coupling appeared normal (20/20 cells; Fig. 2.15G,H). Most transheterozygous *asun*^{d93}/*asun*^{f02815} spermatids exhibited the same constellation of coupling defects as the null mutants (Fig. 2.6D).

LIS-1 localization is ASUN-dependent

Given shared spermatogenesis phenotypes and genetic interaction between *Lis-1* and *asun*, we questioned whether LIS-1 and ASUN might regulate each other's localization. We expressed Cherry-LIS-1 in *asun*^{f02815} testes to assess the effects of decreased ASUN function on LIS-1 localization. We observed severe reduction of Cherry-LIS-1 on the nuclear surface of spermatocytes and spermatids and at spindle poles of dividing spermatocytes in *asun*^{f02815} testes (>97% of G2 spermatocytes and >80% of spermatids, >200 of each cell type scored; Figs 2.16, 2.10). Cherry-LIS-1 accumulation at these sites remains normal in males with mutation of a testes-specific beta-tubulin subunit, suggesting that its recruitment is not microtubule-dependent (data not shown) (Kemphues et al., 1982). We detected wild-type Cherry-LIS-1 levels in *asun*^{f02815} testes; thus, LIS-1 stability does not appear to require ASUN (Fig. 2.17). GFP-ASUN shows a wild-type localization pattern when expressed in *Lis-1*^{k11702} testes (intranuclear during early G2, appearing in cytoplasm during late G2), suggesting that LIS-1 is not reciprocally required for ASUN localization (Fig. 2.18) (Anderson et al., 2009). We infer

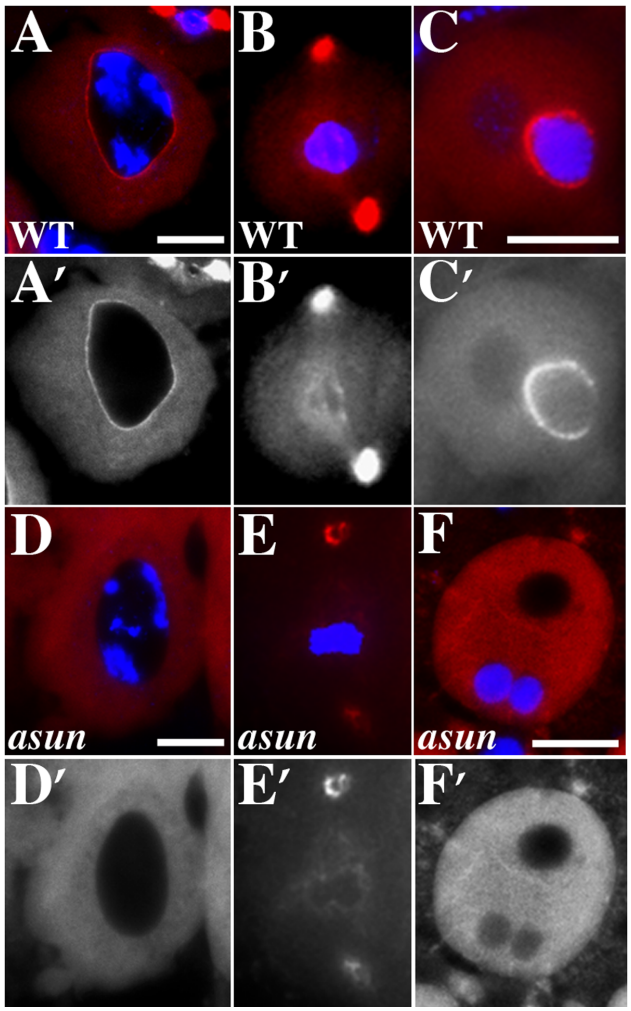

Figure 2.16. Loss of LIS-1 localization in *asun* male germline cells. Male germline cells expressing Cherry-LIS-1 (red, A1-F1; grayscale, A2-F2) and DNA-stained (blue). *asun* cells have reduced Cherry-LIS-1 localization relative to wild-type. Late G2 (A,D) and metaphase I (B,E) spermatocytes and round spermatids (C,F) shown. Bars, 10 μm.

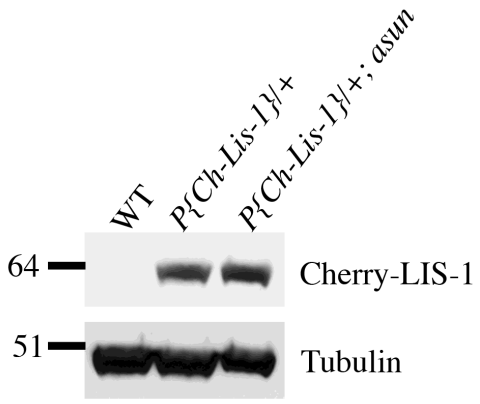

Figure 2.17. Normal LIS-1 levels in *asun* testes. Immunoblots using anti-Cherry antibodies show comparable levels of Cherry-tagged LIS-1 in extracts of wild-type vs. *asun*^{f02815} testes. Loading control: Tubulin.

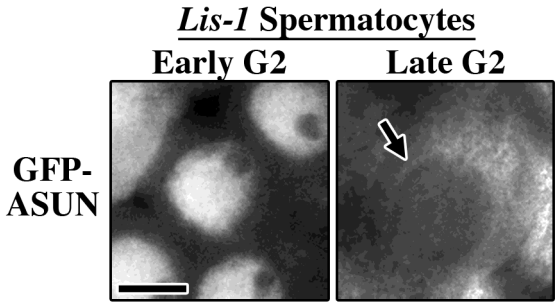

Figure 2.18. Normal ASUN localization in *Lis-1* spermatocytes. GFP-ASUN expressed in *Lis-1*^{k11702} spermatocytes is nuclear in early G2 spermatocytes and cytoplasmic with slight perinuclear enrichment (arrow) in late G2 spermatocytes. Bar, 10 μm.

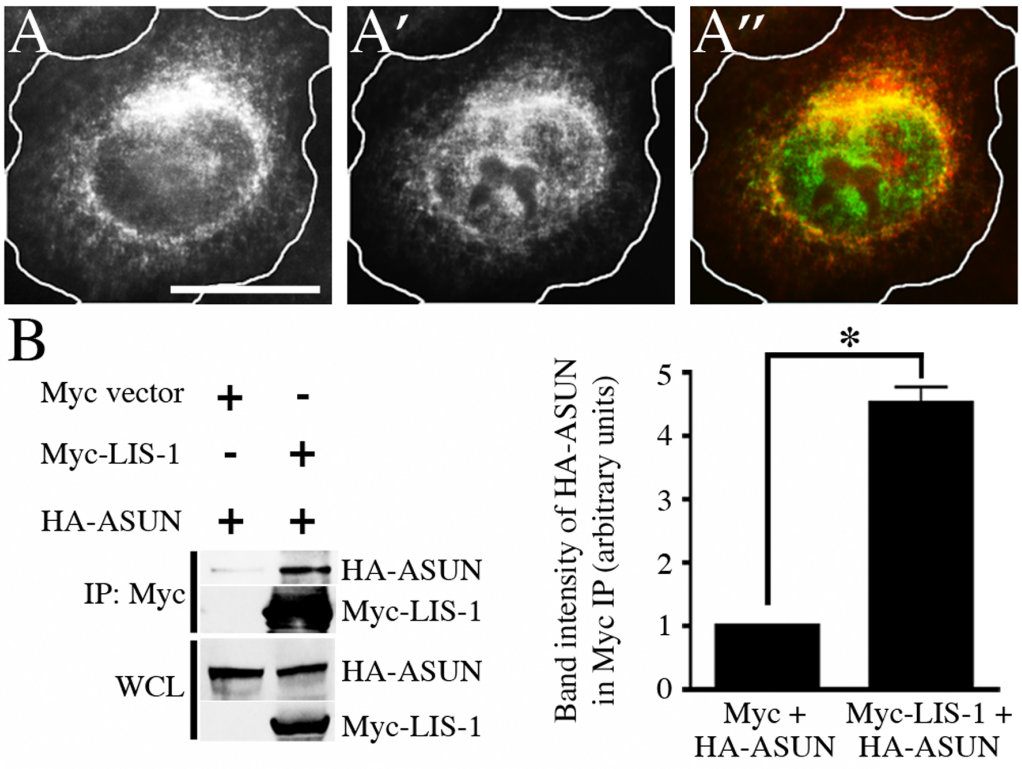

Figure 2.19. LIS-1 and ASUN colocalize and coimmunoprecipitate. (A) Colocalization of Cherry-tagged *Drosophila* LIS-1 (A1; red in A3) and GFP-tagged *Drosophila* ASUN (A2; green in A3) in transfected HeLa cells. Bar, 10 μm. (B) HEK293 cells were transfected with tagged *Drosophila* LIS-1 and ASUN expression plasmids as indicated. Myc (control) or Myc-LIS-1 was immunoprecipitated from lysates. Immunoblots of whole cell lysates (WCL) and Myc immunoprecipitates were probed using HA and Myc antibodies. Representative blot is shown on left, quantification on right (asterisk: $p<0.001$, paired Student's *t*-test, n = 4 experiments, ImageJ analysis of band intensities).

that ASUN regulates localization of LIS-1 and dynein-dynactin, whereas LIS-1 regulates localization of dynein-dynactin but not ASUN.

LIS-1 and ASUN colocalize and coimmunoprecipitate

We hypothesized that LIS-1 and ASUN interact at the nuclear surface of late G2 spermatocytes to recruit dynein-dynactin. Our efforts to demonstrate colocalization of LIS-1 and ASUN at the nuclear surface of spermatocytes, however, were complicated by the low frequency and weak accumulation of GFP-ASUN that we have observed at this site. We previously reported colocalization of endogenous dynein and GFP-tagged *Drosophila* ASUN at the nuclear surface of transfected, nocodazole-treated, cultured mammalian cells (Anderson et al., 2009). Taking a similar approach, we found that 74% of cotransfected cells with perinuclear localization of GFP-tagged *Drosophila* ASUN exhibited colocalization of Cherry-tagged *Drosophila* LIS-1 at this site (Fig. 2.19A; 68/92 cells scored). Furthermore, we demonstrated coimmunoprecipitation of tagged versions of *Drosophila* LIS-1 and ASUN from cultured mammalian cells, suggesting LIS-1 and ASUN can exist within a common complex (Fig. 2.19B).

Discussion and Future Directions

Our analysis of a hypomorphic, male-sterile allele of *Lis-1* revealed that *Lis-1* plays essential roles during *Drosophila* spermatogenesis. Our data suggest that loss of dynein function is the root cause of the defects that we observe in *Lis-1*^{k11702} testes, as mutation of the dynein light chain gene, *tctex-1*, phenocopies mutation of *Lis-1*. Based on their overlapping phenotypes in male germ cells, genetic interaction, colocalization, and

coimmunoprecipitation, we present a model in which *Lis-1* and *asun* cooperate to regulate dynein localization during spermatogenesis.

Our observations suggest that centrosomes of *Lis-1* spermatocytes remain attached to the cell cortex and fail to migrate to the nuclear surface at entry into meiotic prophase. The phenotype of persistent cortical centrosomes during meiotic divisions has been characterized in *abnormal spindles* and *nudE* testes; Wainman et al also noted the presence of cortical centrosomes in *Lis-1*^{k11702} metaphase spermatocytes in their study of *nudE* mutants (Rebollo et al., 2004; Wainman et al., 2009). Dynein-dynactin and LIS-1 localize to the cell periphery in lower eukaryotes and cultured mammalian cells as well as to the posterior cortex of *Drosophila* oocytes (Busson et al., 1998; Dujardin and Vallee, 2002; Faulkner et al., 2000). We have not, however, detected enrichment of dynein-dynactin or LIS-1 at the cortex of *Drosophila* spermatocytes. Cortical dynein has been implicated in regulation of mitotic spindle orientation in several systems, although the mechanism is not clear (Gusnowski and Srayko, 2011; Markus et al., 2009; Woodard et al., 2010). Our data suggest that dynein and LIS-1 are required in spermatocytes to release centrosomes from the cortex prior to meiotic entry.

We showed that *Lis-1* spermatocytes exhibit free centrosomes, albeit at a much lower frequency than the phenotype of cortical centrosomes. Detachment of centrosomes from the cortex of primary spermatocytes is an earlier step in male meiosis than reassociation of the centrosomes with the nuclear surface at G2/M; hence, a failure of centrosomes to detach from the cortex is likely to mask a subsequent failure of nucleus-centrosome coupling. We found that LIS-1 colocalizes with dynein-dynactin at the nuclear surface, and localization of dynein-dynactin to this site is severely impaired in

Lis-1 spermatocytes and spermatids. Dynein-dynactin anchored at the nuclear surface has previously been implicated in mediating interactions between the nucleus and centrosomes during both mitotic and meiotic cell cycles (Anderson et al., 2009; Gonczy et al., 1999; Li et al., 2004; Malone et al., 2003; Robinson et al., 1999; Salina et al., 2002). We propose that defects in nucleus-centrosome coupling in *Lis-1* spermatocytes stem from disruption in localization of dynein-dynactin to the nuclear surface.

Previous studies in other systems concerning the role of LIS1 in dynein-dynactin recruitment to the nuclear surface have yielded conflicting results. In *C. elegans* embryos, dynein-dynactin was reported to localize normally to this site in the absence of *Lis-1* (Cockell et al., 2004). In mammalian neural stem cells, however, *Lis1* was shown to be required for recruitment of dynein to the nuclear surface at prophase entry (Hebbar et al., 2008). Similarly, we observed severe reduction of perinuclear dynein-dynactin in *Drosophila Lis-1* spermatocytes at meiotic onset, suggesting that *Lis-1* is required for this process. Conversely, we found normal levels of *Drosophila* LIS-1 at the nuclear surface of *tctex-1* spermatocytes; thus, dynein-dynactin does not appear to be reciprocally required for LIS-1 recruitment to this site. Our finding of reduced levels of dynein heavy chain on the nuclear surface of *tctex-1* spermatocytes suggest that Tctex-1 light chain plays a specific role in localizing dynein complexes to the nuclear surface; alternatively, complex integrity may be compromised in *tctex-1* mutants.

We previously reported that *asun* regulates dynein localization during *Drosophila* spermatogenesis (Anderson et al., 2009). Our characterization of the hypomorphic *Lis-1*^{k11702} allele and the null *asun*^{d93} allele during *Drosophila* male meiosis reveals overlapping but distinct phenotypes. *Lis-1*^{k11702} spermatocytes exhibit two classes of

centrosome positioning defects: cortical (major phenotype) and free centrosomes (minor phenotype). In contrast, while most *asun*^{d93} spermatocytes have free centrosomes, they do not share with *Lis-1*^{k11702} spermatocytes the phenotype of cortical centrosomes. These observations suggest that the role of *asun* in spermatocytes is limited to events at the nuclear surface, whereas *Lis-1* additionally regulates cortical events. *asun*^{d93} spermatocytes undergo severe prophase arrest, possibly due to failure of astral microtubules of free centrosomes to promote nuclear envelope breakdown. In *Lis-1*^{k11702} spermatocytes, however, meiosis apparently progresses on schedule despite cortical positioning of centrosomes. The high percentage of *asun*^{d93} spermatids with increased numbers of variably sized nuclei, likely a consequence of cytokinesis and chromosome segregation defects, are also absent in *Lis-1*^{k11702} testes. These observations suggest that spindle formation and normal progression through male meiosis require centrosomes to be anchored, either to the nuclear surface or the cortex.

Hypomorphic *Lis-1*^{k11702} and null *asun*^{d93} round spermatids also show similarities and differences in their phenotypes. Both genes are required for recruitment of dynein-dynactin to the nuclear surface; this pool of dynein likely mediates nucleus-basal body and nucleus-Nebenkern attachments, which are defective in both mutants. Genes encoding Spag4 (a SUN protein), Yuri Gagarin (a coiled-coil protein), and GLD2 (a poly(A) polymerase) are required for nucleus-basal body coupling in spermatids, although it is not known whether they interact with ASUN or LIS-1 in this process (Kracklauer et al., 2010; Sartain et al., 2011; Texada et al., 2008). Our studies suggest that *Lis-1*, but not *asun*, is required for proper shaping and Nebenkern-basal body association; these functions might be mediated by dynein/microtubules acting at the

Nebenkern surface. Nebenkerne are generated through fusion of mitochondria following *Drosophila* male meiosis (Fuller, 1993). Two Nebenkerne bodies are occasionally present in *Lis-1* and *tctex-1* spermatids, implicating dynein in regulation of mitochondrial aggregation at this stage. Together, these observations suggest that the role of *asun* in spermatids is limited to events at the nuclear surface, whereas *Lis-1* plays additional roles in regulating Nebenkerne.

Based on our studies of hypomorphic $Lis\text{-}1^{k11702}$ and null $asun^{d93}$ mutant testes, we propose a model in which LIS-1 is required for several dynein-mediated processes during *Drosophila* spermatogenesis, and ASUN is required for the subset of these processes that involve the nuclear surface (Fig. 2.20). Both LIS-1 and ASUN promote recruitment of dynein-dynactin to the nuclear surface of spermatocytes and spermatids. The strong genetic interaction that we observe between *Lis-1* and *asun* suggests that they cooperate in regulating dynein localization during spermatogenesis; our finding that LIS-1 accumulation on the nuclear surface is lost in *asun* male germ cells provides further support for this notion. The observed colocalization and coimmunoprecipitation of LIS-1 and ASUN suggest that they function within a shared complex to promote dynein-dynactin recruitment to the nuclear surface. We did not detect interaction between *Drosophila* LIS-1 and ASUN proteins by in vitro binding or yeast two-hybrid assays, suggesting that their association may be mediated by another protein(s) rather than being direct (P.S. and L.A.L., unpublished observations). Future studies on the nature of the ASUN-LIS-1 interaction should help elucidate the mechanism by which dynein-dynactin localizes to the nuclear surface during spermatogenesis.

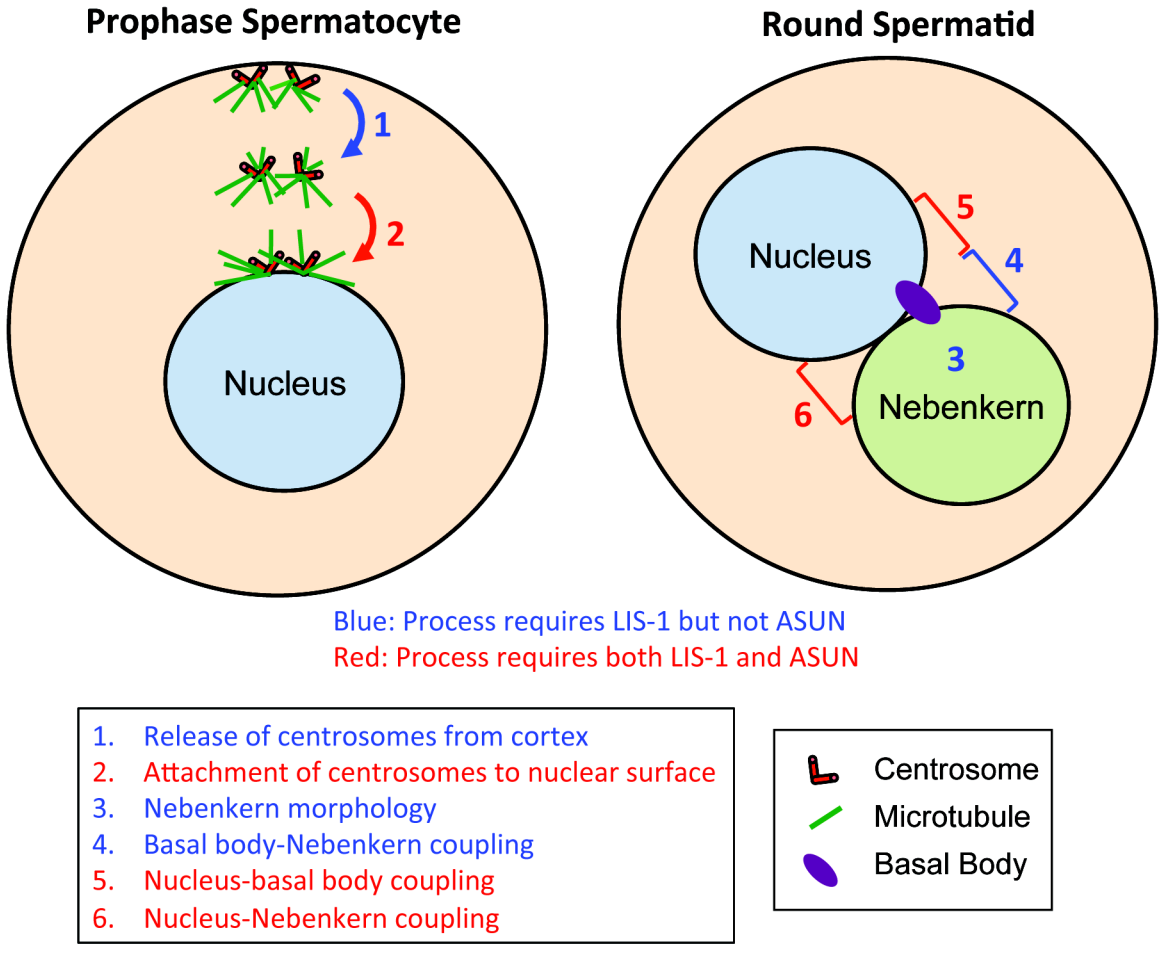

Figure 2.20. Cytoplasmic dynein-mediated processes in *Drosophila* spermatogenesis: differential requirements for LIS-1 and ASUN. See Discussion for details.

Several proteins that promote dynein recruitment and centrosomal tethering to the nuclear surface have been identified. In *C. elegans* embryos, the KASH-domain protein ZYG-12, which localizes to the outer nuclear membrane and binds the inner nuclear membrane protein SUN-1, is required for these events (Malone et al., 2003). Another KASH-domain protein, Syne/Nesprin-1/2, works in concert with SUN-1/2 to mediate nucleus-centrosome interactions during mammalian neuronal migration (Zhang et al., 2009). Two additional pathways required for dynein recruitment to the nuclear surface at prophase have recently been identified in cultured mammalian cells. BicD2 binds dynein and anchors it to the nuclear envelope via its interaction with a nuclear pore complex protein, RanBP2 (Splinter et al., 2010). Similarly, CENP-F and NudE/EL act as a bridge between dynein and Nup133 (Bolhy et al., 2011). It has not yet been determined if mammalian LIS1 and ASUN function within these pathways or if they act via a parallel mechanism to promote dynein recruitment to the nuclear surface.

Our finding that a single copy of *Lis-1*^{k11702} can drastically decrease the size of *asun*^{f02815} testes suggests potential roles for *Lis-1* and *asun* in regulating division of male germline stem cells of *Drosophila*, as loss of cell proliferation can lead to reduction of testes size (Castrillon et al., 1993). Interestingly, *Lis-1* has been reported to regulate germline stem cell renewal in *Drosophila* ovaries (Chen et al., 2010). Orientation of the cleavage plane during male germline stem cell division requires proper migration of centrosomes along the nuclear surface, and misorientation of the plane can lead to stem cell loss (Cheng et al., 2008; Yamashita et al., 2003; Yamashita et al., 2007). Given the importance of *Lis-1* and *asun* in mediating nucleus-centrosome coupling in *Drosophila*

spermatocytes, it is possible that these genes also cooperate to regulate centrosomes during stem cell divisions in testes.

In humans, the *Lis-1* gene is dosage sensitive during brain development, as the disorder lissencephaly results from deletion or mutation of a single copy (Wynshaw-Boris, 2007). *Lis-1* spermatogenesis phenotypes reported herein were observed in flies homozygous for a hypomorphic *Lis-1* allele; flies carrying one copy of this allele displayed many of the same phenotypes but to a lesser degree. These findings suggest that precise regulation of LIS-1 protein levels is essential for normal development in *Drosophila*.

A requirement for *Lis1* during spermatogenesis is conserved in mammals. Deletion of a testis-specific splicing variant of *Lis1* in mice blocks spermiogenesis and prevents spermatid differentiation (Nayernia et al., 2003). LIS1 and dynein were shown to partially colocalize around wild-type spermatid nuclei, but dynein localization in *Lis1* testes was not assessed. It remains to be determined if the functions of LIS1 in mammalian spermatogenesis are mediated through dynein and if the ASUN homolog regulates LIS1 localization in this system.

CHAPTER III

asunder IS REQUIRED FOR DYNEIN LOCALIZATION AND DORSAL FATE DETERMINATION DURING *DROSOPHILA* OOGENESIS

The contents of this chapter have been submitted to the journal *Developmental Biology* (currently in revision).

Introduction

Drosophila oogenesis is a powerful model system for studying various aspects of cell and developmental biology such as control of the cell cycle, axis formation, epithelial morphogenesis, cellular polarity, and cell fate determination. A wild-type *Drosophila* female has a pair of ovaries, each made up of 16 -18 independent "egg assembly lines" known as ovarioles (Bastock and St Johnston, 2008; Spradling, 1993). Each ovariole consists of a specialized anterior region (the germarium) where the progeny of germline and somatic stem cells are organized into distinct egg chambers. Each egg chamber consists of a cyst of 16 germ cells (15 nurse cells and 1 oocyte) interconnected by cytoplasmic bridges called ring canals and surrounded by a single layer of somatic follicle cells. The development of the egg chambers into mature eggs has been divided into 14 stages based on egg chamber morphology (Spradling, 1993). The polarity of the mature egg, formed at the end of oogenesis, is characterized by certain prominent structures: an anteriorly positioned, cone-shaped micropyle that facilitates sperm entry

prior to fertilization and, located above the micropyle, a pair of dorsal appendages that facilitate embryonic respiration.

Determination of eggshell polarity depends on key patterning events that occur during *Drosophila* oogenesis. Within the germarium, centrosomes migrate from the nurse cells into the future oocyte in a manner dependent on a branched cytoplasmic organelle called the fusome, which extends into all the germline cells within a cyst (Bolivar et al., 2001; Lin et al., 1994). A microtubule-organizing center (MTOC) forms in the oocyte posterior; microtubules originating from this MTOC pass through cytoplasmic bridges into adjacent nurse cells and are required for transport of maternal mRNAs and proteins from the nurse cells into the oocyte (Pokrywka and Stephenson, 1991; Theurkauf et al., 1992). Transport and asymmetric localization within the oocyte of *oskar* (*osk*), *nanos* (*nos*), *bicoid* (*bcd*), and *gurken* (*grk*) transcripts are critical for proper establishment of the embryonic body axes (Becalska and Gavis, 2009).

grk mRNA is localized to the posterior of the *Drosophila* oocyte prior to its translation to generate Gurken (Grk) protein, a TGFα-like ligand, which signals posterior follicle cells to adopt a posterior fate (Gonzalez-Reyes et al., 1995; Neuman-Silberberg and Schupbach, 1993). The posterior follicle cells in turn trigger reorganization of the microtubule cytoskeleton of the oocyte that promotes localization of *bcd* transcript to the anterior pole and *osk* and *nos* transcripts to the posterior pole, thus establishing the anterior-posterior axis of the embryo. This microtubule reorganization also results in migration of the oocyte nucleus to the anterior-dorsal region of the oocyte (Zhao et al., 2012). *grk* mRNA, which associates with the oocyte nucleus, begins to accumulate in this region (Neuman-Silberberg and Schupbach, 1993). The resulting localized secretion of

Grk protein, which signals to overlying dorsal-anterior follicle cells, initiates a signaling cascade that ultimately establishes the dorsal-ventral axis of the embryo (Peri and Roth, 2000; Sen et al., 1998; Van Buskirk and Schupbach, 1999; Wasserman and Freeman, 1998).

The microtubule motors, dynein and kinesin, are critical for the transport of various mRNAs to their specific sites during *Drosophila* oogenesis (Becalska and Gavis, 2009; Duncan and Warrior, 2002; Januschke et al., 2002). Localization of *grk* mRNA, which is required for the formation of both major axes, is dependent on the minus-end-directed motor, dynein (MacDougall et al., 2003; Rom et al., 2007; Swan et al., 1999). Dynein is a large complex composed of four types of subunits: heavy, intermediate, light intermediate, and light chains (Hook and Vallee, 2006; Susalka and Pfister, 2000). Dynein regulates multiple cellular processes such as organelle transport, chromosome movements, nucleus-centrosome coupling, nuclear positioning, and spindle assembly (Anderson et al., 2009; Gusnowski and Srayko, 2011; Hebbar et al., 2008; Huang et al., 2011; Jodoin et al., 2012; Salina et al., 2002; Sitaram et al., 2012; Splinter et al., 2010; Stuchell-Brereton et al., 2011; Wainman et al., 2009). During *Drosophila* oogenesis, dynein is required for maintenance of fusome integrity, centrosome migration, oocyte determination, migration of the oocyte nucleus, transport into the oocyte of various mRNAs and proteins that play critical roles in axis determination of the embryo, and localization of these mRNAs and proteins within the oocyte (Bolivar et al., 2001; Januschke et al., 2002; Lei and Warrior, 2000; McGrail and Hays, 1997; Schnorrer et al., 2000; Swan et al., 1999).

We previously identified *asun* as a critical regulator of dynein localization during *Drosophila* spermatogenesis (Anderson et al., 2009). Dynein enrichment on the nuclear surface of G2 spermatocytes and round spermatids is lost in *asun* testes; as a result, *asun* male germ cells exhibit defects in nucleus-centrosome and nucleus-basal body coupling. Northern blot analysis of *Drosophila* tissues revealed that *asun* transcripts, while detected in the testes, were present at much higher levels in ovaries and early embryos, suggesting that *asun* may play roles in oogenesis and/or embryogenesis (Stebbings et al., 1998). In this study, we investigate the role of *asun* during *Drosophila* oogenesis by characterizing the phenotypes of females homozygous for a null allele of *asun* ($asun^{d93}$). We provide evidence to show that, similar to its role in spermatogenesis, *asun* is required for regulating dynein localization and dynein-mediated processes such as nuclear positioning, centrosome migration, and dorsal-ventral patterning during *Drosophila* oogenesis.

Materials and Methods

Drosophila stocks

y w was used as "wild-type" stock. $asun^{d93}$ and $asun^{f02815}$ alleles were previously described (Anderson et al., 2009; Sitaram et al., 2012). png^{50} and png^{1058} were gifts from T. Orr-Weaver (Whitehead Institute, Cambridge, MA).

Transgenesis

A 3.6-kb genomic fragment containing *asun* and its flanking regions (Fig. 1A) was PCR-amplified from BAC clone BAC37I18 (*Drosophila* Genomics Resource Center, Indiana University, IN) and subcloned into modified pCaSpeR4 for expression of full-length ASUN under control of its endogenous promoter (*asun* rescue construct). The following primers were used: 5'-GCA TGG CCG GCC ACT GCA CAA GAT T-3' and 5'-GAC TGG CGC GCC CCG AAG AAA AGT T-3'. Transgenic lines carrying *P[asun^{FL}]* were generated by *P*-element-mediated transformation via embryo injection (Rubin and Spradling, 1982).

Egg-laying assay

Females (2-4 days old) of each genotype tested were placed in a bottle with wild-type males, fattened with wet yeast for two days, and transferred to egg-collection chambers (five females and five wild-type males per chamber; two chambers per genotype) at 25°C. The number of eggs laid by females in each collection chamber was counted each day up to five days. Statistical analysis of the average number of eggs laid per day by females of the indicated genotypes was performed using an unpaired Student's *t*-test.

Cytological analysis of fixed ovaries

Ovaries were dissected and teased apart in Schneider's *Drosophila* medium (Life Technologies, Carlsbad, CA), fixed for 18 minutes in phosphate-buffered saline (PBS) plus 4% formaldehyde, washed for 2 hours in PBS plus 0.1% Triton X-100 (PBT),

incubated for 3 hours in PBT plus 5% normal goat serum (PBT-NGT), and incubated overnight at 4°C in PBT-NGT containing primary antibodies. Ovaries were then washed for 2 hours in PBT, incubated for 4 hours in PBT-NGT containing fluorophore-conjugated secondary antibodies, incubated in PBT plus 0.5 μg/ml DAPI for 6 minutes, washed for 2 hours in PBT, rinsed once in PBS, and mounted in Prolong Gold Antifade Reagent (Life Technologies). All steps were done at room temperature unless otherwise noted. For all experiments, ovaries from all genotypes tested were dissected in parallel and fixed/stained under identical conditions. For staining with anti-PLP antibody, the same protocol was followed except that ovaries were fixed with 100% methanol at -20°C for 10 minutes and rehydrated with decreasing concentrations of methanol in PBT before the first PBT wash.

Primary antibodies directed against the following proteins were used: dynein heavy chain (P1H4, 1:120; gift from T. Hays, University of Minnesota, Minneapolis, MN), PLP (1:500; gift from J. Raff, University of Oxford, Oxford, UK), lamin (ADL67.10, 1:500, Developmental Studies Hybridoma Bank [DSHB], Iowa City, IA), α-spectrin (3A9, 1:20, DSHB), and Gurken (1D12, 1:100, DSHB). Wide-field fluorescent images were obtained using an Eclipse 80i microscope (Nikon, Melville, NY) with Plan-Fluor 40X objective (all micrographs presented unless otherwise indicated). Confocal images were obtained with a Leica TCS SP5 confocal microscope and Leica Application Suite Advanced Fluorescence (LAS-AF) software using maximum-intensity projections of Z-stacks collected at 0.75 μm/step with a 63X objective. Fisher's exact test was used for statistical analyses of data.

Egg-chamber area analysis

Ovaries were fixed in 4% formaldehyde in PBS and stained with Alexa Fluor phalloidin (Life Technologies) to mark actin at the cell membranes. A Leica TCS SP5 confocal microscope was used to obtain images of optical sections of individual stage 10B egg chambers such that the largest areas were obtained. Areas of total egg chambers (oocyte + nurse cells) and oocytes alone were calculated using ImageJ software (National Institutes of Health, Bethesda, MD). 20 egg chambers were imaged per genotype for the calculation of egg chamber and oocyte area. Stage 10B egg chambers were identified by their follicle cell morphology.

Cytological analysis of fixed embryos

Embryos (0-2 hours) were collected on grape plates, dechorionated in 50% bleach, and devitellinized by shaking in a solution of methanol and heptane (1:1). Embryos were then stained with 1 μg/ml propidium iodide plus 1 mg/ml RNase A in PBT for 20 minutes, washed thrice with PBT, once with 50% methanol in PBT, and thrice with 100% methanol. Embryos were cleared and mounted in clearing solution (2:1 benzyl benzoate:benzyl alcohol). Wide-field fluorescent images were obtained using an Eclipse 80i microscope (Nikon) with Plan-Apo 20X objective.

Whole-mount RNA in situ hybridization

Whole-mount enzymatic in situ hybridization was performed as previously described (Suter and Steward, 1991). Fluorescent in situ hybridization was performed following the same protocol with the following modifications: Cy3-conjugated

digoxigenin antibody (Jackson ImmunoResearch Laboratories, West Grove, PA) replaced alkaline phosphatase-conjugated digoxigenin antibody, and the development step was omitted. Digoxigenin-labeled RNA probes were synthesized by in vitro transcription using a digoxigenin RNA labeling kit (Roche Applied Science, Indianapolis, IN). Antisense probes were prepared using the following full-length cDNA clones: *grk* (gift from A. Page-McCaw, Vanderbilt University School of Medicine, Nashville TN), *bcd*, and *osk* (*Drosophila* Genomics Resource Center). No significant signal was observed in control experiments using sense probes. Fluorescent in situ hybridization images were obtained using a Zeiss Apotome mounted on an Axio ImagerM2 with a 20X/0.8 Plan-Apochromat objective, and images were acquired with an AxioCam MRm camera (Zeiss, Thornwood, NY). Enzymatic in situ hybridization images were obtained using a Zeiss LumarV12 fluorescence stereomicroscope with a 1.5X Neolumar objective (zoomed to 80X), and images were acquired with an AxioCam MRc camera (Zeiss).

Immunoblotting

Ovaries from newly eclosed females or embryos (0-2 hour) were homogenized in nondenaturing lysis buffer (50 mM Tris-Cl pH 7.4, 300 mM NaCl, 5 mM EDTA, 1% Triton X-100) and analyzed by SDS-PAGE (25 μg protein/lane) and immunoblotting using standard techniques. Primary antibodies were used as follows: anti-dynein heavy chain (P1H4, 1:2000), anti-dynein intermediate chain (74.1, 1:250, Santa Cruz), anti-Cyclin B (F2F4, 1:100, DSHB), and anti-beta-tubulin (E7, 1:1000, DSHB). HRP-conjugated secondary antibodies were used to detect primary antibodies by chemiluminescence.

Results

asun is required for oogenesis

To address whether *asun* plays a role in *Drosophila* oogenesis, we first tested the fertility of females homozygous for a null allele of *asun* (*asun*^{d93}) that we previously generated (Fig. 3.1A) (Sitaram et al., 2012). We found that *asun*^{d93} females had a severely reduced egg-laying rate (average of <1 egg/day/female compared to 55 eggs/day/female for a control stock; Fig. 3.1B). Heterozygous *asun*^{d93} females, however, exhibited egg-laying rates comparable to that of control females, indicating that *asun* is a haplosufficient locus (Fig. 3.1B). To confirm that the egg-laying defect of *asun*^{d93} females was a direct consequence of loss of *asun* function, we generated transgenic *Drosophila* lines (*P[asun*^{FL}*]*) expressing full-length ASUN under control of its endogenous promoter (Fig. 3.1A). The egg-laying rate of *asun*^{d93} females was restored nearly to control levels by introduction of the *P[asun*^{FL}*]* transgene (Fig. 3.1B).

We then sought to determine if *asun*^{d93} females had gross defects in oogenesis that could account for their reduced egg-laying rate. We dissected whole ovaries from two-day old female flies fattened by addition of wet yeast paste to their food. Ovaries isolated from a majority of *asun*^{d93} females were considerably smaller in size than those isolated from wild-type females or *asun*^{d93} females carrying the *P[asun*^{FL}*]* transgene (herein referred to as "rescued *asun*^{d93}" line) (Fig. 3.1C-F). To test if the reduced size of *asun*^{d93} ovaries was due to a decrease in egg chamber and/or oocyte size, we measured the area of stage 10B egg chambers and oocytes (as a representative stage) isolated from wild-type or *asun*^{d93} females. We found no striking difference in stage 10B egg chamber

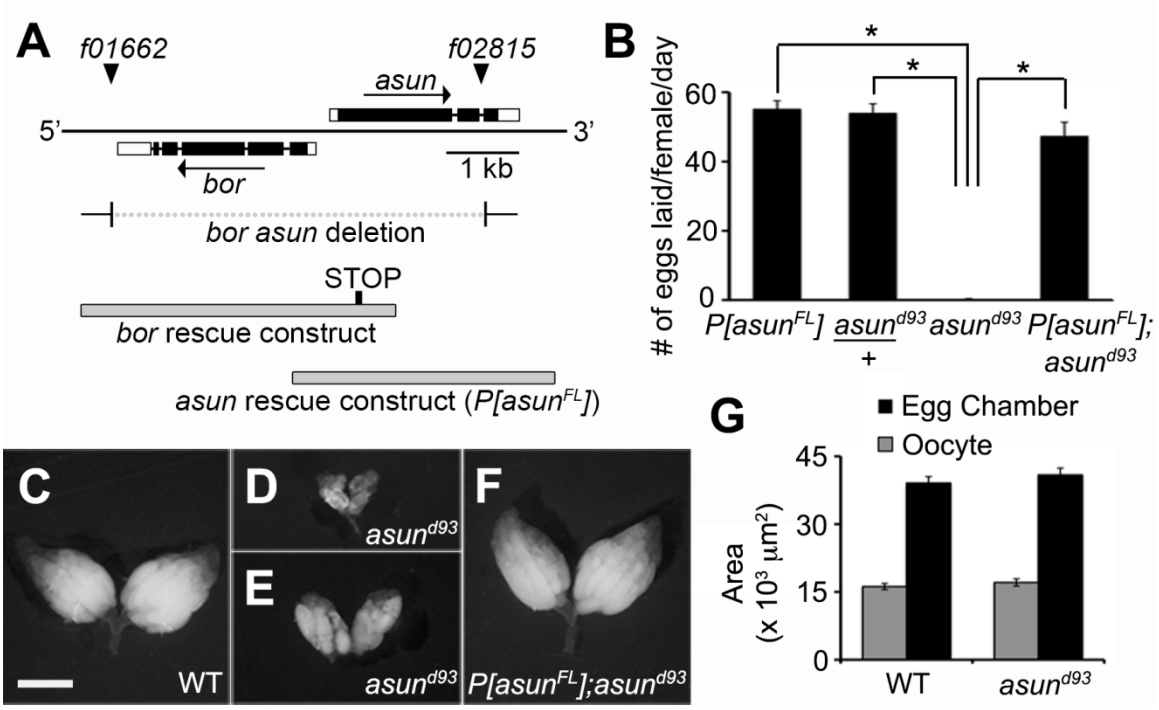

Figure 3.1. Reduced egg-laying rates and ovary size of *asun*^{d93} females. **(A)** Schematic diagram of the *asun* gene region. Coding regions and UTRs are represented as filled and unfilled boxes, respectively, introns as thin lines, and *piggyBac* transposons *f01662* and *f02815* as triangles. Breakpoints of a *bor asun* two-gene deletion (generated through FLP-mediated recombination of FRT sites within the transposons) and design of a *bor* transgene are shown; as previously described, *asun*^{d93} flies are homozygous for the *bor asun* two-gene deletion and *bor* transgene (Sitaram et al., 2012). Design of the full-length *asun* transgene (*P[asun*^{FL}*]*) generated for this study is also shown. (B) Quantification of egg-laying rates for females of the indicated genotypes. Asterisks, $p<0.0001$. (C-F) Whole ovaries dissected from 2-day old fattened females of the indicated genotypes. Ovaries from *asun*^{d93} females (D,E) are highly reduced in size compared to those from wild-type (C) or *P[asun*^{FL}*];asun*^{d93} rescue (F) females. Scale bar, 1 mm. (G) Quantification of the average area of stage 10B egg chambers and oocytes isolated from females of the indicated genotypes.

or oocyte area between these genotypes (Fig. 3.1G), suggesting that the reduction in *asun*^{d93} ovary size might be due to defects in proper progression to later developmental stages of oogenesis.

Whereas individual ovarioles isolated from wild-type or rescued *asun*^{d93} ovaries were clearly ordered by increasing stages of development (Fig. 3.2A,C), the arrangement of a majority of ovarioles isolated from *asun*^{d93} ovaries was highly disorganized (Figs 3.2B, 3.1E). Ovarioles from the larger *asun*^{d93} ovaries typically contained early- and late-stage egg chambers with a paucity of intermediate stages (for example, Fig. 3.2B shows an *asun*^{d93} ovariole with two mature oocytes to the right immediately adjacent to a stage 5 egg chamber). Thus, the mature oocytes that are occasionally produced by *asun*^{d93} females tend to accumulate within the ovaries. These findings suggest that, in addition to abnormal oogenesis, *asun*^{d93} females have defects in related processes downstream of oogenesis such as ovulation, mating, sperm storage, fertilization, and/or egg laying (Sun and Spradling, 2013). We did not observe any overt differences, however, in the morphological appearance of the reproductive glands (parovaria, spermathecae, or seminal receptacles) of *asun*^{d93} females compared to wild-type controls (Fig. 3.2D,E).

asun^{d93} egg chambers exhibit structural defects

We occasionally observed abnormal numbers of oocytes and nurse cells within *asun*^{d93} egg chambers. Whereas wild-type egg chambers normally contain 15 nurse cells and one oocyte, we found that 20% of *asun*^{d93} egg chambers (compared to <1% and <4% of wild-type and rescued *asun*^{d93} egg chambers, respectively) contained an increased number of germ cells, possibly as a consequence of fusion of two or more egg chambers

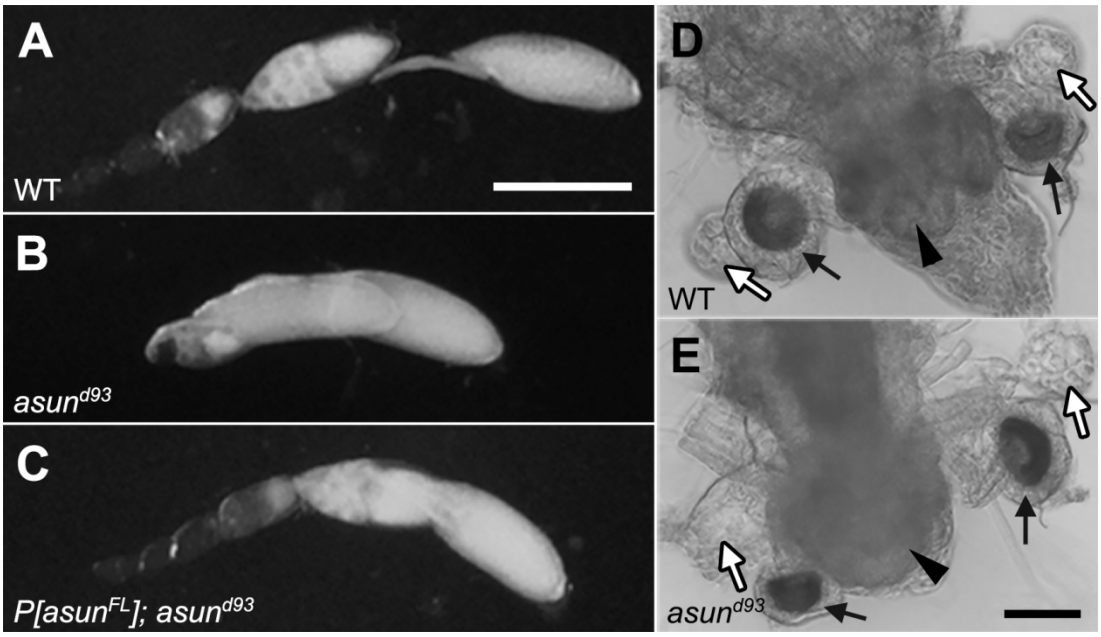

Figure 3.2. Defective ovulation with normal reproductive glands in *asun*^{d93} females. (A-C) Micrographs of ovarioles isolated from fattened females of indicated genotypes. Mature eggs, right; germaria, left. Wild-type and rescued *asun*^{d93} ovarioles (A and C, respectively) contain a linear sequence of egg chambers of increasing developmental stages. *asun*^{d93} ovarioles (B) contain juxtaposed mature and early egg chambers with intermediate stages missing. Scale bar, 500 μm. (D,E) Phase-contrast images of female reproductive glands from wild-type and *asun*^{d93} females. As in wild type (D), a seminal receptacle (black arrowhead), a pair of spermathecae (black arrows), and a pair of parovaria (white arrows) are present in *asun*^{d93} (E) females. Scale bar, 200 μm.

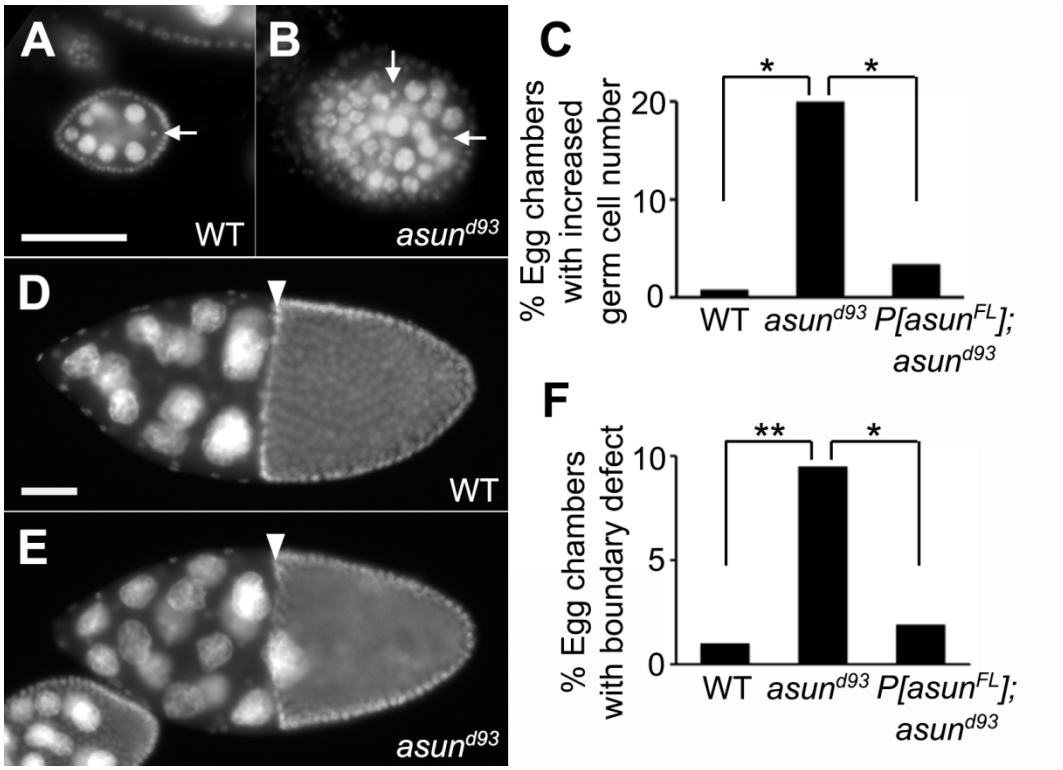

Figure 3.3. Defects in the cellular composition and arrangement of *asun*^{d93} egg chambers. (A,B) DAPI-stained stage 5 egg chambers from wild-type and *asun*^{d93} ovaries (dorsal, top; anterior, left). Wild-type egg chambers (A) contain 15 polyploid nurse cells and 1 haploid oocyte. *asun*^{d93} ovaries occasionally contain compound/fused egg chambers (B). White arrows, oocyte nuclei. (C) Quantification of fused egg chamber defect in ovaries of indicated genotypes (>250 chambers scored per genotype). Asterisks, $p<0.0001$. (D,E) DAPI-stained stage 10 egg chambers from wild-type and *asun*^{d93} ovaries (dorsal, top; anterior, left). There is a clear boundary of follicle cells (white arrowhead) between the nurse cells and the oocyte in stage 10 wild-type egg chambers (D). Nurse cells occasionally extend past this boundary in *asun*^{d93} stage 10 egg chambers (E). (F) Quantification of nurse cell-oocyte boundary defect in ovaries of indicated genotypes (>200 chambers scored per genotype). Single asterisk, $p=0.0006$; double asterisk, $p<0.0001$. Scale bars, 50 μm.

(Fig. 3.3A-C). Furthermore, we occasionally observed disruption of the follicle cell border that clearly demarcates nurse cells and the oocyte in wild-type egg chambers at or beyond stage 10 (Fig. 3.3D); in 10% of *asun*^{d93} egg chambers at or beyond stage 10 (compared to 1% and 2% of wild-type and rescued *asun*^{d93} egg chambers, respectively), nurse cells appeared to protrude across this border and into the oocyte (Fig. 3.3E,F).

asun-derived embryos do not phenocopy _png_ mutants

ASUN was identified in an *in vitro* screen for substrates of the serine/threonine protein kinase encoded by *pan gu* (*png*), a critical regulator of the S-M cell cycles of early embryogenesis in *Drosophila* (Fenger et al., 2000; Lee et al., 2005; Shamanski and Orr-Weaver, 1991). Based on this association, we assessed *asun*^{d93}-derived embryos for the presence of *png*-like phenotypes. We found that *asun*^{d93}-derived embryos did not exhibit the giant nuclei phenotype that is characteristic of *png*-derived embryos (Fig. 3.4A-D). Furthermore, we did not observe genetic interaction between *png* and *asun*: introduction of a single copy of *asun*^{f02815} into the *png*^{50} background failed to modify the *png*^{50} giant nuclei phenotype (Fig. 3.4E). PNG kinase mediates derepression of translation during early embryogenesis, thereby ensuring that Cyclin B levels are sufficiently high to promote mitotic entry (Fenger et al., 2000; Lee et al., 2001; Vardy and Orr-Weaver, 2007). In contrast, immunoblotting revealed normal levels of cyclin B in *asun*^{d93}-derived embryos, suggesting that ASUN is not required for this function (Fig. 3.4F). We therefore concluded that ASUN does not function as a substrate of the PNG kinase during early embryogenesis in *Drosophila*.

asun^{d93}-derived embryos have dorsal-ventral patterning defects

While performing experiments with *asun*^{d93}-derived embryos, we noticed abnormalities in the appearance of the dorsal appendages, a pair of paddle-shaped eggshell structures located on the anterior-dorsal surface of the embryo that form as a result of normal dorsal-ventral patterning events (Schupbach, 1987; Spradling, 1993). We used a previously reported scheme for classifying dorsal appendage defects to characterize this phenotype in *asun*^{d93}-derived embryos (Fig. 3.5A) (Lei and Warrior, 2000). Class I embryos have a pair of distinct dorsal appendages (wild-type appearance) that are positioned much closer to each other in class II embryos, fused at the base in class III embryos, and fused along their entire lengths in class IV embryos; class V embryos lack visible dorsal appendages. We found that a majority (54%) of *asun*^{d93}-derived embryos had dorsal appendage defects (compared to 1% and 3% for wild-type and rescued *asun*^{d93} embryos, respectively), including 23% in class V (Fig. 3.5B). These data suggest that *asun* is required for proper dorsal-ventral patterning of the *Drosophila* embryo. We also examined *asun*^{d93}-derived embryos for the presence of the micropyle, another eggshell structure located at the anterior end of the embryo that is required for sperm entry (Spradling, 1993). We found that a small fraction of *asun*^{d93}-derived embryos lacked a micropyle (6% compared to 1% in wild-type and *asun*^{d93}-derived embryos; Fig. 3.6).

grk mRNA localization is abnormal in *asun*^{d93} oocytes

The dorsal appendage defects of *asun*^{d93}-derived embryos resemble those reported for embryos produced by females homozygous for a hypomorphic allele of the dynein

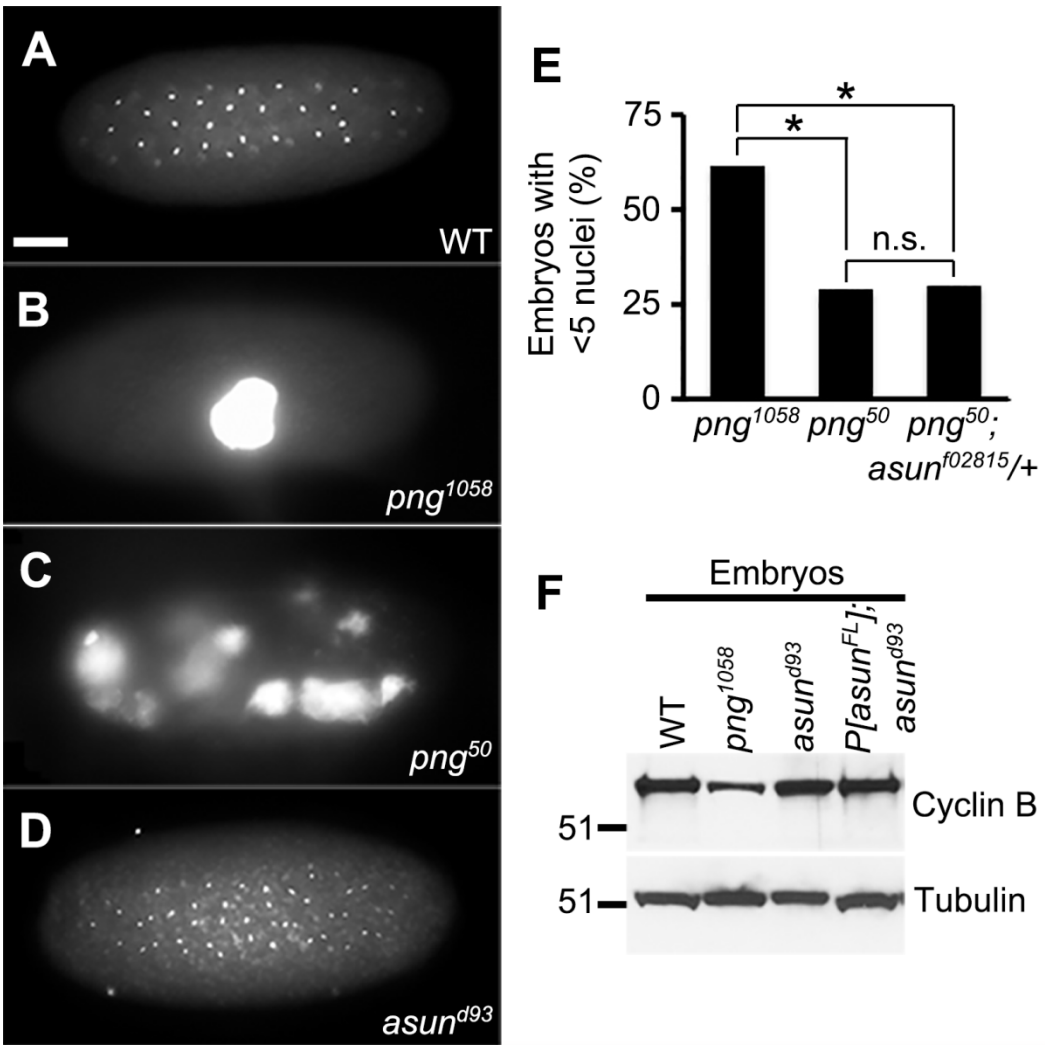

Figure 3.4. *asun*^{d93}-derived embryos do not exhibit the giant nuclei phenotype. (A-D) DNA-stained embryos (0-2 hour) from wild-type, *png*, or *asun*^{d93} females. Embryos from wild-type (A) and *asun*^{d93} (D) females exhibit a normal DNA staining pattern, unlike the giant nuclei phenotype observed in the strong (B) and weak (C) alleles of *png*. Scale bar, 50 μm. (E) Quantification of embryos (0-2 hour) containing fewer than 5 nuclei (>350 embryos scored per genotype). Asterisks, $p<0.0001$; n.s., not significant. (F) Immunoblot showing wild-type levels of Cyclin B in extracts of embryos (0-2 hour) from *asun*^{d93} and rescued *asun*^{d93} females. Cyclin B levels are reduced in *png*^{1058}-derived embryos. Tubulin, loading control.

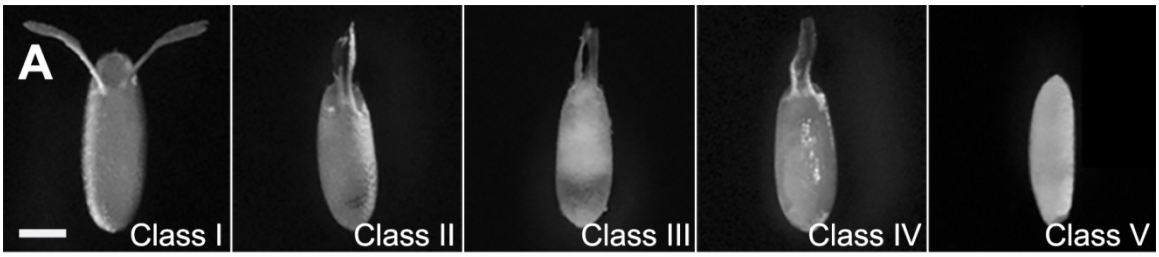

B

Maternal genotype	Dorsal appendage phenotype				
	Class I	Class II	Class III	Class IV	Class V
yw	98.8%	0.9%	0.1%	0.1%	0.1%
$asun^{d93}$	46.4%	12.7%	7.3%	10.7%	22.9%
$P[asun^{FL}];asun^{d93}$	96.9%	0.7%	0.6%	0.5%	1.3%

Figure 3.5. Ventralization of $asun^{d93}$-derived eggs. (A) Eggs laid by $asun^{d93}$ females. Anterior, top; dorsal side facing outward. Classification scheme for ventralized eggs is adapted from (Lei and Warrior, 2000). Class I eggs appear wild type with a pair of dorsal appendages in the anterior-dorsal region. Dorsal appendages in class II eggs are positioned abnormally close to each other. Class III and class IV eggs contain dorsal appendages that are partially fused at the base and completely fused along the length, respectively. Class V eggs lack dorsal appendages. Scale bar, 250 μm. (B) Quantification of dorsal appendage phenotypes in embryos from wild-type, $asun^{d93}$, and rescued $asun^{d93}$ females (>200 embryos scored per genotype).

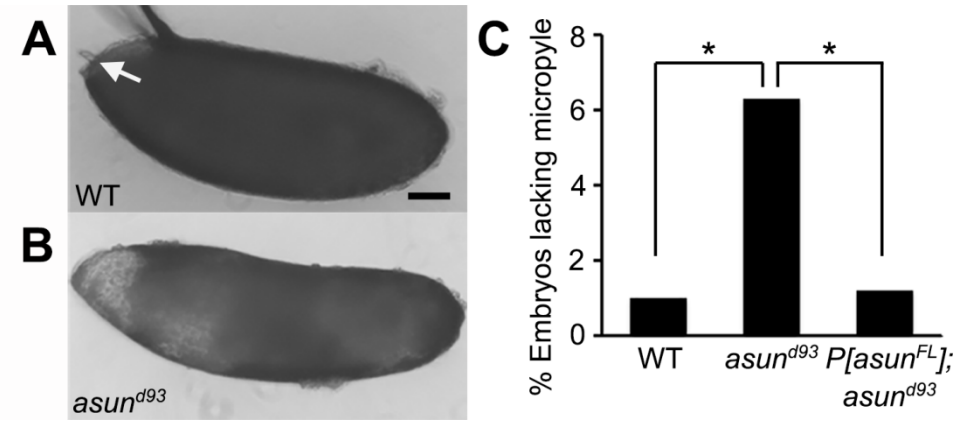

Figure 3.6. Lack of a micropyle is a low-penetrance phenotype of *asun*-derived embryos. (A,B) Phase-contrast images of whole embryos derived from wild-type (A) or *asun*^{d93} (B) females. Anterior, left; dorsal, top. The micropyle (white arrow) is occasionally absent in embryos derived from *asun*^{d93} females. Scale bar, 200 μm. (C) Quantification of wild-type and *asun*^{d93}-derived embryos lacking a micropyle (>200 embryos scored per genotype). Asterisks, $p<0.005$.

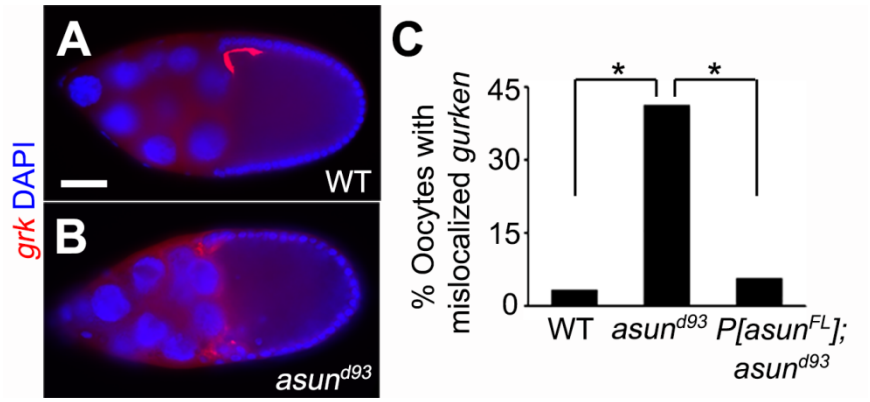

Figure 3.7. Diffuse localization of *grk* transcripts in *asun*^{d93} oocytes. (A-B) Fluorescent in situ hybridization of stage 9 egg chambers using *grk* probe (red). Dorsal, top; anterior, left. *grk* mRNA localization is tightly restricted to the anterior-dorsal region of the oocyte in wild-type egg chambers (A). In *asun*^{d93} egg chambers, *grk* transcripts are more diffusely localized throughout the anterior oocyte (B). Scale bars, 50 μm. (C) Quantification of abnormal *gurken* mRNA localization in wild-type, *asun*^{d93}, and rescued *asun*^{d93} egg chambers (>100 chambers scored per genotype) by fluorescent in situ hybridization. Asterisks, $p<0.0001$.

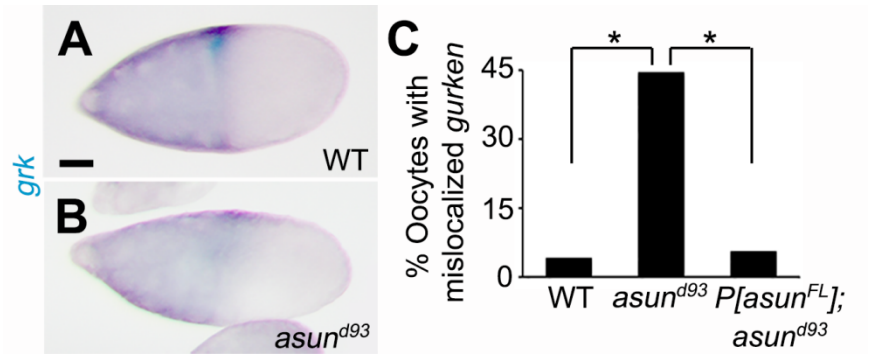

Figure 3.8. Diffuse localization of *grk* transcripts in *asun*^{d93} oocytes. (A-B) Enzymatic in situ hybridization of stage 9-10 egg chambers using *grk* probe (dorsal, up; anterior, left). *grk* mRNA localization is tightly restricted to the anterior-dorsal region of the oocyte in wild-type egg chambers (A). In *asun*^{d93} egg chambers, *grk* transcripts are more diffusely localized throughout the anterior oocyte (B). Scale bars, 50 μm. (C) Quantification of diffusely localized *gurken* transcripts in wild-type, *asun*^{d93}, and rescued *asun*^{d93} oocytes (>100 chambers scored per genotype) by enzymatic in situ hybridization. Asterisks, $p<0.0001$.

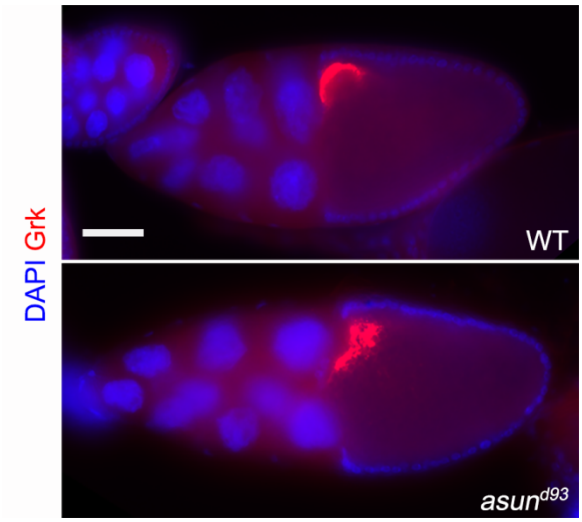

Figure 3.9. Localization of Grk protein in *asun*^{d93} oocytes. Immunostaining of stage 10 wild-type and *asun*^{d93} egg chambers using Gurken antibody (red). DNA is in blue. Anterior, left; dorsal, top. Gurken protein localizes normally to the anterior-dorsal region of *asun*^{d93} oocytes, but occasionally with a more diffuse pattern than that observed in wild-type oocytes. Scale bar, 50 μm.

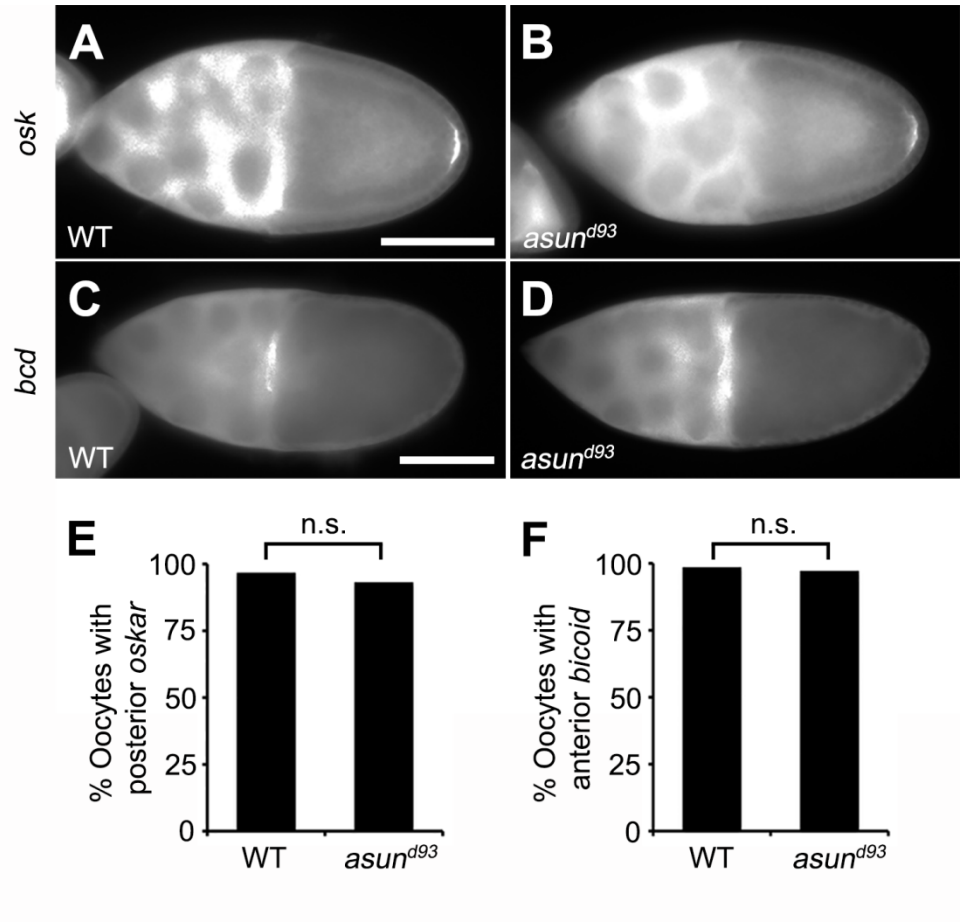

Figure 3.10. Wild-type localizations of *osk* and *bcd* transcripts in *asun*^{d93} oocytes. Fluorescent in situ hybridizations of stage 10 egg chambers using *osk* and *bcd* probes (dorsal, up; anterior, left). (A,B) Representative images showing normal localization of *osk* mRNA to the posterior pole of the oocyte in wild-type (A) and *asun*^{d93} (B) egg chambers. (C,D) Representative images showing normal localization of *bcd* mRNA to the anterior region of the oocyte in wild-type (C) and *asun*^{d93} (D) egg chambers. Scale bars, 100 μm. (E,F) Quantification of properly localized *osk* (E) and *bcd* (F) transcripts in wild-type and *asun*^{d93} egg oocytes (>100 chambers scored per sample). n.s., not significant.

accessory factor, *Lis-1* (Lei and Warrior, 2000). The defect in dorsal-ventral patterning in *Lis-1*-derived embryos was attributed to loss of anterior-dorsal anchoring of *grk* mRNA in the oocyte. This asymmetric anchoring of *gurken* transcripts allows Grk, a TGFα-like protein that acts as a ligand, to asymmetrically activate the EGF receptor homolog, Torpedo/DER, specifically within the dorsal-anterior follicle cells (Neuman-Silberberg and Schupbach, 1993). Dynein light chain, a cargo-binding subunit of dynein, directly binds to *grk* mRNA and is required for its tight localization to the anterior-dorsal region of the oocyte (Rom et al., 2007).

To determine if the dorsal-ventral patterning defects observed in $asun^{d93}$ egg chambers could be due to a loss of dynein-mediated regulation of *grk* transcripts, we assessed the localization of *grk* mRNA using both enzymatic and fluorescent in situ hybridization methods. We consistently observed a loss of the tight anterior-dorsal localization of *grk* transcripts (in 42% and 45% of $asun^{d93}$ egg chambers by enzymatic and fluorescent in situ hybridization, respectively (compared to 4% and 6% of wild-type and rescued $asun^{d93}$ egg chambers, respectively), suggesting that the ventralization of $asun^{d93}$-derived embryos could be a consequence of loss of dynein regulation by ASUN (Figs 3.7, 3.8). In contrast, Grk protein appeared to localize normally to the anterior-dorsal region of the oocyte in $asun^{d93}$ egg chambers, albeit occasionally in a more diffuse manner than what we observed in wild-type egg chambers (Fig. 3.9). We did not observe any defects, however, in the localization of *osk* or *bcd* transcripts, which encode anterior-posterior patterning factors, in $asun^{d93}$ egg chambers (Fig. 3.10).

Dynein localization is disrupted in *asun*^{d93} oocytes

We previously identified *asun* as a critical regulator of dynein localization in *Drosophila* spermatogenesis and in cultured mammalian cells (Anderson et al., 2009; Jodoin et al., 2012; Sitaram et al., 2012). To determine if *asun* performs the same function during *Drosophila* oogenesis, we examined the localization of dynein in *asun*^{d93} oocytes using antibodies against the dynein heavy chain. Dynein accumulates within the oocyte in region 2b of the germarium and remains there throughout oogenesis (Li et al., 1994). In early egg chambers of wild-type females, dynein is enriched around the oocyte nucleus, and it localizes to the posterior pole of the oocyte in stage 9 chambers (Fig. 3.11A,D). We observed a significant loss of dynein localization to these sites in >35% of *asun*^{d93} egg chambers (compared to <1% and <3% of wild-type and rescued *asun*^{d93} egg chambers, respectively; Fig. 3.11A-G). Immunoblotting revealed normal levels of dynein heavy and intermediate chains in *asun*^{d93} ovaries, suggesting that the loss of dynein localization was not due to instability of core components of the complex (Fig. 3.11H).

Nucleus-centrosome coupling and nuclear positioning are abnormal in *asun*^{d93} oocytes

The dynein motor is required at multiple steps during *Drosophila* oogenesis, and its role in this system has been well characterized (Januschke et al., 2002; Lei and Warrior, 2000; McGrail and Hays, 1997; Schnorrer et al., 2000; Swan et al., 1999). Because we observed a loss of dynein localization in *asun*^{d93} ovaries, we sought to determine if dynein-mediated processes (in addition to *grk* transcript localization) were disrupted. We observed oocyte nucleus-centrosome coupling defects in 18% of *asun*^{d93}

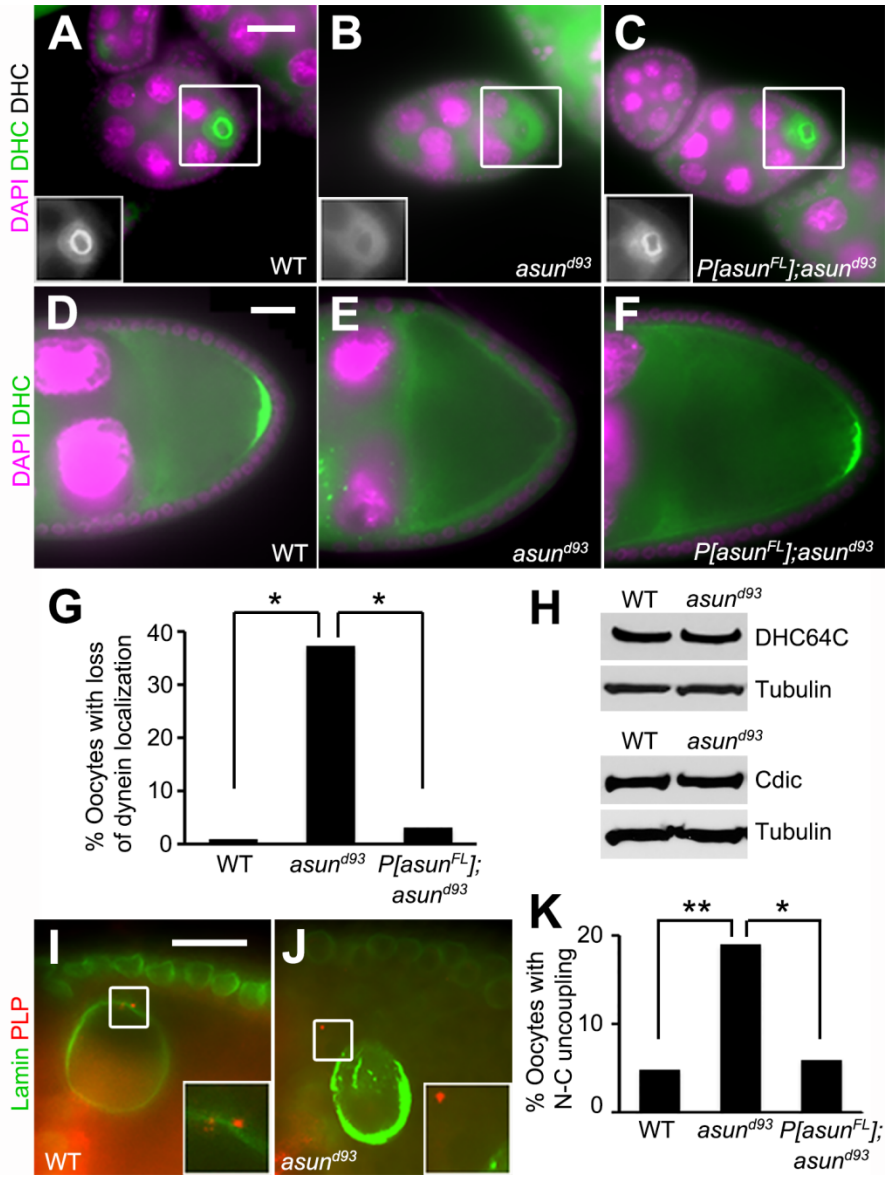

Figure 3.11. Loss of dynein localization and nucleus-centrosome coupling in *asun*^{d93} oocytes. (A-F) Stage 5 (A-C) and stage 9 (D-F) egg chambers stained for dynein heavy chain (green; grayscale in inset) and DNA (magenta). Dorsal, top; anterior, left. *asun*^{d93} oocytes (B,E) have reduced dynein localization relative to wild-type (A,D) or rescued *asun*^{d93} (C,F) oocytes. (G) Quantification of loss of dynein localization in egg chambers of indicated genotypes (>200 chambers scored per genotype). Asterisks, $p<0.0001$. (H) Immunoblot showing wild-type levels of dynein heavy (DHC64C) and intermediate (Cdic) chains in extracts of *asun*^{d93} ovaries. Loading control, tubulin. (I,J) Stage 10 egg chambers stained for lamin (green; nuclear envelope marker) and PLP (red; centriole marker) (enlarged insets shown below). Dorsal, top; anterior, left. Unlike wild-type oocytes (I), centrosomes are not tightly coupled to the nuclear envelope in *asun*^{d93} oocytes (J). (K) Quantification of nucleus-centrosome coupling defect in ovaries of indicated genotypes (>100 chambers scored for wild-type and *asun*^{d93}; >50 chambers scored for rescue). Single asterisk, $p<0.05$; double asterisk, $p<0.0025$. Scale bars, 20 μm.

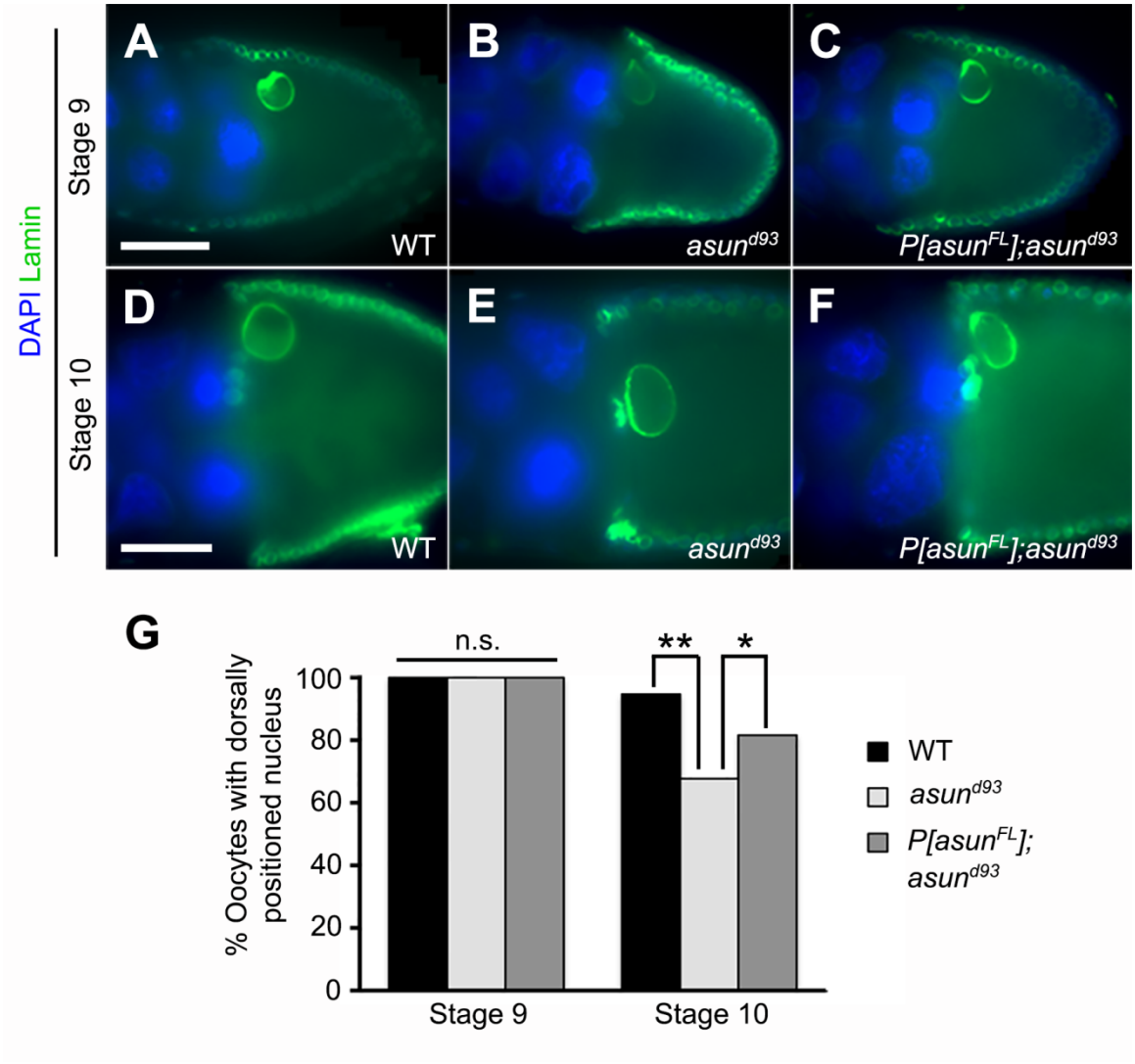

Figure 3.12. Loss of anterior-dorsal positioning of the oocyte nucleus in *asun*^{d93} egg chambers. (A-F) Stage 9 (A-C) and stage 10 (D-F) egg chambers stained for lamin (green; nuclear envelope marker) and DNA (blue). Dorsal, top; anterior, left. Wild-type anterior-dorsal positioning of the oocyte nucleus (A,D) is observed in stage 9 *asun*^{d93} oocytes (B), but this positioning is not maintained in stage 10 *asun*^{d93} oocytes (E). Scale bars, 50 μm. (G) Quantification of anterior-dorsal positioning of oocyte nucleus in wild-type, *asun*^{d93}, and rescued *asun*^{d93} stage 9 and 10 egg chambers (>100 chambers scored per genotype). Single asterisk, $p<0.006$; double asterisk, $p<0.0001$; n.s., not significant.

egg chambers (compared to 5% and 6% in wild-type and rescued *asun*^{d93} egg chambers, respectively), suggesting that, similar to its role in male germ cells, *Drosophila* ASUN promotes dynein-mediated association between the nucleus and centrosomes during oogenesis (Fig. 3.11I-K).

We next assessed the positioning of the oocyte nucleus in *asun*^{d93} egg chambers. The oocyte nucleus, which normally migrates from the posterior of the oocyte to the future anterior-dorsal region in stage 7 egg chambers, is incorrectly positioned in the absence of dynein or its accessory factors (Januschke et al., 2002; Lei and Warrior, 2000; Swan et al., 1999). This phenotype has been attributed to a failure in the dynein-dependent anchoring of the nucleus at the anterior-dorsal of the oocyte (Zhao et al., 2012). We found that oocyte nuclei in stage 9 egg chambers from wild-type and *asun*^{d93} females were similarly positioned, suggesting that nuclear migration takes place normally in *asun*^{d93} females (Fig. 3.12A-C,G). By stage 10, however, only 67% of *asun*^{d93} egg chambers (compared to 94% of wild-type egg chambers) exhibited normal anterior-dorsal anchoring of the oocyte nucleus, suggesting that the attachment of the oocyte nucleus at that position is not maintained in the absence of ASUN; introduction of the genomic *asun* transgene into the *asun*^{d93} background partially rescued this defect with 81% of these egg chambers containing a properly positioned oocyte nucleus (Fig. 3.12D-G).

asun^{d93} egg chambers exhibit defects in centrosome migration

At the end of the four mitotic germ cell divisions, centrosomes migrate from the nurse cells into the pro-oocyte in a manner dependent on a large cytoplasmic organelle called the fusome, which extends into all 16 cells within a cyst through the ring canals

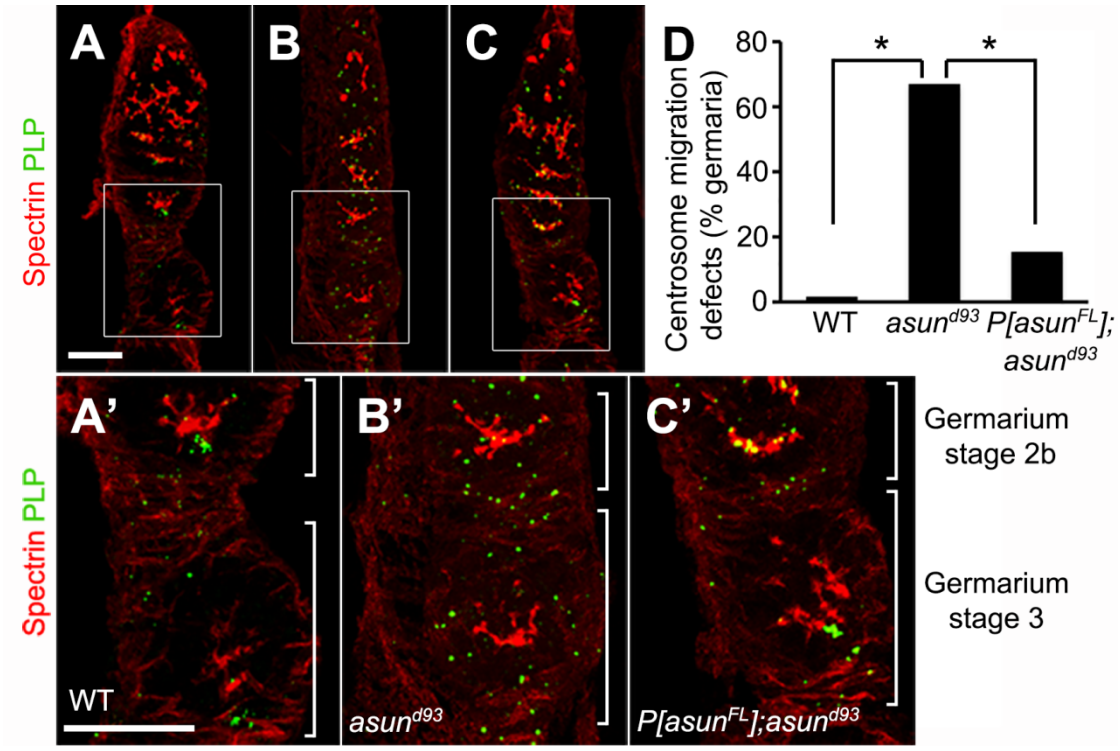

Figure 3.13. Centrosome migration defects of *asun*^{d93} germaria. (A-C) Projections of confocal sections of wild-type, *asun*^{d93}, and rescued *asun*^{d93} germaria stained for spectrin (red; fusome marker) and PLP (green; centriole marker). Enlarged insets shown below. Anterior, top; dorsal, left. Within wild-type cysts, most centrosomes have migrated from the nurse cells into the oocyte (located at posterior of egg chamber) by stage 2b of the germarium (A, A'). Centrosomes do not properly migrate into the oocyte in *asun*^{d93} germaria and are found distributed throughout the entire cyst (B, B'). Centrosome migration occurs in rescued germaria but is delayed (C, C'). Scale bars, 20 μm. (D) Quantification of centrosome migration defects in wild-type, *asun*^{d93}, and rescued *asun*^{d93} germaria (>100 germaria scored per genotype). Asterisks, $p<0.0001$.

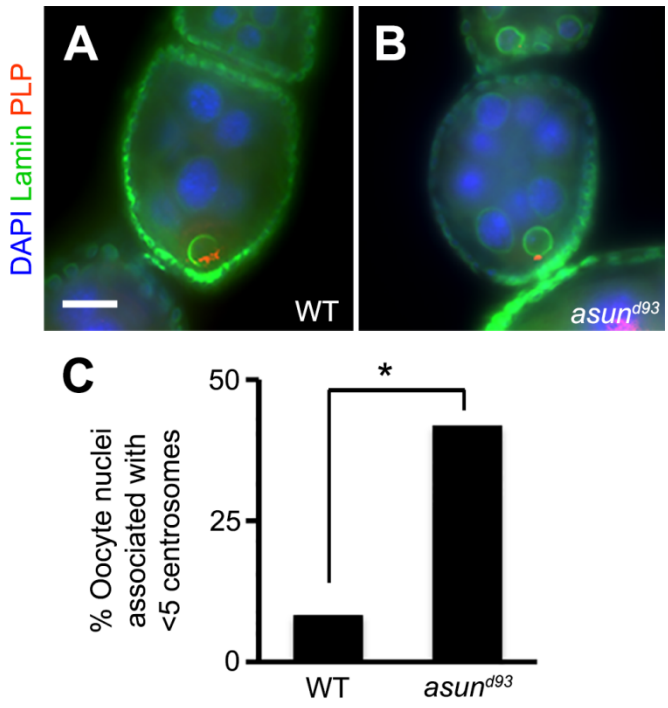

Figure 3.14. Reduced centrosome number in *asun*^{d93} oocytes. (A,B) Stage 5 egg chambers stained for lamin (green; NE marker), PLP (red; centriole marker), and DNA (blue). Anterior, top; dorsal, right. Fewer centrosomes are associated with the oocyte nucleus in *asun*^{d93} (B) than wild-type (A) egg chambers. Scale bar, 20 μm. (C) Quantification of reduced centrosome number in wild-type and *asun*^{d93} ovaries (>40 chambers scored per genotype). Asterisk, $p<0.0001$.

(Bolivar et al., 2001; Grieder et al., 2000). Mutation of dynein heavy chain has been reported to result in loss of fusome integrity and centrosome migration (Bolivar et al., 2001; McGrail and Hays, 1997).

We assessed *asun*^{d93} germaria for fusome integrity and centrosome migration. We observed no obvious differences in fusome structure in wild-type and *asun*^{d93} germaria (Fig. 3.13A,A',B,B'). *asun*^{d93} germaria, however, exhibited defects in centrosome migration. Most nurse cell centrosomes have migrated to the oocyte (located at the posterior of the egg chamber) by stage 2B in wild-type germaria (Fig. 3.13A,A',D). Centrosome migration was disrupted in 67% of *asun*^{d93} stage 3 germaria (compared to <2% in wild-type stage 3 germaria) with centrosomes still distributed throughout the cyst (Fig. 3.13B,B',D). Centrosome migration was significantly restored in rescued *asun*^{d93} ovaries (with only 15% of their stage 3 germaria showing disruption of centrosome migration) (Fig. 3.13C,C',D). The timing of this process, however, appeared to be delayed: in contrast to wild-type ovaries, most centrosomes were found scattered throughout stage 2B germaria of rescued *asun*^{d93} ovaries (Fig. 3.13C'). Possibly as a result of the loss of centrosome migration in *asun*^{d93} germaria, we observed a decreased number of centrosomes (fewer than five) associated with the oocyte nucleus in 42% of *asun*^{d93} stage 5 egg chambers (compared to 8% of wild-type egg chambers; Fig. 3.14).

Discussion and Future Directions

We report herein that *asun* is a critical regulator of *Drosophila* oogenesis. *Drosophila* females that are homozygous for a null allele of *asun* (*asun*^{d93}) have highly reduced egg-laying rates as a result of defects in oogenesis as well as in processes

downstream of oogenesis. We have focused in this study on characterizing the oogenesis defects in *asun*^{d93} females and have found that eggs laid by these females are ventralized. This phenotype may be secondary to the improper localization of mRNA transcripts encoding the dorsal fate determinant, Grk, in *asun*^{d93} oocytes. The dynein motor, which is required for transport of *grk* mRNA during *Drosophila* oogenesis, is also mislocalized in a significant fraction of *asun*^{d93} oocytes. We have also determined that other reported dynein-mediated processes such as nuclear positioning, nucleus-centrosome coupling, and centrosome migration are also defective in *asun*^{d93} egg chambers.

We previously identified ASUN as a regulator of dynein localization during *Drosophila* spermatogenesis and in cultured human cells (Anderson et al., 2009; Jodoin et al., 2012). Loss of ASUN in *Drosophila* spermatocytes results in the loss of perinuclear localization of dynein at the G2-M transition, leading to defects in coupling between the nucleus and centrosomes, spindle assembly, chromosome segregation, and cytokinesis during the meiotic divisions (Anderson et al., 2009). Similar defects were observed in mitotically dividing cultured human cells following siRNA-mediated down-regulation of the human homologue of ASUN (Jodoin et al., 2012).

The role of dynein during *Drosophila* oogenesis has been well characterized. The dynein motor has been implicated in maintaining fusome integrity, centrosome migration, and oocyte determination within the germarium (Bolivar et al., 2001; McGrail and Hays, 1997; Mische et al., 2008; Swan et al., 1999). Additionally, dynein is critical for the transport and normal localizations of various patterning factors throughout oogenesis as well as maintenance of the anterior-dorsal positioning of the oocyte nucleus in late-stage

egg chambers (Clark et al., 2007; Duncan and Warrior, 2002; Januschke et al., 2002; Lan et al., 2010; Lei and Warrior, 2000; Rom et al., 2007; Swan et al., 1999).

We have observed disruption of several of these dynein-regulated processes in *asun*^{d93} ovaries, likely as a result of the loss of dynein localization that occurs in the absence of ASUN. *asun*^{d93} ovaries exhibit defects in centrosome migration, *grk* mRNA localization, and nuclear positioning. *asun*^{d93} ovaries exhibit additional defects in the structure of the egg chamber and in the coupling between the oocyte nucleus and centrosomes. Dynein has been shown to facilitate nucleus-centrosome coupling in other systems, and fused egg chambers have been observed in *Drosophila* dynein light chain mutants; thus, these defects of *asun*^{d93} egg chambers could potentially also be due to loss of dynein function (Anderson et al., 2009; Bolhy et al., 2011; Dick et al., 1996; Jodoin et al., 2012; Malone et al., 2003; Robinson et al., 1999; Sitaram et al., 2012; Splinter et al., 2010).

All reported dynein-mediated processes occurring during *Drosophila* oogenesis, however, were not affected in *asun*^{d93} ovaries. The fusome, a cytoplasmic organelle, is highly disorganized in ovaries that lack dynein or its accessory factor, LIS-1 (Bolivar et al., 2001; McGrail and Hays, 1997). The normal asymmetric distribution of the fusome within the different cells of a female germline cyst plays an important role in the determination of the future oocyte (de Cuevas and Spradling, 1998; Lin and Spradling, 1995; McKearin, 1997). Not surprisingly, *Drosophila* lines mutant for dynein or LIS-1 exhibit defects in oocyte determination (McGrail and Hays, 1997; Mische et al., 2008; Swan et al., 1999). We observed, however, that fusome structure within *asun*^{d93} germaria was indistinguishable from that of wild-type females, and oocyte determination appeared

to occur normally in *asun*^{d93} ovaries (P.S. and L.A.L., unpublished observations). The migration of centrosomes from the nurse cells into the oocyte within the germaria is considered to be a fusome-dependent process (Bolivar et al., 2001; Grieder et al., 2000). Despite our observations of wild-type fusome structure in *asun*^{d93} germaria, they exhibit defects in centrosome migration. This discrepancy suggests that either an additional factor required for centrosome migration is affected in *asun*^{d93} mutants, the function (but not structure) of the fusome is compromised in *asun*^{d93} germaria, or that the fusomes of *asun*^{d93} germaria have subtle structural defects that we were unable to detect.

asun^{d93}-derived embryos exhibit defects in dorsal-ventral patterning. We found that the localization of *grk* mRNA to the anterior-dorsal region of the oocyte is lost in late-stage *asun*^{d93} egg chambers, suggesting that the ventralization of *asun*^{d93}-derived eggs could be a consequence of this defect. Surprisingly, we only occasionally observed mild defects in the localization of the Grk protein in *asun*^{d93} egg chambers. We speculate that our method of detecting Grk protein by immunofluorescence, which generates a strong signal, may have caused us to underestimate the severity of mislocalization of Grk protein in *asun*^{d93} egg chambers. Alternatively, the function of the Grk protein could be compromised due to its dissociation from the oocyte nucleus as a result of nuclear mislocalization in late-stage *asun*^{d93} egg chambers. Similar defects in the localization of *grk* mRNA as well as the dissociation between Grk protein and the oocyte nucleus have been reported in *Drosophila* females mutant for a dynein light chain (Rom et al., 2007). Furthermore, additional unknown defects within the signaling cascade activated by the Grk ligand might exist within the dorsal-anterior follicle cells in *asun*^{d93} egg chambers that could contribute to the ventralization phenotype.

The oogenesis defects reported herein for *asun*^{d93} females appear to be only partially penetrant. Centrosome migration, the most penetrant ovarian phenotype that we observed (with 65% of germaria showing defects), occurs at a relatively early stage of oogenesis. The remaining defects reported in *asun*^{d93} egg chambers and *asun*^{d93}-derived embryos had a maximum penetrance of ~50%, with some, such as the structural defects of egg chambers, occurring at a frequency of less than 20%. In contrast, the defects observed in *asun*^{d93} testes are generally present at a higher frequency (Sitaram et al., 2012). Additionally, we observed that females that are heterozygous for the null allele of *asun* as well as females that are homozygous for a weak allele of *asun* (*asun*^{f02815}) do not exhibit any obvious defects in oogenesis, whereas spermatogenesis is severely compromised in *asun*^{f02815} males (P.S. and L.A.L., unpublished observations) (Anderson et al., 2009). Taken together, these data suggest that either ASUN plays a less critical role during *Drosophila* oogenesis in comparison to spermatogenesis and/or that other factors can better compensate for the loss of ASUN in this system.

ASUN was previously identified as an in vitro substrate of the PNG kinase (Lee et al., 2005). PNG has been reported to critically regulate the syncytial cell cycles during early embryogenesis in *Drosophila* by maintaining proper levels of Cyclin B (Fenger et al., 2000; Shamanski and Orr-Weaver, 1991). We observed no genetic interaction between *asun*^{d93} and a weak allele of *png*. *asun*^{d93}-derived embryos did not exhibit the giant nuclei phenotype typical of embryos derived from *png* females, nor were Cyclin B levels reduced in *asun*^{d93}-derived embryos. These results suggest that either *asun* does not function as a substrate of PNG during *Drosophila* embryogenesis, or that the loss of *asun* can be compensated by some other factor during this developmental window.

ASUN has also been identified as a functional component of an evolutionarily conserved nuclear complex known as the Integrator in cultured mammalian cells (Chen et al., 2012; Malovannaya et al., 2010). Integrator, composed of at least 14 distinct subunits (including ASUN), mediates 3'-end processing of small nuclear RNAs (Baillat et al., 2005; Chen and Wagner, 2010). We have recently determined that several Integrator subunits, like ASUN, are required in cultured human cells for recruitment of dynein motors to the nuclear envelope during mitosis (Jodoin et al., 2013). The nuclear localization of ASUN has been shown to be critical for perinuclear dynein recruitment in cultured human cells as well as during *Drosophila* spermatogenesis (Jodoin et al., 2013). Our current model for the role of ASUN in controlling dynein localization is that ASUN, in conjunction with other subunits of the Integrator complex, mediates the proper processing of a specific mRNA target encoding a critical regulator of dynein recruitment to the nuclear envelope in cultured human cells. The high degree of conservation between *Drosophila* ASUN and its human homologue, and our data showing that *Drosophila* ASUN can be used to rescue loss of mammalian ASUN and vice versa, makes it likely that *Drosophila* ASUN functions in a similar manner to regulate the localization of dynein during oogenesis and spermatogenesis (Anderson et al., 2009; Jodoin et al., 2012).

In addition to the defects in oogenesis that we report herein, the capacity of $asun^{d93}$ females to produce mature eggs that accumulate within the ovary suggests that these females also have defects downstream of oogenesis. Given that we have been able to ascribe a majority of the defects in $asun^{d93}$ mutants to disruption of dynein-mediated processes, it is possible that these downstream phenotypes of $asun^{d93}$ females may represent novel functions of dynein. Alternatively, these processes may be directly

regulated by ASUN or by a different target of the ASUN/Integrator complex. It would therefore be of importance in future studies to determine if ASUN functions as a component of the Integrator complex in this system and if so, to identify the targets of this complex required for normal progression through *Drosophila* oogenesis.

CHAPTER IV

DOMINANT MODIFIER SCREEN TO IDENTIFY POTENTIAL INTERACTORS AND REGULATORS OF *asun*

Introduction

We have previously reported a role for *asun* in the fertility of *Drosophila* males (Anderson et al., 2009; Sitaram et al., 2012). *asun* spermatocytes undergo prophase arrest with defects in nucleus-centrosome coupling; cells that overcome this arrest also exhibit defects in meiotic spindle assembly, chromosome segregation, and cytokinesis. Similarly, defects in the attachment between the nucleus and basal body were observed in post-meiotic stages of spermatogenesis in *asun* testes. We observed reduction of perinuclear dynein in *asun* male germ cells that we hypothesized causes loss of nucleus-centrosome and nucleus-basal body coupling. These data suggest that ASUN is a critical regulator of dynein localization during *Drosophila* spermatogenesis (Anderson et al., 2009; Sitaram et al., 2012).

The mechanism by which ASUN regulates the localization of dynein is not well understood. During spermatogenesis and in cultured human cells, ASUN localization fluctuates between the nucleus and cytoplasm in a cell cycle-dependent manner (Anderson et al., 2009; Jodoin et al., 2012). Using a transgene expressing GFP-tagged ASUN, we were able to show that during *Drosophila* spermatogenesis, ASUN localizes within the nucleus of early to mid-G2 spermatocytes and within both the nucleus and cytoplasm of late G2 spermatocytes (Anderson et al., 2009). The cytoplasmic appearance

of ASUN coincides with the perinuclear enrichment of dynein, suggesting that this pool of ASUN may play a direct role in recruiting dynein to the nuclear surface during spermatogenesis.

To help place ASUN within a molecular network, we sought to identify additional genes involved in the regulation of dynein localization during *Drosophila* spermatogenesis by screening for enhancement or suppression of a hypomorphic *asun* phenotype upon loss of one copy of other genes. This general approach, known as a dominant modifier genetic screen, has been used successfully to define molecular pathways, such as the Ras signaling pathway, in *Drosophila* (Therrien et al., 2000).

The phenotype we chose to use for the dominant modifier screen was the multi-nucleated spermatid phenotype of *asun* testes. Defective chromosome segregation and cytokinesis in *asun* testes can be easily identified by the morphological appearance of immature spermatids, which are the cells that are formed at the end of the second meiotic division. Wild-type spermatids have a very distinct appearance: they contain a phase-light nucleus and a phase-dark mitochondrial aggregate (the Nebenkern) of the same size. Secondary to aberrant meiotic divisions, ~66% of immature spermatids from testes homozygous for a weak allele of *asun* (*asun*^{f02815}) contain one large, irregularly shaped Nebenkern and multiple smaller nuclei. We previously employed this phenotype in demonstrating genetic interaction between *asun* and components of dynein and dynactin complexes (Anderson et al., 2009). Loss of a single copy of genes encoding dynein heavy chain or the Glued subunit of dynactin enhanced the multi-nucleated phenotype of *asun*^{f02815}. These data provide proof of principle that the screening phenotype is highly

sensitive and that additional components of ASUN-mediated dynein localization could potentially be identified by this screening approach.

To perform the screen, we utilized a publicly available, predefined set of deficiency lines on the 2nd chromosome known as the "Bloomington Deficiency Kit for 2". Deficiency kits have been used successfully for dominant modifier screens in *Drosophila* (Lee et al., 2001). This kit covers almost the entirety of the 2nd chromosome with a minimum number of deletions, and all of these deletions are molecularly mapped. Each deficiency within this kit deletes a large number of genes, thereby making it feasible to screen all the genes located within ~98% of the second chromosome (nearly 6000 euchromatic genes) with a minimum number of stocks and fly crosses. We chose to initiate the screen using deficiencies on the 2nd chromosome because *asun* is located on the third chromosome, so crosses to introduce a single copy of a given deficiency into the $asun^{f02815}$ background are easier and faster for 2nd chromosome deficiencies than for 3rd chromosome deficiencies (which would require recombination). The use of chromosomal deficiencies on the X chromosome (most of which are hemizygous lethal) is complicated by our need to obtain male flies to assess a spermatogenesis phenotype. The 4th chromosome of *Drosophila* is relatively tiny and contains few genes, so it is rarely used in this type of genetic screen.

Materials and Methods

Drosophila stocks

y w was used as "wild-type" stock. *piggyBac* insertion line *asun*^{f02815} was from the Exelixis Collection (Harvard Medical School, Boston, MA). The 2nd chromosome deficiency stocks were from Bloomington Stock Center (Indiana University, IN).

Cytological analysis of live testes

Live testes cells were prepared for phase-contrast microscopy as described (Anderson et al., 2009). Individual round spermatids from a minimum of six pairs of testes per genotype were classified as either mono-nucleated or multi-nucleated based on their appearance under a phase-contrast microscope. The percent of multi-nucleated spermatids was calculated for each genotype (>500 spermatids scored per genotype). Wild-type and mutant testes were isolated and prepared for microscopy under identical conditions for all experiments.

Results

Our lab has previously described that <1% of spermatids from wild-type males are multi-nucleated, while ~67% of spermatids from *asun*^{f02815} males are multi-nucleated (Anderson et al., 2009). We re-examined this phenotype in our control fly stocks (*y w* and *asun*^{f02815}) and were able to reproduce the previously reported results.

Table 4.1. Results of dominant modifier screen for *asun* interactors

Bloomington stock #	Chromosome region deleted	% Multi-nucleated spermatids	Modification of *asun* phenotype
24958	21B7--21B8	67%	n.s.[a]
8673	21C2--21E2	68%	n.s.
24959	22D5--22E1	34%	Suppression[b]
9610	23B7--23C3	85%	Enhancement[c]
23677	23F6--24A2	80%	n.s.
9600	24D4--24D8	38%	n.s.
9605	25B10--25C1	35%	Suppression
8835	25C1--25C4	68%	n.s.
8674	25C4--25C8	65%	n.s.
9560	25E5--25F3	87%	Enhancement
9615	26F1--27A2	70%	n.s.
23676	27D6--27F2	64%	n.s.
7807	28E1--28F1	32%	Suppression
9704	28E8--29B1	60%	n.s.
8836	28F5--29B1	35%	Suppression
9631	29D5--29F8	70%	n.s.
9715	30C7--30F2	65%	n.s.
9503	31B1--31D9	65%	n.s.
1469	31C--32E5	88%	Enhancement
9635	31D7--31D11	89%	Enhancement

9637	31D7--31E1	68%	n.s.
9642	31F5--32B4	57%	n.s.
9641	32B1--32C1	53%	n.s.
9505	32C1--32C1	92%	Enhancement
9716	32C1--32F2	15%	Suppression
9718	32F2--33B6	99%	Enhancement
23152	34D1--34F1	64%	n.s.
7839	36E2--36E6	66%	n.s.
23156	36E3--36F2	90%	Enhancement
9508	36F5--36F10	85%	Enhancement
9510	40A5--40E5	57%	n.s.
32253	41F11--42A13 (Estimated)	98%	Enhancement
24335	44A4--44F1 44A4--44C4 (Estimated)	61%	n.s.
23665	45C4--45F4	30%	Suppression
23682	46B2--46C7	55%	n.s.
23686	46E1--46F3	94%	Enhancement
23666	46F1--47A9	76%	n.s.
9626	48C5--48E4	70%	n.s.
24929	48F1--49A1	98%	Enhancement
23688	49A4--49A10	80%	n.s.
24989	49B10--49E6	70%	n.s.
7871	49F1--49F10	70%	n.s.

23169	49F4--50A13	85%	Enhancement
23690	50B6--50C18	58%	n.s.
24385	50C3--50F1	90%	Enhancement
24407	50C6--50D2	90%	Enhancement
7875	50D4--50E4	52%	n.s.
7876	50E4--50F6	52%	n.s.
24933	51C2--51D1	75%	n.s.
25078	53C1--53C6	71%	n.s.
7888	53C8--53D2	65%	n.s.
24356	53D14--54A1	53%	n.s.
9596	54B2--54B17	65%	n.s.
24379	54B16--54C3	60%	n.s.
7890	54C10--54D5	50%	n.s.
24371	54D2--54E9	99%	Enhancement
7893	55B9--55C1	75%	n.s.
27354	56D8--56D14 (Estimated)	100%	Enhancement
30588	56E1--56F11 (Estimated)	58%	n.s.
7896	56F11--56F16	79%	n.s.
6609	56F12--57A4	2%	Suppression
24424	56F16--57B1	99%	Enhancement
26554	57A2--57B3 (Estimated)	80%	n.s.
30590	57D2--57D10 (Estimated)	50%	n.s.

26516	57D12--58A3 (Estimated)	98%	Enhancement
25430	58A2--58F1	82%	n.s.
25431	58F3--59A1	94%	Enhancement
24380	60B8--60C4	81%	n.s.
27352	60C2--60D14 (Estimated)	69%	n.s.
25441	60E11--60F2	68%	n.s.
24758	60F5--60F5	75%	n.s.

Single copies of 2nd chromosome deficiencies were introduced into the *asun*^{f02815} background. Testes were dissected from flies heterozygous for the deficiency and homozygous for *asun*^{f02815}, and the percent of multi-nucleated spermatids was determined. The percent of multi-nucleated spermatids was compared to that for testes homozygous for *asun*^{f02815} (the screening phenotype; ~67% multi-nucleated spermatids) to determine if the introduction of the deficiency in one copy enhanced or suppressed the *asun* phenotype.

[a]n.s.= not significant

[b]Suppression ≤ 35% multi-nucleated spermatids

[c]Enhancement ≥ 85% multi-nucleated spermatids

We sought to identify genes that could either enhance or suppress the multi-nucleated spermatid phenotype of *asun*^{f02815}. Out of 190 deficiency lines available in the Bloomington 2nd chromosome deficiency kit, we were able to test 73 deficiencies, in single copy, for their capacity to enhance or suppress this phenotype by performing multi-generation crosses to introduce the deficiencies into the hypomorphic *asun* (*asun*^{f02815}) background. We calculated the percent of multi-nucleated spermatids observed in males that were heterozygous for a 2nd chromosome deficiency and homozygous for the *f02815* transposon insertion.

For our screen, we used an arbitrary cutoff of ≥85% multi-nucleated spermatids to define enhancement of the multi-nucleated spermatid phenotype and an arbitrary cutoff of ≤35% to define suppression of the phenotype. Using this scoring system, we determined that out of the 73 deficiencies screened, single copies of 22 deficiency lines had the capacity to enhance the *asun*^{f02815} phenotype, and 7 deficiency lines suppressed this phenotype. The list of deficiencies tested, the region of the 2nd chromosome deleted, and the percent of multi-nucleated spermatids observed for each deficiency are summarized in Table 4.1.

Discussion and Future Directions

We have performed the first step of a large-scale genetic screen to identify potential interactors of *asun*. We have tested 73 out of the 190 2nd chromosome deficiency lines for their capacity to modify the multi-nucleated phenotype of *asun*. We found that a total of 29 deficiency lines strongly modified the *asun* phenotype. We placed these deficiencies into one or more of five broad classes based on candidate genes

mapped to the deleted chromosomal regions (Tables 4.2, 4.3, 4.4, and 4.5). To make the classification simpler, different candidate genes uncovered by a single deficiency were used to place that deficiency chromosome within more than one class; however, if a given deficiency could be placed into more than one class based on a single candidate gene, we chose to place such a deficiency into whichever class would best fit the gene in question.

The first class comprises those deficiencies in which one or more genes previously reported to play a role in spermatogenesis have been deleted (Table 4.2). Eight out of the 29 deficiencies obtained as hits from the screen lack at least one gene with known roles in spermatogenesis. Examples of such genes are *no mitochondrial derivative* (*nmd*) deleted in the deficiency line BL1469, *mitoshell* (*mtsh*) deleted in the deficiency line BL8836, and *Peroxin 13* (*Pex13*) deleted in the deficiency line BL23169.

The second class of deficiencies lack (in one copy) one or more genes that are related to the dynein motor or are involved in the various functions of dynein within the cell (Table 4.3). ASUN has been shown to be a critical regulator of dynein localization and nucleus-centrosome coupling in *Drosophila* spermatocytes and in cultured human cells; therefore, we would expect other proteins involved in this process to dominantly modify the *asun* phenotype (Anderson et al., 2009). Additionally, we have previously demonstrated that loss of single copies of genes encoding certain subunits of dynein or dynactin complexes can modify the *asun* phenotype. Fourteen out of the 29 hits belong to the second class, as each line lacks a single copy of at least one gene that could potentially be involved in the cellular functions of dynein. As ASUN regulates nucleus-centrosome coupling by regulating dynein localization, we have included deficiencies

Table 4.2. Class 1 deficiencies: spermatogenesis regulators

Bloomington stock #	Candidate genes deleted		
	Flybase ID	**Gene symbol**	**Gene name**
9560	FBgn0051989	*Cap-D3*	*Chromosome associated protein D3*
	FBgn0031715	*tomb*	*tombola*
	FBgn0031728	*Hsp60C*	*Hsp60C*
7807	FBgn0011230	*poe*	*purity of essence*
	FBgn0010287	*Trf*	*TBP-related factor*
	FBgn0261822	*Bsg*	*Basigin*
1469	FBgn0005322	*nmd*	*no mitochondrial derivative*
	FBgn0032269	*w-cup*	*world cup*
9716	FBgn0000287	*salr*	*spalt-related*
9508	FBgn0261349	*Mst36Fa*	*Male-specific transcript 36Fa*
	FBgn0086681	*Mst36Fb*	*Male-specific transcript 36Fb*
23169	FBgn0033812	*Pex13*	*Peroxin 13*
25431	FBgn0034740	*nsr*	*novel spermatogenesis regulator*
8836	FBgn0262598	*mtsh*	*mitoshell*

This table includes deficiencies that dominantly modify the *asun*^{f02815} phenotype and lack one or more genes that are known to play a role in *Drosophila* spermatogenesis. The specific candidate genes within each deficiency have been listed.

Table 4.3. Class 2 deficiencies: genes related to the dynein motor and its cellular function

Bloomington stock #	Candidate genes deleted		
	Flybase ID	Gene symbol	Gene name
24959	FBgn0028570	*robl22E*	*Dynein light chain, roadblock-type*
9560	FBgn0002525	*Lam*	*Lamin*
1469	FBgn0032243	*Klp31E*	*Kinesin-like protein at 31E*
	FBgn0026431	*Grip75*	*Grip75*
	FBgn0027868	*Nup107*	*Nucleoporin 107kD*
	FBgn0021761	*Nup154*	*Nucleoporin 154kD*
	FBgn0262647	*Nup160*	*Nucleoporin 160kD*
	FBgn0040232	*cmet*	*CENP-meta*
	FBgn0040233	*cana*	*CENP-ana*
9716	FBgn0021761	*Nup154*	*Nucleoporin 154kD*
	FBgn0262647	*Nup160*	*Nucleoporin 160kD*
	FBgn0040232	*cmet*	*CENP-meta*
	FBgn0040233	*cana*	*CENP-ana*
9505	FBgn0021761	*Nup154*	*Nucleoporin 154kD*
9718	FBgn0032368	*spag4*	*sperm-associated antigen 4*
	FBgn0032390	*dgt2*	*dim γ-tubulin 2*
23156	FBgn0023096	*btv*	*beethoven*
23686	FBgn0265512	*mlt*	*mulet*
24929	FBgn0266111	*ana3*	*anastral spindle 3*
23169	FBgn0013765	*cnn*	*centrosomin*
	FBgn0086757	*cbs*	*centrosomin's beautiful sister*
24385	FBgn0033912	*RpS23*	*Ribosomal protein S23*
24371	FBgn0003545	*sub*	*subito*
27354	FBgn0003887	*βTub56D*	*β-Tubulin at 56D*
24424	FBgn0034530	*Rcd6*	*Reduction in Cnn dots 6*

This table includes deficiencies that dominantly modify the *asun*^{f02815} phenotype and lack one or more genes that are related to the dynein motor or are involved in the various functions of dynein within the cell. The specific candidate genes within each deficiency have been listed.

that lack genes encoding nuclear envelope proteins or centrosomal proteins in this category. For example, the gene *sperm-associated antigen 4* (*spag4*) encoding the *Drosophila* homolog of the mammalian SUN protein sperm-associated antigen 4, deleted in the deficiency line BL9718, has been shown to be required for spermatogenesis by facilitating dynein localization and nucleus-centrosome coupling (Kracklauer et al., 2010). This is very similar to the role played by ASUN during spermatogenesis. Additionally, this category includes deficiency lines that uncover genes encoding dynein subunits (*robl22E* and *btv*), tubulin (*βtub56D*), lamin (*lam*), as well as several nucleoporins (*Nup107*, *Nup160*, and *Nup154*).

The third class of deficiencies lack (in one copy) one or more genes involved in mRNA binding and/or processing (Table 4.4). Seven out of the 29 hits obtained from the screen belong to this category; examples include *bancal* (*bl*) deleted in the deficiency line BL24424 and the *FLASH ortholog* (*FLASH*) deleted in the deficiency line BL23169. We expected to find such hits because recent studies have identified ASUN as a functional component of the nuclear Integrator complex (Chen et al., 2012; Malovannaya et al., 2010). Integrator is a nuclear complex that plays a crucial role in the 3'-end processing of small nuclear RNAs. Our lab has further demonstrated that, in addition to ASUN, several other components of the Integrator complex are required for dynein recruitment to the nuclear surface in cultured human cells (Jodoin et al., 2013). We also showed that the pool of ASUN localized within the nucleus is critical for the recruitment of dynein to the nuclear surface during *Drosophila* spermatogenesis and in cultured human cells. These data have led to our current model in which ASUN functions within the nuclear

Table 4.4. Class 3 deficiencies: genes involved in mRNA binding and/or processing

Bloomington stock #	Candidate genes deleted		
	Flybase ID	**Gene symbol**	**Gene name**
9610	FBgn0010263	*rbp9*	*RNA-binding protein 9*
9560	FBgn0014189	*Hel25E*	*Helicase at 25E*
	FBgn0041719	*snRNA:U4:25F*	
	FBgn0024191	*sip1*	*septin interacting protein 1*
1469	FBgn0067622	*LSm4*	*Like Sm protein 4*
23169	FBgn0033806	*FLASH*	*FLASH ortholog*
24385	FBgn0086895	*pea*	*peanuts*
	FBgn0000662	*fl(2)d*	*female lethal d*
24407	FBgn0000662	*fl(2)d*	*female lethal d*
24424	FBgn0015907	*bl*	*bancal*

This table includes deficiencies that dominantly modify the *asun*^{f02815} phenotype and lack one or more genes that are involved in mRNA binding and/or processing. The specific candidate genes within each deficiency have been listed.

Table 4.5. Class 4 deficiencies: genes with moderate to high expression in testes

Bloomington stock #	Candidate genes deleted		
	Flybase ID	**Gene symbol**	**Gene name**
9635	FBgn0032219	*Tsp42A*	
32253	FBgn0033042	*CG4995*	*Tetraspanin 42A*

This table includes deficiencies that dominantly modify the *asun*^{f02815} phenotype and lack one or more genes that moderate to high expression within the testes. The specific candidate genes within each deficiency have been listed. This category does not include deficiencies that are found within any of the first three categories.

Integrator complex to regulate the localization of dynein. According to this model, Integrator is required for the processing of snRNA that then plays a role in the splicing of one or more mRNA transcripts encoding a regulator(s) of dynein localization. Therefore, reduction of the levels of components of the spliceosome, or of proteins involved in other mRNA processing events, via reduction of their gene dosage, could conceivably lead to modification of the *asun* phenotype. None of the genes encoding known components of the Integrator complex, however, are deleted in the 73 deficiency lines tested in this preliminary screen thus explaining why we did not identify any of the components of the Integrator complex as candidate *asun* interactors.

The fourth class of deficiencies lack (in one copy) one or more genes known to have moderate to high expression within the *Drosophila* testes, although there is little else known about their functions (Table 4.5). Two out of the 29 deficiencies - BL32253 with *Tetraspanin 42A* (*Tsp42A*) deleted (in one copy) and BL9635 with *CG4995* deleted (in one copy) – belong to this category. The deficiencies included in this category could not be placed in any of the first three categories. The final and fifth class includes those deficiencies for which we were unable to identify any obvious candidate genes of interest. Four out of the 29 deficiencies (BL9605, BL23665, BL6609, and BL26516) belonged to this category. These two categories of deficiencies would be most interesting to pursue further to identify novel proteins that play a role in spermatogenesis and/or are part of the molecular network of ASUN.

One disadvantage of having performed the genetic screen by testing for modification of only one *asun* phenotype is that we might have missed those genes among the deficiencies tested that could dominantly modify a different *asun* phenotype.

The multi-nucleated phenotype that we used for the screen, however, is a phenotype observed at nearly the very end of spermatogenesis. Therefore, we are more likely to obtain a larger number of false positives from the screen as a result of haplo-insufficiency of the allele tested rather than being unable to identify all the genes that could potentially modify the *asun* phenotype.

To follow up on the above-mentioned hits, firstly, we would have to confirm the genetic interaction by repeating the experiment and by determining if the deficiency line is haplo-insufficient. If a single copy of the chromosome deletion, in an otherwise wild-type background, also exhibits a multi-nucleated spermatid phenotype, it is possible that the perceived genetic interaction is actually the result of an independent effect of the deficiency on spermatogenesis. After testing the hits from the screen for the absence of haplo-insufficiency, the next step would be to test smaller deficiencies (publicly available stocks from the Bloomington Stock Center) within the large genomic region deleted in the deficiency lines identified in our screen to narrow down the potential candidates. The ultimate goal would be to identify individual genes that dominantly modify the $asun^{f02815}$ phenotype. Any genes identified in this manner would then require further characterization to determine their molecular placement in ASUN-dependent processes.

CHAPTER V

CONCLUDING REMARKS

Summary

Our lab previously characterized *asun* as a novel regulator of dynein localization in *Drosophila* spermatogenesis and in cultured human cells (Anderson et al., 2009; Jodoin et al., 2012). Male flies homozygous for the $asun^{f02815}$ allele, which is predicted to encode a truncated version of the ASUN protein, are sterile (Anderson et al., 2009). *asun* spermatocytes and spermatids exhibit loss of perinuclear dynein resulting in nucleus-centrosome coupling defects in spermatocytes and nucleus-basal body coupling defects in spermatids. As a result of the nucleus-centrosome coupling defects, *asun* spermatocytes undergo a prophase arrest, and spermatocytes that overcome this arrest exhibit defects in spindle formation and in further progression through meiosis. Similarly, siRNA-mediated knockdown of human ASUN in cultured human cells resulted in loss of perinuclear dynein and nucleus-centrosome coupling, indicating that this role of ASUN is conserved through phyla (Jodoin et al., 2012).

During *Drosophila* spermatogenesis, we determined that the *asun* phenotype is dominantly enhanced by the introduction of a single mutant copy of a dynein accessory factor, *Lis-1* (Sitaram et al., 2012). Human *LIS1* was initially identified as the causative factor of the human brain disorder, Lissencephaly-1, when lost in one copy. *Drosophila Lis-1* is essential for the viability of the fly. During *Drosophila* spermatogenesis, we observed that flies homozygous for a hypomorphic allele of *Lis-1* ($Lis\text{-}1^{k11702}$) are male

sterile. *Lis-1* spermatocytes and spermatids exhibit loss of perinuclear dynein as well as the nucleus-centrosome and nucleus-basal body coupling defects observed in *asun* mutants. *Lis-1* male germ cells also exhibit additional defects such as failure of centrosomes to detach from the cell cortex at the G2-M transition of meiosis and defects in the coupling of the Nebenkern with the nucleus and basal body. We also observed all of these *Lis-1* defects in flies null for the dynein light chain, *tctex-1*, suggesting that *Lis-1* is required for all dynein-mediated processes, whereas *asun* is required only for a subset of dynein-mediated processes during *Drosophila* spermatogenesis. Additionally, we observed that ASUN is required for the perinuclear localization of LIS-1 and that the *Drosophila* homologs of LIS-1 and ASUN co-localize and co-immunoprecipitate in cultured human cells. These data, along with the data showing genetic interaction between *Lis-1* and *asun* mentioned earlier, led us to propose a model in which *Lis-1* and *asun* cooperate to regulate dynein localization and dynein-mediated processes during *Drosophila* spermatogenesis.

Northern blot analysis of *asun* mRNA expression in *Drosophila* tissues revealed that, while *asun* is expressed within *Drosophila* testes, its expression is much higher in *Drosophila* ovaries and embryos (Stebbings et al., 1998). Additionally, ASUN was previously identified as an *in vitro* substrate of the PAN GU kinase, which is critical during the syncytial divisions of early embryogenesis (Lee et al., 2005). These data suggested that ASUN might play an important role during oogenesis and/or embryogenesis. We used flies carrying a null allele of *asun* ($asun^{d93}$) to determine whether ASUN is required for these processes. We observed no genetic interaction between *asun* and *png*, and *asun*-derived embryos did not exhibit the giant nuclei

phenotype that is characteristic of *png*-derived embryos, suggesting that *asun* may not function within the molecular network of *png* during early embryogenesis in *Drosophila*.

We did, however, find that *asun* plays an essential role during *Drosophila* oogenesis. $asun^{d93}$ females have a highly reduced egg laying rate and more than half of the eggs laid by these females exhibit various degrees of ventralization. This ventralization is likely due to the mislocalization of mRNA transcripts encoding the dorsal fate determinant, Gurken, in *asun* egg chambers. Dynein has been previously implicated in the proper localization of *gurken* mRNA. We observed that the localization of dynein is disrupted in *asun* egg chambers, suggesting that this defect may be the root cause of the ventralization phenotype of *asun*-derived embryos. We also observed defects in other dynein-mediated processes such as centrosome migration, nucleus-centrosome coupling, and nuclear positioning in *asun* ovaries. Therefore, similar to its role in spermatogenesis, our studies have revealed that *asun* is required for dynein localization and dynein function during *Drosophila* oogenesis.

Discussion and Future Directions

ASUN has been identified as a functional component of the nuclear Integrator complex in a genome-wide RNAi screen performed in *Drosophila* S2 cells (Chen et al., 2012). The Integrator plays a role in 3'-end processing of small nuclear RNAs (Chen and Wagner, 2010). Work in our lab has further determined that, in cultured human cells, the regulation of dynein localization by ASUN occurs through its role in the Integrator complex (Jodoin et al., 2013). The Integrator complex is conserved across phyla, although it has not yet been determined if *Drosophila* ASUN is a functional component

of the Integrator complex *in vivo*. Future experiments utilizing available mutants of additional components of the *Drosophila* Integrator complex would need to be performed to determine if, firstly, the results of the RNAi screen in *Drosophila* S2 cells indicating that ASUN is a component of this complex holds true for the organism, and, secondly, if the *Drosophila* Integrator complex is required for the localization of dynein during gametogenesis. We have shown in *Drosophila* that localization of ASUN within the nucleus of primary spermatocytes is critical for perinuclear accumulation of dynein during spermatogenesis (Jodoin et al., 2013). These data strengthen our hypothesis that ASUN may function as a component of the Integrator complex in *Drosophila* and that a nuclear function of this complex (most likely in RNA processing) is required for the regulation of dynein localization during *Drosophila* spermatogenesis.

As the Integrator is a nuclear complex, the current model for its role in regulating cytoplasmic dynein in human cells is that Integrator is required for the proper 3'-end processing of snRNA, which in turn is required for the proper processing of one or more mRNA transcripts encoding key regulator(s) of dynein localization within the cytoplasm (Jodoin et al., 2013). Therefore, to obtain more information on how dynein is regulated by the Integrator complex within the cell, it would be critical to identify and characterize the target(s) of the complex involved in mediating dynein localization. If we find that the Integrator complex plays a role in regulating dynein localization in *Drosophila*, further characterization of any hits obtained from the genetic screen described in Chapter IV could potentially be useful in identifying such Integrator targets. As ASUN is a component of the Integrator complex, and because ASUN was the first identified component of the complex that regulates dynein localization, it stands to reason that any

target of the Integrator complex that plays a role in regulating dynein localization could potentially dominantly modify the *asun* phenotype. Therefore, one method we could use to identify the above mentioned target(s) of the Integrator complex would be to identify hits from the genetic screen that are found to be required for the regulation of the perinuclear localization of dynein during *Drosophila* spermatogenesis and to determine if the mRNA processing of the target(s) is affected in the absence of one or more Integrator components.

ASUN exhibits a dynamic, cell cycle-dependent localization in *Drosophila* primary spermatocytes (Anderson et al., 2009). Using a transgene encoding GFP-tagged *Drosophila* ASUN, we demonstrated that in early G2 spermatocytes, ASUN is restricted to the nucleus, and in late G2 spermatocytes, ASUN first appears in the cytoplasm at approximately the same time as the enrichment of dynein on the nuclear surface. Based on this coincidence in the localizations of ASUN and dynein, we initially hypothesized that cytoplasmic ASUN was critical for the perinuclear localization of dynein. We performed experiments in which we restricted the localization of ASUN to either the nucleus or the cytoplasm by the addition of a strong exogenous nuclear localization sequence (NLS) or by mutating the endogenous NLS of ASUN, respectively (Jodoin et al., 2013). As mentioned earlier, we observed that the cytoplasmic-restricted form of ASUN failed to rescue the loss of dynein localization in *asun* mutants. This result suggests that nuclear ASUN plays an important role in dynein recruitment. This was further validated by the results obtained by the introduction of nuclear-restricted ASUN into the *asun* background, as nuclear ASUN fully rescued the *asun* phenotype. However, because we observed some leakage of the nuclear-restricted ASUN protein into the

cytoplasm, we cannot completely deny a possible role for cytoplasmic ASUN in regulating the localization of dynein. Additionally, the weak but conserved physical interaction that we observed between ASUN and LIS-1 would suggest that ASUN, in addition to functioning within the nucleus as a component of the Integrator complex, may also interact more directly with LIS-1 within the cytoplasm to regulate dynein. A new transgenic line, better capable of restricting ASUN to the nucleus (possibly by the addition of multiple strong exogenous nuclear localization sequences to the *asun* transgene), would have to be generated and tested to determine if cytoplasmic ASUN may play a minor role in regulating the localization of dynein during *Drosophila* spermatogenesis.

In addition to the role of ASUN as a component of the Integrator complex, ASUN has also been previously identified as an *in vitro* substrate of the PNG kinase (Lee et al., 2005). The PNG kinase is a serine/threonine kinase that ensures mitotic entry by maintaining Cyclin B levels during early embryogenesis in *Drosophila* (Fenger et al., 2000; Lee et al., 2005; Shamanski and Orr-Weaver, 1991; Vardy and Orr-Weaver, 2007). We observed that *asun*-derived embryos expressed normal levels of Cyclin B and failed to exhibit the giant nuclei phenotype that is characteristic of *png*-derived embryos, suggesting that ASUN is not critical during early embryogenesis. However, ASUN could still be an *in vivo* substrate of PNG and perform non-essential functions within the embryo. It would therefore be interesting to perform biochemical experiments to test if ASUN is phosphorylated by PNG during *Drosophila* embryogenesis.

asun^{d93} females have a highly reduced egg laying rate, although a significant number of *asun* females accumulate mature eggs within their ovaries. This suggested that

these females have defects in processes downstream of oogenesis that facilitate the movement of mature eggs from the ovary, down the oviduct and out the vulva. Current research has not implicated dynein or its accessory proteins in processes downstream of oogenesis. Therefore, it would be very interesting to determine if the loss of egg laying in *asun* females is a result of dynein-dependent defects in processes such as ovulation, egg release from the ovary, sperm storage, and/or fertilization or if ASUN plays dynein-independent roles in these processes. Our preliminary data suggest that the morphological appearance of the reproductive glands such as the parovaria glands and the spermathecae is similar to wild type in *asun* females. It would therefore be necessary to test the secretory cells of these glands for their capacity to release hormones that are required for proper activation and movement of the embryo down the oviduct. Our preliminary data also suggest that *asun* females mate normally and that motile sperm is stored within the seminal receptacle. It would therefore be of interest to determine if these females exhibit defects in the process of fertilization, as only half of the eggs laid by *asun* females undergo hatching.

The localization of mRNA transcripts encoding the dorsal fate determinant, Grk, to the anterior-dorsal region of late stage egg chambers is defective in *asun* females, likely as a result of loss of dynein localization. The Grk protein, however, was found to generally localize properly to the anterior-dorsal region of the oocyte in a majority of *asun* egg chambers, although the association of Grk with the oocyte nucleus appears to be disrupted as a result of nuclear mispositioning in *asun* egg chambers. These observations could suggest that the activation of the dorsal-anterior follicle cells by Grk depends on its activation and/or association with the oocyte nucleus. It is therefore of important to test

the activity of the Grk protein in *asun* egg chambers by observing the localization and activity of proteins activated and inhibited by Grk, such as Rhomboid and EGFR within the dorsal follicle cells and Pipe within the ventral follicle cells, respectively.

Based on our current knowledge, ASUN performs several critical functions during mitosis in human cells and during gametogenesis in *Drosophila*, and it has been shown to be a functional component of the Integrator complex. Additionally, recent evidence from our lab has demonstrated that ASUN and other components of the Integrator complex are required for the formation of primary cilia in cultured human cells via a mechanism that is independent of dynein (unpublished observations; Jeanne Jodoin and Laura Lee). These findings indicate that ASUN regulates dynein-dependent as well as dynein-independent cellular activities. It is therefore of importance to obtain more information on the potential interactors of ASUN. We have initiated a dominant modifier screen in *Drosophila* to identify genes that enhance or suppress the *asun* phenotype. We have tested 73 out of 190 deficiencies on the 2nd chromosome using this approach. These experiments have so far provided us with a small number of hits to pursue. To get a complete picture of the interactions and functions of ASUN within the cell, the remaining deficiencies on the 2nd chromosome as well as deficiencies on the other two major chromosomes would need to be tested to complete the first stage of the screen. Any hits obtained from this screen could then be further pursued to identify individual genes that would represent potential components of the molecular network of ASUN. Genes identified by this screen could then be characterized to determine their function during the cell cycle and their potential association with ASUN.

Significance

Dynein is an essential component of the cell. As mentioned in earlier chapters, dynein performs a myriad of functions ranging from the transport of cargo to various parts of the cell during interphase to the regulation of the rearrangement of microtubules and chromosomes during cell division. Loss of the majority of dynein components or accessory proteins or the disruption of the dynein complex would, in most cases, prove lethal to individual cells and the whole organism.

Loss or disruption of dynein function has been shown to be the cause of several diseases. As mentioned earlier, loss of one copy of the dynein accessory factor, *Lis1*, leads to type 1 lissencephaly, a human brain disorder resulting from defects in neuronal migration, which is a dynein-dependent process. Dynein has also been implicated in several other neurodegenerative diseases such as amyotrophic lateral sclerosis (ALS) and Huntington's disease (Moughamian and Holzbaur, 2011). Mutations in dynactin subunits also lead to neurodegenerative diseases such as Perry syndrome.

Our lab has demonstrated using *Drosophila* as a model that the misregulation of dynein localization can lead to male and female sterility, as dynein plays several critical roles during *Drosophila* gametogenesis. A similar requirement for dynein and LIS-1 was observed during spermatogenesis in mice, as deletion of a testis-specific splicing variant of *Lis1* in mice resulted in male sterility (Nayernia et al., 2003). Based on this conservation, it is likely that a subset of cases of sterility observed in humans could likewise be related to defects in cytoplasmic dynein function.

For dynein to perform its functions, others and we have shown that the regulation of its subunit composition and its subcellular localization is critical. Multiple proteins

have so far been identified as regulators of dynein localization and function, although it is clear that this knowledge is not complete. It is therefore very important to obtain a more precise understanding of the functions of cytoplasmic dynein and the various mechanisms by which it is regulated within the cell.

BIBLIOGRAPHY

Alberts, B., Johnson, A., Lewis, J., Martin, R., Roberts, K., and Walter, P. 2007. Molecular Biology of the Cell. Garland Science, Taylor and Francis Group, LLC, New York, NY.

Anderson, E.G. (1925) Crossing over in a Case of Attached X Chromosomes in DROSOPHILA MELANOGASTER. *Genetics*, **10**, 403-417.

Anderson, M.A., Jodoin, J.N., Lee, E., Hales, K.G., Hays, T.S., and Lee, L.A. (2009) Asunder is a critical regulator of dynein-dynactin localization during Drosophila spermatogenesis. *Mol Biol Cell*, **20**, 2709-2721.

Baillat, D., Hakimi, M.A., Naar, A.M., Shilatifard, A., Cooch, N., and Shiekhattar, R. (2005) Integrator, a multiprotein mediator of small nuclear RNA processing, associates with the C-terminal repeat of RNA polymerase II. *Cell*, **123**, 265-276.

Basto, R., Lau, J., Vinogradova, T., Gardiol, A., Woods, C.G., Khodjakov, A., and Raff, J.W. (2006) Flies without centrioles. *Cell*, **125**, 1375-1386.

Bastock, R., and St Johnston, D. (2008) Drosophila oogenesis. *Current biology : CB*, **18**, R1082-1087.

Beaudouin, J., Gerlich, D., Daigle, N., Eils, R., and Ellenberg, J. (2002) Nuclear envelope breakdown proceeds by microtubule-induced tearing of the lamina. *Cell*, **108**, 83-96.

Becalska, A.N., and Gavis, E.R. (2009) Lighting up mRNA localization in Drosophila oogenesis. *Development*, **136**, 2493-2503.

Bettencourt-Dias, M., Rodrigues-Martins, A., Carpenter, L., Riparbelli, M., Lehmann, L., Gatt, M.K., Carmo, N., Balloux, F., Callaini, G., and Glover, D.M. (2005) SAK/PLK4 is required for centriole duplication and flagella development. *Current biology : CB*, **15**, 2199-2207.

Blangy, A., Arnaud, L., and Nigg, E.A. (1997) Phosphorylation by p34cdc2 protein kinase regulates binding of the kinesin-related motor HsEg5 to the dynactin subunit p150. *J Biol Chem*, **272**, 19418-19424.

Bolhy, S., Bouhlel, I., Dultz, E., Nayak, T., Zuccolo, M., Gatti, X., Vallee, R., Ellenberg, J., and Doye, V. (2011) A Nup133-dependent NPC-anchored network tethers centrosomes to the nuclear envelope in prophase. *J Cell Biol*, **192**, 855-871.

Bolivar, J., Huynh, J.R., Lopez-Schier, H., Gonzalez, C., St Johnston, D., and Gonzalez-Reyes, A. (2001) Centrosome migration into the Drosophila oocyte is independent of BicD and egl, and of the organisation of the microtubule cytoskeleton. *Development*, **128**, 1889-1897.

Boschi, M., Belloni, M., and Robbins, L.G. (2006) Genetic evidence that nonhomologous disjunction and meiotic drive are properties of wild-type Drosophila melanogaster male meiosis. *Genetics*, **172**, 305-316.

Brendza, R.P., Serbus, L.R., Duffy, J.B., and Saxton, W.M. (2000) A function for kinesin I in the posterior transport of oskar mRNA and Staufen protein. *Science*, **289**, 2120-2122.

Bridges, C.B. (1916) Non-Disjunction as Proof of the Chromosome Theory of Heredity. *Genetics*, **1**, 1-52.

Busson, S., Dujardin, D., Moreau, A., Dompierre, J., and De Mey, J.R. (1998) Dynein and dynactin are localized to astral microtubules and at cortical sites in mitotic epithelial cells. *Current biology : CB*, **8**, 541-544.

Castrillon, D.H., Gonczy, P., Alexander, S., Rawson, R., Eberhart, C.G., Viswanathan, S., DiNardo, S., and Wasserman, S.A. (1993) Toward a molecular genetic analysis of spermatogenesis in Drosophila melanogaster: characterization of male-sterile mutants generated by single P element mutagenesis. *Genetics*, **135**, 489-505.

Cenci, G., Bonaccorsi, S., Pisano, C., Verni, F., and Gatti, M. (1994) Chromatin and microtubule organization during premeiotic, meiotic and early postmeiotic stages of Drosophila melanogaster spermatogenesis. *J Cell Sci*, **107 (Pt 12)**, 3521-3534.

Cha, B.J., Koppetsch, B.S., and Theurkauf, W.E. (2001) In vivo analysis of Drosophila bicoid mRNA localization reveals a novel microtubule-dependent axis specification pathway. *Cell*, **106**, 35-46.

Chen, J., Ezzeddine, N., Waltenspiel, B., Albrecht, T.R., Warren, W.D., Marzluff, W.F., and Wagner, E.J. (2012) An RNAi screen identifies additional members of the Drosophila Integrator complex and a requirement for cyclin C/Cdk8 in snRNA 3'-end formation. *Rna*, **18**, 2148-2156.

Chen, J., and Wagner, E.J. (2010) snRNA 3' end formation: the dawn of the Integrator complex. *Biochemical Society transactions*, **38**, 1082-1087.

Cheng, J., Turkel, N., Hemati, N., Fuller, M.T., Hunt, A.J., and Yamashita, Y.M. (2008) Centrosome misorientation reduces stem cell division during ageing. *Nature*, **456**, 599-604.

Chuang, J.Z., Milner, T.A., and Sung, C.H. (2001) Subunit heterogeneity of cytoplasmic dynein: Differential expression of 14 kDa dynein light chains in rat hippocampus. *J Neurosci*, **21**, 5501-5512.

Clark, A., Meignin, C., and Davis, I. (2007) A Dynein-dependent shortcut rapidly delivers axis determination transcripts into the Drosophila oocyte. *Development*, **134**, 1955-1965.

Cockell, M.M., Baumer, K., and Gonczy, P. (2004) lis-1 is required for dynein-dependent cell division processes in C. elegans embryos. *J Cell Sci*, **117**, 4571-4582.

Cole, D.G. (2003) The intraflagellar transport machinery of Chlamydomonas reinhardtii. *Traffic*, **4**, 435-442.

Collins, K.A., Callicoat, J.G., Lake, C.M., McClurken, C.M., Kohl, K.P., and Hawley, R.S. (2012) A germline clone screen on the X chromosome reveals novel meiotic mutants in Drosophila melanogaster. *G3*, **2**, 1369-1377.

Coquelle, F.M., Caspi, M., Cordelieres, F.P., Dompierre, J.P., Dujardin, D.L., Koifman, C., Martin, P., Hoogenraad, C.C., Akhmanova, A., Galjart, N., De Mey, J.R., and Reiner, O. (2002) LIS1, CLIP-170's key to the dynein/dynactin pathway. *Molecular and cellular biology*, **22**, 3089-3102.

Culver-Hanlon, T.L., Lex, S.A., Stephens, A.D., Quintyne, N.J., and King, S.J. (2006) A microtubule-binding domain in dynactin increases dynein processivity by skating along microtubules. *Nature cell biology*, **8**, 264-270.

Day, C.L., Puthalakath, H., Skea, G., Strasser, A., Barsukov, I., Lian, L.Y., Huang, D.C., and Hinds, M.G. (2004) Localization of dynein light chains 1 and 2 and their pro-apoptotic ligands. *The Biochemical journal*, **377**, 597-605.

de Cuevas, M., Lilly, M.A., and Spradling, A.C. (1997) Germline cyst formation in Drosophila. *Annual review of genetics*, **31**, 405-428.

de Cuevas, M., and Spradling, A.C. (1998) Morphogenesis of the Drosophila fusome and its implications for oocyte specification. *Development*, **125**, 2781-2789.

Deacon, S.W., Serpinskaya, A.S., Vaughan, P.S., Lopez Fanarraga, M., Vernos, I., Vaughan, K.T., and Gelfand, V.I. (2003) Dynactin is required for bidirectional organelle transport. *J Cell Biol*, **160**, 297-301.

Dick, T., Ray, K., Salz, H.K., and Chia, W. (1996) Cytoplasmic dynein (ddlc1) mutations cause morphogenetic defects and apoptotic cell death in Drosophila melanogaster. *Molecular and cellular biology*, **16**, 1966-1977.

Dillman, J.F., 3rd, and Pfister, K.K. (1994) Differential phosphorylation in vivo of cytoplasmic dynein associated with anterogradely moving organelles. *J Cell Biol*, **127**, 1671-1681.

Dujardin, D.L., and Vallee, R.B. (2002) Dynein at the cortex. *Curr Opin Cell Biol*, **14**, 44-49.

Duncan, J.E., and Warrior, R. (2002) The cytoplasmic dynein and kinesin motors have interdependent roles in patterning the Drosophila oocyte. *Current biology : CB*, **12**, 1982-1991.

Faulkner, N.E., Dujardin, D.L., Tai, C.Y., Vaughan, K.T., O'Connell, C.B., Wang, Y., and Vallee, R.B. (2000) A role for the lissencephaly gene LIS1 in mitosis and cytoplasmic dynein function. *Nature cell biology*, **2**, 784-791.

Fenger, D.D., Carminati, J.L., Burney-Sigman, D.L., Kashevsky, H., Dines, J.L., Elfring, L.K., and Orr-Weaver, T.L. (2000) PAN GU: a protein kinase that inhibits S phase and promotes mitosis in early Drosophila development. *Development*, **127**, 4763-4774.

Fuller, M.T. 1993. Spermatogenesis. *In* The Development of *Drosophila melanogaster*. e. M. Bate and A. Martinez-Arias, editor. Cold Spring Harbor Laboratory Press, Cold Spring Harbor, NY. 71-147.

Gambello, M.J., Darling, D.L., Yingling, J., Tanaka, T., Gleeson, J.G., and Wynshaw-Boris, A. (2003) Multiple dose-dependent effects of Lis1 on cerebral cortical development. *J Neurosci*, **23**, 1719-1729.

Gassmann, R., Essex, A., Hu, J.S., Maddox, P.S., Motegi, F., Sugimoto, A., O'Rourke, S.M., Bowerman, B., McLeod, I., Yates, J.R., 3rd, Oegema, K., Cheeseman, I.M., and Desai, A. (2008) A new mechanism controlling kinetochore-microtubule interactions revealed by comparison of two dynein-targeting components: SPDL-1 and the Rod/Zwilch/Zw10 complex. *Genes & development*, **22**, 2385-2399.

Gibbons, I.R., and Rowe, A.J. (1965) Dynein: A Protein with Adenosine Triphosphatase Activity from Cilia. *Science*, **149**, 424-426.

Gill, S.R., Cleveland, D.W., and Schroer, T.A. (1994) Characterization of DLC-A and DLC-B, two families of cytoplasmic dynein light chain subunits. *Mol Biol Cell*, **5**, 645-654.

Gill, S.R., Schroer, T.A., Szilak, I., Steuer, E.R., Sheetz, M.P., and Cleveland, D.W. (1991) Dynactin, a conserved, ubiquitously expressed component of an activator of vesicle motility mediated by cytoplasmic dynein. *J Cell Biol*, **115**, 1639-1650.

Gonczy, P., Pichler, S., Kirkham, M., and Hyman, A.A. (1999) Cytoplasmic dynein is required for distinct aspects of MTOC positioning, including centrosome separation, in the one cell stage Caenorhabditis elegans embryo. *J Cell Biol*, **147**, 135-150.

Gonzalez-Reyes, A., Elliott, H., and St Johnston, D. (1995) Polarization of both major body axes in Drosophila by gurken-torpedo signalling. *Nature*, **375**, 654-658.

Grieder, N.C., de Cuevas, M., and Spradling, A.C. (2000) The fusome organizes the microtubule network during oocyte differentiation in Drosophila. *Development*, **127**, 4253-4264.

Griffis, E.R., Stuurman, N., and Vale, R.D. (2007) Spindly, a novel protein essential for silencing the spindle assembly checkpoint, recruits dynein to the kinetochore. *J Cell Biol*, **177**, 1005-1015.

Gusnowski, E.M., and Srayko, M. (2011) Visualization of dynein-dependent microtubule gliding at the cell cortex: implications for spindle positioning. *J Cell Biol*, **194**, 377-386.

Ha, J., Lo, K.W., Myers, K.R., Carr, T.M., Humsi, M.K., Rasoul, B.A., Segal, R.A., and Pfister, K.K. (2008) A neuron-specific cytoplasmic dynein isoform preferentially transports TrkB signaling endosomes. *J Cell Biol*, **181**, 1027-1039.

Hassold, T., and Chiu, D. (1985) Maternal age-specific rates of numerical chromosome abnormalities with special reference to trisomy. *Human genetics*, **70**, 11-17.

Hassold, T., and Hunt, P. (2001) To err (meiotically) is human: the genesis of human aneuploidy. *Nature reviews. Genetics*, **2**, 280-291.

Hebbar, S., Mesngon, M.T., Guillotte, A.M., Desai, B., Ayala, R., and Smith, D.S. (2008) Lis1 and Ndel1 influence the timing of nuclear envelope breakdown in neural stem cells. *J Cell Biol*, **182**, 1063-1071.

Herskowitz, I.H., and Muller, H.J. (1954) Evidence against a Straight End-to-End Alignment of Chromosomes in Drosophila Spermatozoa. *Genetics*, **39**, 836-850.

Hirotsune, S., Fleck, M.W., Gambello, M.J., Bix, G.J., Chen, A., Clark, G.D., Ledbetter, D.H., McBain, C.J., and Wynshaw-Boris, A. (1998) Graded reduction of Pafah1b1 (Lis1) activity results in neuronal migration defects and early embryonic lethality. *Nat Genet*, **19**, 333-339.

Hook, P., and Vallee, R.B. (2006) The dynein family at a glance. *J Cell Sci*, **119**, 4369-4371.

Hu, D.J., Baffet, A.D., Nayak, T., Akhmanova, A., Doye, V., and Vallee, R.B. (2013) Dynein recruitment to nuclear pores activates apical nuclear migration and mitotic entry in brain progenitor cells. *Cell*, **154**, 1300-1313.

Huang, J., Roberts, A.J., Leschziner, A.E., and Reck-Peterson, S.L. (2012) Lis1 acts as a "clutch" between the ATPase and microtubule-binding domains of the dynein motor. *Cell*, **150**, 975-986.

Huang, X., Wang, H.L., Qi, S.T., Wang, Z.B., Tong, J.S., Zhang, Q.H., Ouyang, Y.C., Hou, Y., Schatten, H., Qi, Z.Q., and Sun, Q.Y. (2011) DYNLT3 is required for chromosome alignment during mouse oocyte meiotic maturation. *Reprod Sci*, **18**, 983-989.

Hughes, S.M., Vaughan, K.T., Herskovits, J.S., and Vallee, R.B. (1995) Molecular analysis of a cytoplasmic dynein light intermediate chain reveals homology to a family of ATPases. *J Cell Sci*, **108 (Pt 1)**, 17-24.

Inoue, Y.H., Savoian, M.S., Suzuki, T., Mathe, E., Yamamoto, M.T., and Glover, D.M. (2004) Mutations in orbit/mast reveal that the central spindle is comprised of two microtubule populations, those that initiate cleavage and those that propagate furrow ingression. *J Cell Biol*, **166**, 49-60.

Januschke, J., Gervais, L., Dass, S., Kaltschmidt, J.A., Lopez-Schier, H., St Johnston, D., Brand, A.H., Roth, S., and Guichet, A. (2002) Polar transport in the Drosophila oocyte requires Dynein and Kinesin I cooperation. *Current biology : CB*, **12**, 1971-1981.

Jin, Q., Ding, W., and Mulder, K.M. (2007) Requirement for the dynein light chain km23-1 in a Smad2-dependent transforming growth factor-beta signaling pathway. *J Biol Chem*, **282**, 19122-19132.

Jin, Q., Gao, G., and Mulder, K.M. (2009) Requirement of a dynein light chain in TGFbeta/Smad3 signaling. *Journal of cellular physiology*, **221**, 707-715.

Jodoin, J.N., Shboul, M., Sitaram, P., Zein-Sabatto, H., Reversade, B., Lee, E., and Lee, L.A. (2012) Human Asunder promotes dynein recruitment and centrosomal tethering to the nucleus at mitotic entry. *Mol Biol Cell*, **23**, 4713-4724.

Jodoin, J.N., Sitaram, P., Albrecht, T.R., May, S.B., Shboul, M., Lee, E., Reversade, B., Wagner, E.J., and Lee, L.A. (2013) Nuclear-localized Asunder regulates cytoplasmic dynein localization via its role in the Integrator complex. *Mol Biol Cell*.

Karki, S., and Holzbaur, E.L. (1995) Affinity chromatography demonstrates a direct binding between cytoplasmic dynein and the dynactin complex. *J Biol Chem*, **270**, 28806-28811.

Kemphues, K.J., Kaufman, T.C., Raff, R.A., and Raff, E.C. (1982) The testis-specific beta-tubulin subunit in Drosophila melanogaster has multiple functions in spermatogenesis. *Cell*, **31**, 655-670.

King, S.J., and Schroer, T.A. (2000) Dynactin increases the processivity of the cytoplasmic dynein motor. *Nature cell biology*, **2**, 20-24.

Kiyomitsu, T., and Cheeseman, I.M. (2012) Chromosome- and spindle-pole-derived signals generate an intrinsic code for spindle position and orientation. *Nature cell biology*, **14**, 311-317.

Kracklauer, M.P., Wiora, H.M., Deery, W.J., Chen, X., Bolival, B., Jr., Romanowicz, D., Simonette, R.A., Fuller, M.T., Fischer, J.A., and Beckingham, K.M. (2010) The Drosophila SUN protein Spag4 cooperates with the coiled-coil protein Yuri Gagarin to maintain association of the basal body and spermatid nucleus. *J Cell Sci*, **123**, 2763-2772.

Lam, C., Vergnolle, M.A., Thorpe, L., Woodman, P.G., and Allan, V.J. (2010) Functional interplay between LIS1, NDE1 and NDEL1 in dynein-dependent organelle positioning. *J Cell Sci*, **123**, 202-212.

Lan, L., Lin, S., Zhang, S., and Cohen, R.S. (2010) Evidence for a transport-trap mode of Drosophila melanogaster gurken mRNA localization. *PloS one*, **5**, e15448.

Lee, L.A., Elfring, L.K., Bosco, G., and Orr-Weaver, T.L. (2001) A genetic screen for suppressors and enhancers of the Drosophila PAN GU cell cycle kinase identifies cyclin B as a target. *Genetics*, **158**, 1545-1556.

Lee, L.A., Lee, E., Anderson, M.A., Vardy, L., Tahinci, E., Ali, S.M., Kashevsky, H., Benasutti, M., Kirschner, M.W., and Orr-Weaver, T.L. (2005) Drosophila genome-scale screen for PAN GU kinase substrates identifies Mat89Bb as a cell cycle regulator. *Developmental cell*, **8**, 435-442.

Lee, W.L., Oberle, J.R., and Cooper, J.A. (2003) The role of the lissencephaly protein Pac1 during nuclear migration in budding yeast. *J Cell Biol*, **160**, 355-364.

Lei, Y., and Warrior, R. (2000) The Drosophila Lissencephaly1 (DLis1) gene is required for nuclear migration. *Developmental biology*, **226**, 57-72.

Li, J., Lee, W.L., and Cooper, J.A. (2005) NudEL targets dynein to microtubule ends through LIS1. *Nature cell biology*, **7**, 686-690.

Li, M., McGrail, M., Serr, M., and Hays, T.S. (1994) Drosophila cytoplasmic dynein, a microtubule motor that is asymmetrically localized in the oocyte. *J Cell Biol*, **126**, 1475-1494.

Li, M.G., Serr, M., Newman, E.A., and Hays, T.S. (2004) The Drosophila tctex-1 light chain is dispensable for essential cytoplasmic dynein functions but is required during spermatid differentiation. *Mol Biol Cell*, **15**, 3005-3014.

Lin, H., and Spradling, A.C. (1995) Fusome asymmetry and oocyte determination in Drosophila. *Developmental genetics*, **16**, 6-12.

Lin, H., Yue, L., and Spradling, A.C. (1994) The Drosophila fusome, a germline-specific organelle, contains membrane skeletal proteins and functions in cyst formation. *Development*, **120**, 947-956.

Lindsley, D.L., and Sandler, L. (1977) The genetic analysis of meiosis in female Drosophila melanogaster. *Philosophical transactions of the Royal Society of London. Series B, Biological sciences*, **277**, 295-312.

Ma, S., Trivinos-Lagos, L., Graf, R., and Chisholm, R.L. (1999) Dynein intermediate chain mediated dynein-dynactin interaction is required for interphase microtubule organization and centrosome replication and separation in Dictyostelium. *J Cell Biol*, **147**, 1261-1274.

MacDougall, N., Clark, A., MacDougall, E., and Davis, I. (2003) Drosophila gurken (TGFalpha) mRNA localizes as particles that move within the oocyte in two dynein-dependent steps. *Developmental cell*, **4**, 307-319.

Malone, C.J., Misner, L., Le Bot, N., Tsai, M.C., Campbell, J.M., Ahringer, J., and White, J.G. (2003) The C. elegans hook protein, ZYG-12, mediates the essential attachment between the centrosome and nucleus. *Cell*, **115**, 825-836.

Malovannaya, A., Li, Y., Bulynko, Y., Jung, S.Y., Wang, Y., Lanz, R.B., O'Malley, B.W., and Qin, J. (2010) Streamlined analysis schema for high-throughput identification of endogenous protein complexes. *Proceedings of the National Academy of Sciences of the United States of America*, **107**, 2431-2436.

Markus, S.M., Punch, J.J., and Lee, W.L. (2009) Motor- and tail-dependent targeting of dynein to microtubule plus ends and the cell cortex. *Current biology : CB*, **19**, 196-205.

Martinez-Campos, M., Basto, R., Baker, J., Kernan, M., and Raff, J.W. (2004) The Drosophila pericentrin-like protein is essential for cilia/flagella function, but appears to be dispensable for mitosis. *J Cell Biol*, **165**, 673-683.

McGrail, M., and Hays, T.S. (1997) The microtubule motor cytoplasmic dynein is required for spindle orientation during germline cell divisions and oocyte differentiation in Drosophila. *Development*, **124**, 2409-2419.

McKearin, D. (1997) The Drosophila fusome, organelle biogenesis and germ cell differentiation: if you build it. *BioEssays : news and reviews in molecular, cellular and developmental biology*, **19**, 147-152.

McKenney, R.J., Vershinin, M., Kunwar, A., Vallee, R.B., and Gross, S.P. (2010) LIS1 and NudE induce a persistent dynein force-producing state. *Cell*, **141**, 304-314.

McKenney, R.J., Weil, S.J., Scherer, J., and Vallee, R.B. (2011) Mutually exclusive cytoplasmic dynein regulation by NudE-Lis1 and dynactin. *J Biol Chem*, **286**, 39615-39622.

Mesngon, M.T., Tarricone, C., Hebbar, S., Guillotte, A.M., Schmitt, E.W., Lanier, L., Musacchio, A., King, S.J., and Smith, D.S. (2006) Regulation of cytoplasmic dynein ATPase by Lis1. *J Neurosci*, **26**, 2132-2139.

Miller, M.P., Amon, A., and Unal, E. (2013) Meiosis I: when chromosomes undergo extreme makeover. *Curr Opin Cell Biol*.

Mische, S., He, Y., Ma, L., Li, M., Serr, M., and Hays, T.S. (2008) Dynein light intermediate chain: an essential subunit that contributes to spindle checkpoint inactivation. *Mol Biol Cell*, **19**, 4918-4929.

Mische, S., Li, M., Serr, M., and Hays, T.S. (2007) Direct observation of regulated ribonucleoprotein transport across the nurse cell/oocyte boundary. *Mol Biol Cell*, **18**, 2254-2263.

Morris, N.R. (2000) Nuclear migration. From fungi to the mammalian brain. *J Cell Biol*, **148**, 1097-1101.

Moughamian, A.J., and Holzbaur, E.L.F. 2011. Cytoplasmic Dynein Dysfunction and Neurodegenerative Disease.

Nayernia, K., Vauti, F., Meinhardt, A., Cadenas, C., Schweyer, S., Meyer, B.I., Schwandt, I., Chowdhury, K., Engel, W., and Arnold, H.H. (2003) Inactivation of a testis-specific Lis1 transcript in mice prevents spermatid differentiation and causes male infertility. *J Biol Chem*, **278**, 48377-48385.

Neuman-Silberberg, F.S., and Schupbach, T. (1993) The Drosophila dorsoventral patterning gene gurken produces a dorsally localized RNA and encodes a TGF alpha-like protein. *Cell*, **75**, 165-174.

Nyarko, A., Song, Y., and Barbar, E. (2012) Intrinsic disorder in dynein intermediate chain modulates its interactions with NudE and dynactin. *J Biol Chem*, **287**, 24884-24893.

O'Connor, C. (2008) Chromosomal Abnormalities: Aneuploidies. *Nature Education*, **1**.

Ong, S., and Tan, C. (2010) Germline cyst formation and incomplete cytokinesis during Drosophila melanogaster oogenesis. *Developmental biology*, **337**, 84-98.

Ori-McKenney, K.M., McKenney, R.J., and Vallee, R.B. 2011. Studies of Lissencephaly and Neurodegenerative Disease Reveal Novel Aspects of Cytoplasmic Dynein Regulation. *In* Dyneins. S.M. King, editor. Elsevier publishing.

Orr-Weaver, T.L. (1995) Meiosis in Drosophila: seeing is believing. *Proceedings of the National Academy of Sciences of the United States of America*, **92**, 10443-10449.

Palmer, K.J., Hughes, H., and Stephens, D.J. (2009) Specificity of cytoplasmic dynein subunits in discrete membrane-trafficking steps. *Mol Biol Cell*, **20**, 2885-2899.

Parks, A.L., Cook, K.R., Belvin, M., Dompe, N.A., Fawcett, R., Huppert, K., Tan, L.R., Winter, C.G., Bogart, K.P., Deal, J.E., Deal-Herr, M.E., Grant, D., Marcinko, M., Miyazaki, W.Y., Robertson, S., Shaw, K.J., Tabios, M., Vysotskaia, V., Zhao, L., Andrade, R.S., Edgar, K.A., Howie, E., Killpack, K., Milash, B., Norton, A., Thao, D., Whittaker, K., Winner, M.A., Friedman, L., Margolis, J., Singer, M.A., Kopczynski, C., Curtis, D., Kaufman, T.C., Plowman, G.D., Duyk, G., and Francis-Lang, H.L. (2004) Systematic generation of high-resolution deletion coverage of the Drosophila melanogaster genome. *Nat Genet*, **36**, 288-292.

Paschal, B.M., Mikami, A., Pfister, K.K., and Vallee, R.B. (1992) Homology of the 74-kD cytoplasmic dynein subunit with a flagellar dynein polypeptide suggests an intracellular targeting function. *J Cell Biol*, **118**, 1133-1143.

Paschal, B.M., and Vallee, R.B. (1987) Retrograde transport by the microtubule-associated protein MAP 1C. *Nature*, **330**, 181-183.

Peri, F., and Roth, S. (2000) Combined activities of Gurken and decapentaplegic specify dorsal chorion structures of the Drosophila egg. *Development*, **127**, 841-850.

Pfarr, C.M., Coue, M., Grissom, P.M., Hays, T.S., Porter, M.E., and McIntosh, J.R. (1990) Cytoplasmic dynein is localized to kinetochores during mitosis. *Nature*, **345**, 263-265.

Pfister, K.K., Shah, P.R., Hummerich, H., Russ, A., Cotton, J., Annuar, A.A., King, S.M., and Fisher, E.M. (2006) Genetic analysis of the cytoplasmic dynein subunit families. *PLoS genetics*, **2**, e1.

Pokrywka, N.J., and Stephenson, E.C. (1991) Microtubules mediate the localization of bicoid RNA during Drosophila oogenesis. *Development*, **113**, 55-66.

Quintyne, N.J., and Schroer, T.A. (2002) Distinct cell cycle-dependent roles for dynactin and dynein at centrosomes. *J Cell Biol*, **159**, 245-254.

Raaijmakers, J.A., Tanenbaum, M.E., and Medema, R.H. (2013) Systematic dissection of dynein regulators in mitosis. *J Cell Biol*, **201**, 201-215.

Raaijmakers, J.A., van Heesbeen, R.G., Meaders, J.L., Geers, E.F., Fernandez-Garcia, B., Medema, R.H., and Tanenbaum, M.E. (2012) Nuclear envelope-associated dynein drives prophase centrosome separation and enables Eg5-independent bipolar spindle formation. *The EMBO journal*, **31**, 4179-4190.

Rebollo, E., and Gonzalez, C. (2000) Visualizing the spindle checkpoint in Drosophila spermatocytes. *EMBO reports*, **1**, 65-70.

Rebollo, E., Llamazares, S., Reina, J., and Gonzalez, C. (2004) Contribution of noncentrosomal microtubules to spindle assembly in Drosophila spermatocytes. *PLoS Biol*, **2**, E8.

Reiner, O., and Lombroso, P.J. (1998) Development of the cerebral cortex: II. Lissencephaly. *Journal of the American Academy of Child and Adolescent Psychiatry*, **37**, 231-232.

Reinsch, S., and Gonczy, P. (1998) Mechanisms of nuclear positioning. *J Cell Sci*, **111 (Pt 16)**, 2283-2295.

Reinsch, S., and Karsenti, E. (1994) Orientation of spindle axis and distribution of plasma membrane proteins during cell division in polarized MDCKII cells. *J Cell Biol*, **126**, 1509-1526.

Robinson, J.T., Wojcik, E.J., Sanders, M.A., McGrail, M., and Hays, T.S. (1999) Cytoplasmic dynein is required for the nuclear attachment and migration of centrosomes during mitosis in Drosophila. *J Cell Biol*, **146**, 597-608.

Rom, I., Faicevici, A., Almog, O., and Neuman-Silberberg, F.S. (2007) Drosophila Dynein light chain (DDLC1) binds to gurken mRNA and is required for its localization. *Biochimica et biophysica acta*, **1773**, 1526-1533.

Roth, S., Neuman-Silberberg, F.S., Barcelo, G., and Schupbach, T. (1995) cornichon and the EGF receptor signaling process are necessary for both anterior-posterior and dorsal-ventral pattern formation in Drosophila. *Cell*, **81**, 967-978.

Roulier, E.M., Panzer, S., and Beckendorf, S.K. (1998) The Tec29 tyrosine kinase is required during Drosophila embryogenesis and interacts with Src64 in ring canal development. *Molecular cell*, **1**, 819-829.

Rubin, G.M., and Spradling, A.C. (1982) Genetic transformation of Drosophila with transposable element vectors. *Science*, **218**, 348-353.

Salata, M.W., Dillman, J.F., 3rd, Lye, R.J., and Pfister, K.K. (2001) Growth factor regulation of cytoplasmic dynein intermediate chain subunit expression preceding neurite extension. *Journal of neuroscience research*, **65**, 408-416.

Salina, D., Bodoor, K., Eckley, D.M., Schroer, T.A., Rattner, J.B., and Burke, B. (2002) Cytoplasmic dynein as a facilitator of nuclear envelope breakdown. *Cell*, **108**, 97-107.

Sartain, C.V., Cui, J., Meisel, R.P., and Wolfner, M.F. (2011) The poly(A) polymerase GLD2 is required for spermatogenesis in Drosophila melanogaster. *Development*, **138**, 1619-1629.

Sasaki, S., Shionoya, A., Ishida, M., Gambello, M.J., Yingling, J., Wynshaw-Boris, A., and Hirotsune, S. (2000) A LIS1/NUDEL/cytoplasmic dynein heavy chain complex in the developing and adult nervous system. *Neuron*, **28**, 681-696.

Schliwa, M., and Woehlke, G. (2003) Molecular motors. *Nature*, **422**, 759-765.

Schnorrer, F., Bohmann, K., and Nusslein-Volhard, C. (2000) The molecular motor dynein is involved in targeting swallow and bicoid RNA to the anterior pole of Drosophila oocytes. *Nature cell biology*, **2**, 185-190.

Schroer, T.A. (1994) New insights into the interaction of cytoplasmic dynein with the actin-related protein, Arp1. *J Cell Biol*, **127**, 1-4.

Schroer, T.A. (2004) Dynactin. *Annual review of cell and developmental biology*, **20**, 759-779.

Schroer, T.A., and Sheetz, M.P. (1991) Two activators of microtubule-based vesicle transport. *J Cell Biol*, **115**, 1309-1318.

Schupbach, T. (1987) Germ line and soma cooperate during oogenesis to establish the dorsoventral pattern of egg shell and embryo in Drosophila melanogaster. *Cell*, **49**, 699-707.

Sen, J., Goltz, J.S., Stevens, L., and Stein, D. (1998) Spatially restricted expression of pipe in the Drosophila egg chamber defines embryonic dorsal-ventral polarity. *Cell*, **95**, 471-481.

Shamanski, F.L., and Orr-Weaver, T.L. (1991) The Drosophila plutonium and pan gu genes regulate entry into S phase at fertilization. *Cell*, **66**, 1289-1300.

Siller, K.H., and Doe, C.Q. (2008) Lis1/dynactin regulates metaphase spindle orientation in Drosophila neuroblasts. *Developmental biology*, **319**, 1-9.

Siller, K.H., Serr, M., Steward, R., Hays, T.S., and Doe, C.Q. (2005) Live imaging of Drosophila brain neuroblasts reveals a role for Lis1/dynactin in spindle assembly and mitotic checkpoint control. *Mol Biol Cell*, **16**, 5127-5140.

Sitaram, P., Anderson, M.A., Jodoin, J.N., Lee, E., and Lee, L.A. (2012) Regulation of dynein localization and centrosome positioning by Lis-1 and asunder during Drosophila spermatogenesis. *Development*, **139**, 2945-2954.

Sivaram, M.V., Wadzinski, T.L., Redick, S.D., Manna, T., and Doxsey, S.J. (2009) Dynein light intermediate chain 1 is required for progress through the spindle assembly checkpoint. *The EMBO journal*, **28**, 902-914.

Smith, D.S., Niethammer, M., Ayala, R., Zhou, Y., Gambello, M.J., Wynshaw-Boris, A., and Tsai, L.H. (2000) Regulation of cytoplasmic dynein behaviour and microtubule organization by mammalian Lis1. *Nature cell biology*, **2**, 767-775.

Splinter, D., Tanenbaum, M.E., Lindqvist, A., Jaarsma, D., Flotho, A., Yu, K.L., Grigoriev, I., Engelsma, D., Haasdijk, E.D., Keijzer, N., Demmers, J., Fornerod, M., Melchior, F., Hoogenraad, C.C., Medema, R.H., and Akhmanova, A. (2010) Bicaudal D2, dynein, and kinesin-1 associate with nuclear pore complexes and regulate centrosome and nuclear positioning during mitotic entry. *PLoS Biol*, **8**, e1000350.

Spradling, A. 1993. Developmental Genetics of Oogenesis. *In* The Development of Drosophila melanogaster. Cold Spring Harbor Laboratory Press, Plainview, NY.

Starr, D.A., Williams, B.C., Hays, T.S., and Goldberg, M.L. (1998) ZW10 helps recruit dynactin and dynein to the kinetochore. *J Cell Biol*, **142**, 763-774.

Stebbings, L., Grimes, B.R., and Bownes, M. (1998) A testis-specifically expressed gene is embedded within a cluster of maternally expressed genes at 89B in Drosophila melanogaster. *Development genes and evolution*, **208**, 523-530.

Steuer, E.R., Wordeman, L., Schroer, T.A., and Sheetz, M.P. (1990) Localization of cytoplasmic dynein to mitotic spindles and kinetochores. *Nature*, **345**, 266-268.

Stuchell-Brereton, M.D., Siglin, A., Li, J., Moore, J.K., Ahmed, S., Williams, J.C., and Cooper, J.A. (2011) Functional interaction between dynein light chain and intermediate chain is required for mitotic spindle positioning. *Mol Biol Cell*, **22**, 2690-2701.

Sun, J., and Spradling, A.C. (2013) Ovulation in Drosophila is controlled by secretory cells of the female reproductive tract. *eLife*, **2**, e00415.

Susalka, S.J., and Pfister, K.K. (2000) Cytoplasmic dynein subunit heterogeneity: implications for axonal transport. *J Neurocytol*, **29**, 819-829.

Suter, B., and Steward, R. (1991) Requirement for phosphorylation and localization of the Bicaudal-D protein in Drosophila oocyte differentiation. *Cell*, **67**, 917-926.

Swan, A., Nguyen, T., and Suter, B. (1999) Drosophila Lissencephaly-1 functions with Bic-D and dynein in oocyte determination and nuclear positioning. *Nature cell biology*, **1**, 444-449.

Tai, A.W., Chuang, J.Z., and Sung, C.H. (2001) Cytoplasmic dynein regulation by subunit heterogeneity and its role in apical transport. *J Cell Biol*, **153**, 1499-1509.

Tai, C.Y., Dujardin, D.L., Faulkner, N.E., and Vallee, R.B. (2002) Role of dynein, dynactin, and CLIP-170 interactions in LIS1 kinetochore function. *J Cell Biol*, **156**, 959-968.

Tanaka, T., Serneo, F.F., Higgins, C., Gambello, M.J., Wynshaw-Boris, A., and Gleeson, J.G. (2004) Lis1 and doublecortin function with dynein to mediate coupling of the nucleus to the centrosome in neuronal migration. *J Cell Biol*, **165**, 709-721.

Tanenbaum, M.E., Akhmanova, A., and Medema, R.H. (2010) Dynein at the nuclear envelope. *EMBO reports*, **11**, 649.

Tarricone, C., Perrina, F., Monzani, S., Massimiliano, L., Kim, M.H., Derewenda, Z.S., Knapp, S., Tsai, L.H., and Musacchio, A. (2004) Coupling PAF signaling to dynein regulation: structure of LIS1 in complex with PAF-acetylhydrolase. *Neuron*, **44**, 809-821.

Texada, M.J., Simonette, R.A., Johnson, C.B., Deery, W.J., and Beckingham, K.M. (2008) Yuri gagarin is required for actin, tubulin and basal body functions in Drosophila spermatogenesis. *J Cell Sci*, **121**, 1926-1936.

Therrien, M., Morrison, D.K., Wong, A.M., and Rubin, G.M. (2000) A genetic screen for modifiers of a kinase suppressor of Ras-dependent rough eye phenotype in Drosophila. *Genetics*, **156**, 1231-1242.

Theurkauf, W.E., Smiley, S., Wong, M.L., and Alberts, B.M. (1992) Reorganization of the cytoskeleton during Drosophila oogenesis: implications for axis specification and intercellular transport. *Development*, **115**, 923-936.

Tsai, L.H., and Gleeson, J.G. (2005) Nucleokinesis in neuronal migration. *Neuron*, **46**, 383-388.

Vallee, R.B., and Hook, P. (2006) Autoinhibitory and other autoregulatory elements within the dynein motor domain. *Journal of structural biology*, **156**, 175-181.

Vallee, R.B., and Tsai, J.W. (2006) The cellular roles of the lissencephaly gene LIS1, and what they tell us about brain development. *Genes & development*, **20**, 1384-1393.

Vallee, R.B., Williams, J.C., Varma, D., and Barnhart, L.E. (2004) Dynein: An ancient motor protein involved in multiple modes of transport. *Journal of neurobiology*, **58**, 189-200.

Van Buskirk, C., and Schupbach, T. (1999) Versatility in signalling: multiple responses to EGF receptor activation during Drosophila oogenesis. *Trends in cell biology*, **9**, 1-4.

Vardy, L., and Orr-Weaver, T.L. (2007) The Drosophila PNG kinase complex regulates the translation of cyclin B. *Developmental cell*, **12**, 157-166.

Vaughan, K.T., and Vallee, R.B. (1995) Cytoplasmic dynein binds dynactin through a direct interaction between the intermediate chains and p150Glued. *J Cell Biol*, **131**, 1507-1516.

Vaughan, P.S., Leszyk, J.D., and Vaughan, K.T. (2001) Cytoplasmic dynein intermediate chain phosphorylation regulates binding to dynactin. *J Biol Chem*, **276**, 26171-26179.

Vaughan, P.S., Miura, P., Henderson, M., Byrne, B., and Vaughan, K.T. (2002) A role for regulated binding of p150(Glued) to microtubule plus ends in organelle transport. *J Cell Biol*, **158**, 305-319.

Vergnolle, M.A., and Taylor, S.S. (2007) Cenp-F links kinetochores to Ndel1/Nde1/Lis1/dynein microtubule motor complexes. *Current biology : CB*, **17**, 1173-1179.

Wainman, A., Creque, J., Williams, B., Williams, E.V., Bonaccorsi, S., Gatti, M., and Goldberg, M.L. (2009) Roles of the Drosophila NudE protein in kinetochore function and centrosome migration. *J Cell Sci*, **122**, 1747-1758.

Wasserman, J.D., and Freeman, M. (1998) An autoregulatory cascade of EGF receptor signaling patterns the Drosophila egg. *Cell*, **95**, 355-364.

Waterman-Storer, C.M., Karki, S., and Holzbaur, E.L. (1995) The p150Glued component of the dynactin complex binds to both microtubules and the actin-related protein centractin (Arp-1). *Proceedings of the National Academy of Sciences of the United States of America*, **92**, 1634-1638.

Whyte, J., Bader, J.R., Tauhata, S.B., Raycroft, M., Hornick, J., Pfister, K.K., Lane, W.S., Chan, G.K., Hinchcliffe, E.H., Vaughan, P.S., and Vaughan, K.T. (2008) Phosphorylation regulates targeting of cytoplasmic dynein to kinetochores during mitosis. *J Cell Biol*, **183**, 819-834.

Wojcik, E., Basto, R., Serr, M., Scaerou, F., Karess, R., and Hays, T. (2001) Kinetochore dynein: its dynamics and role in the transport of the Rough deal checkpoint protein. *Nature cell biology*, **3**, 1001-1007.

Wong, R., Hadjiyanni, I., Wei, H.C., Polevoy, G., McBride, R., Sem, K.P., and Brill, J.A. (2005) PIP2 hydrolysis and calcium release are required for cytokinesis in Drosophila spermatocytes. *Current biology : CB*, **15**, 1401-1406.

Woodard, G.E., Huang, N.N., Cho, H., Miki, T., Tall, G.G., and Kehrl, J.H. (2010) Ric-8A and Gi alpha recruit LGN, NuMA, and dynein to the cell cortex to help orient the mitotic spindle. *Molecular and cellular biology*, **30**, 3519-3530.

Wynshaw-Boris, A. (2007) Lissencephaly and LIS1: insights into the molecular mechanisms of neuronal migration and development. *Clin Genet*, **72**, 296-304.

Xiang, X., and Fischer, R. (2004) Nuclear migration and positioning in filamentous fungi. *Fungal genetics and biology : FG & B*, **41**, 411-419.

Yamashita, Y.M., Jones, D.L., and Fuller, M.T. (2003) Orientation of asymmetric stem cell division by the APC tumor suppressor and centrosome. *Science*, **301**, 1547-1550.

Yamashita, Y.M., Mahowald, A.P., Perlin, J.R., and Fuller, M.T. (2007) Asymmetric inheritance of mother versus daughter centrosome in stem cell division. *Science*, **315**, 518-521.

Zhang, J., Li, S., Fischer, R., and Xiang, X. (2003) Accumulation of cytoplasmic dynein and dynactin at microtubule plus ends in Aspergillus nidulans is kinesin dependent. *Mol Biol Cell*, **14**, 1479-1488.

Zhang, X., Lei, K., Yuan, X., Wu, X., Zhuang, Y., Xu, T., Xu, R., and Han, M. (2009) SUN1/2 and Syne/Nesprin-1/2 complexes connect centrosome to the nucleus during neurogenesis and neuronal migration in mice. *Neuron*, **64**, 173-187.

Zhao, T., Graham, O.S., Raposo, A., and St Johnston, D. (2012) Growing microtubules push the oocyte nucleus to polarize the Drosophila dorsal-ventral axis. *Science*, **336**, 999-1003.

Zimyanin, V.L., Belaya, K., Pecreaux, J., Gilchrist, M.J., Clark, A., Davis, I., and St Johnston, D. (2008) In vivo imaging of oskar mRNA transport reveals the mechanism of posterior localization. *Cell*, **134**, 843-853.